OULUN YLIOPISTO
UNIVERSITY of OULU

Department of Process and Environmental Engineering
Mass and Heat Transfer Laboratory

Master's Thesis

Waste Material Mediated CO_2 Capture and Storage

Oulu 30th May 2011

Author: _____
Johannes Ritamäki

Supervisors: _____
Riitta Keiski, Professor

_____
Jyri-Pekka Mikkola, Professor

Advisors: _____
Eva Pongracz, D.Sc.(Tech.)

_____
Mika Huuhtanen, D.Sc.(Tech.)

UNIVERSITY OF OULU **Abstract of thesis**
Faculty of technology

Department	Laboratory
Dep. of Process and Environmental Engineering	Mass and Heat Transfer Process Laboratory
Author	**Supervisor**
Ritamäki, Johannes Miikka Petteri	Keiski, R. Professor

Name of the thesis

Waste Material Mediated CO_2 Capture and Storage

Subject	Level of studies	Date	Number of pages
Process Engineering	Master's Thesis	May 2011	98 p., 6 appendices

Abstract

CO_2 emissions are suspected to be the primary cause for the climate change. Carbon dioxide levels have risen from 280 ppm to 385 ppm over the last century. At the same time, the average surface temperature has increased by 0.6°C, globally. For this reason carbon dioxide capture and storage (CCS) is under research worldwide.

World oil shale, as a source of energy, is almost a pristine resource and it is expected to be an important fuel in the future. Unfortunately, oil shale utilisation yields large amounts of CO_2 emissions and ash, which is classified mainly as waste. Therefore, it is very important to research novel applications for the utilisation of ash, as has been done in this work. The second waste material in this work is green liquor sludge, which is originating from pulp and paper industry. Green liquor sludge is the largest single waste fraction in chemical pulping. Both of the waste materials have prerequisite for CCS.

CCS was studied via chemical and physical adsorption, chemisorption and physisorption, respectively. Chemisorption is present in a process called mineral carbonation, in which CO_2 is transformed to its solid, carbonate form. Carbonates are found to be a geologically stable form for CO_2 storage. Physisorption, alternately, can be used in gas purification. Both waste materials need to be pre-treated, activated, before adsorption. The activation increases the specific surface area or yield minerals that are able to react with CO_2.

Activated oil shale ash was feasible for chemisorption, with an adsorption capacity of 90 kg CO_2 per ton of ash. The process was analysed with a variety of analyses, but concrete evidence of chemical reaction was not found. Green liquor sludge was not found to be practical for CO_2 storage. Physisorption measurements for oil shale ash indicated 1.6 wt.-% CO_2 uptake and for green liquor sludge the value was 0.2 wt.-%.

The thesis was conducted in frames of the EU's Northern Periphery Programme funded Micro Waste to Energy Solutions (MicrE) project, in collaboration between the University of Oulu's Thule Institute and Mass and Heat Transfer Process Laboratory, the Department of Chemistry at Umeå University, and the National Institute of Chemical Physics and Biophysics in Estonia.

Library location

University of Oulu, Science Library Tellus

Additional information

OULUN YLIOPISTO **Tiivistelmä**
opinnäytetyöstä
Teknillinen tiedekunta

Osasto	Laboratorio
Prosessi- ja ympäristötekniikan osasto	Lämpö- ja diffuusiotekniikan laboratorio
Tekijä	**Työn valvoja**
Ritamäki, Johannes Miikka Petteri	Keiski, R. Professori

Työn nimi

Jätemateriaalit hiilidioksidin talteenotossa ja varastoinnissa

Oppiaine	Työn laji	Aika	Sivumäärä
Prosessitekniikka	Diplomityö	Toukokuu 2011	98 s., 6 liitettä

Tiivistelmä

Hiilidioksidipäästöjen on epäilty olevan tärkein syy ilmastonmuutokseen. Ilmakehän hiilidioksiditasot on noussut tasolta 280 ppm tasolle 385 ppm viimeisen vuosisadan kuluessa. Samaan aikaan keskimääräinen maapallon pintalämpötila on noussut 0.6 °C. Tästä johtuen hiilidioksidin talteenottoa ja varastointia tutkitaan maailmanlaajuisesti.

Maailman öljyliuskevarannot energialähteenä ovat pääosin koskemattomat ja öljyliuskeen odotetaan olevan tärkeä polttoaine tulevaisuudessa. Öljyliuskeen hyödyntäminen tuottaa valtavan määrän hiilidioksidia ja tuhkaa, joka on määritelty pääasiassa jätteeksi. Tästä johtuen on tärkeä etsiä uusia käyttökohteita tuhkalle, kuten tässä työssä on tutkittu. Toinen työn jätemateriaaleista on viherlipeäsakka, joka on peräisin sellu ja paperiteollisuudesta. Viherlipeäsakka on suurin yksittäinen jätejae kemiallisessa sellun valmistuksessa. Molemmilla jätemateriaaleilla on edellytyksiä hiilidioksidin talteenottoon ja varastointiin.

Hiilidioksidin talteenottoa ja varastointia tutkittiin kemiallisessa ja fysikaalisessa adsorptiossa, kemisorptiossa ja fysisorptiossa. Kemisorptio on osallisena prosessissa, jota kutsutaan mineraalien karbonoinniksi, jossa CO_2 reagoi karbonaattiksi. Karbonaattien on todettu olevan geologisesti vakaa hiilidioksidin varastointimuoto. Toisaalta fysisorptiota voidaan käyttää kaasujen puhdistuksessa. Jätemateriaalit tulee esikäsitellä, aktivoida, ennen adsorptiota. Aktivoinnilla lisätään ominaispinta-alaa tai tuotetaan mineraaleja, jotka ovat kykeneviä reagoimaan CO_2 kanssa.

Aktivoitu öljyliuske osoittautui kemisorptioon soveltuvaksi, jopa 90 kg CO_2 adsorboitui tonniin tuhkaa. Prosessia analysoitiin useilla analysaattoreilla, mutta konkreettista näyttöä kemialliselle reaktiolle ei löydetty. Viherlipeäsakka ei osoittanut käytännölliseksi hiilidioksidin varastoinnissa. Öljyliuskeen fysisorptiomittaukset osoittivat 1.6%:n hiilidioksidikertymää ja viherlipeäsakkaan kertymä oli vastaavasti 0.2%.

Työ tehtiin EU:n Northern Periphery Programme –ohjelmaan kuuluvassa MicrE-projektissa yhteistyössä Oulun yliopiston Thule instituutin ja lämpö- ja diffuusiotekniikan laboratorion, Uumajan yliopiston kemian osaston, ja Viron kansallisen kemiallisen fysiikan ja biofysiikan instituutin kanssa.

Säilytyspaikka

Oulun yliopisto, Tiedekirjasto Tellus

Muita tietoja

Table of contents

Abbreviations

AD	Anaerobic Digestion
BET	Brunauer Emmett Teller theory
BJH	Barret Joyer Halenda method
CCS	Carbon Capture and Storage
CFB	Circulating Fluidized Bed boiler
EDS	Energy-dispersive X-ray spectroscopy
EFTEM	Energy Filtered Transmission Electron Microscope
FESEM	Field Emission Scanning Electron Microscope
GLS	Green Liquor Sludge
NMR	Nuclear Magnetic Resonance
OSA	Oil Shale Ash
ppm	parts per million
PF	Pulverized firing
TGA	Thermogravimetric Analysis
XRD	X-ray Diffraction analysis

List of appendices

Preface

The research in this thesis was funded by the EU in MicrE-project, which is a project to develop small scale renewable energy solutions for rural small and medium sized enterprises as well as local organisations in the northern periphery. This thesis was compiled as a collaborative project between the Thule institute, the Department of Chemistry at Umeå University in Sweden, the Mass and Heat Transfer Process Laboratory at the University of Oulu, and the National Institute of Chemical Physics and Biophysics (KBFI) in Estonia. The work was carried out at Umeå and Oulu Universities.

I would like to acknowledge my supervisors Professor Riitta Keiski and Professor Jyri-Pekka Mikkola. I would also like to thank my advisors Dr. Eva Pongrácz and Dr. Mika Huuhtanen. I would also like to thank Dr. Willian Larsson and Dr. Janek Reinik for guidance and new ideas. Many thanks are due to Lic. Niko Hänninen.

I would also like to thank the staff of Chemical Biological Centre at Umeå University, especially Dr. Janice Kenney. Finally, I would like to thank my family and Hilkka Keränen for supporting me throughout this project.

Oulu, April 2011

Johannes Ritamäki

Theoretical part

1 Introduction

In this work, two waste materials, oil shale fly ash and green liquor sludge, were researched with respect to carbon capture and storage (CCS). These waste materials were examined as precursor materials for mineral carbonation and adsorption, as well as various mixtures of these two materials.

The aim of the work was to determine if these low value waste materials could be utilised in carbon dioxide sequestration. The EU Emission Trading System (EU ETS) considers carbon dioxide as a greenhouse gas and due to CO_2 allowances, the price to release CO_2 into the environment is significant. The objective of the trading system is to lower CO_2 emissions over time by reducing the number of allowances (The EU ETS 2011). Today, there are serious concerns that climate change might be caused primarily by carbon dioxide. If something as simple as these waste materials could be used in carbon dioxide capture and storage, it would have significant advantages for bioenergy and oil shale industries and eventually could affect the carbon dioxide level in the atmosphere.

The work in this study was carried out under the Micro Energy to Rural Enterprises (MicrE) project financed by the European Union's Northern Periphery Programme. The project aims to develop small scale renewable energy solutions. One of the most successful technologies to produce renewable energy in small scale in Northern Periphery conditions is anaerobic digestion (AD), as well as gasification and small scale combustion of biomass (Kauriinoja 2010). The drawback of those technologies is the high content of carbon dioxide in the biogas and flue gases produced. CO_2 needs to be removed from the biogas before it can be used in modern industrial applications, e.g. fuel cells, gas motors, or gas burners. One third of the mass of biogas consists of carbon dioxide, which needs to be removed. The leftover CO_2 cannot be released into environment, therefore, it is imperative to determine what to do with it after removal. The surplus CO_2 could be turned into a stable form, for example through the mineral carbonation to calcium carbonate.

There are several methods which exist for the final disposal of carbon dioxide, for example, storage in spent natural gas mines or in the deep sea. Unfortunately, these methods do not provide a feasible solution for the growing need of CO_2 sequestration. Therefore, much effort has been put into developing new CCS methods globally. One promising method could be mineral carbonation of carbon dioxide into the form of calcium carbonate. Oil shale ash has naturally good properties to offer a nucleation site for mineral carbonation. Other possible sorption methods are evaluated as well.

Both, the oil shale fly ash and the green liquor sludge have significant potential for biogas scrubbing and mineral carbonation of CO_2, which is why they seem to be promising precursors in CO_2 sequestration. They are both inexpensive, there is plenty of both materials available, and their chemical compositions make them feasible for the sequestration. The residual material could thereafter be used as a road bottom material or landfill foundation.

2 CO_2 and sustainable energy production

Carbon dioxide was originally discovered as a gas approximately 250 years ago by a Scottish University student Joseph Black, at the University of Edinburgh. The results were published in 1756 under the title *Experiments upon Magnesia alba, Quick lime, and some other Alcaline substances*. Among other things, Black discovered that *magnesia alba* ($4MgCO_3 \cdot Mg(OH)_2 \cdot 4H_2O$) produced a gas during heating and transformed to *magnesia calcinata* (MgO). Black found out, that it was possible to obtain *magnesia calcinata* back to *magnesia alba* reacting *magnesia calcinata* with sodium or potassium carbonates. The gas released in the reaction was called 'fixed air' by Black, because it was fixed in solid form of magnesia. Black was thus the first person to realise the nature of CO_2 production and sequestration. (Marini 2007)

The concentration of atmospheric carbon dioxide has been monitored for over 50 years. Likewise, air bubbles trapped in ice core samples from the Antarctic can be used to estimate the variations of atmospheric CO_2 concentration during the last 400 000 years. In such a long time span there are always uncertainties, however, there is no doubt that the level of atmospheric CO_2 concentrations have started rising immediately after the industrial revolution and has continued rising since. It is assumed that the concentration of atmospheric CO_2 has risen to 385 ppm by volume from the preindustrial levels of 280 ppm, and annual increase is increasing by 2 ppm. (Brierley & Kingsford 2009). However, it is possible that the increase has induced to the atmospheric green house effect, thus leading to climate change. This could explain most of the 0.6°C on average temperature increase during the last century. The positive correlation between CO_2 level and temperature is presented in Figure 1. The climate change also has many serious consequences to global ecosystems, which can be seriously affected by phenomena such as drought, floods, dearth and stronger storms. Additionally, many animal and plant species are under threat of becoming extinct. (Marini 2007)

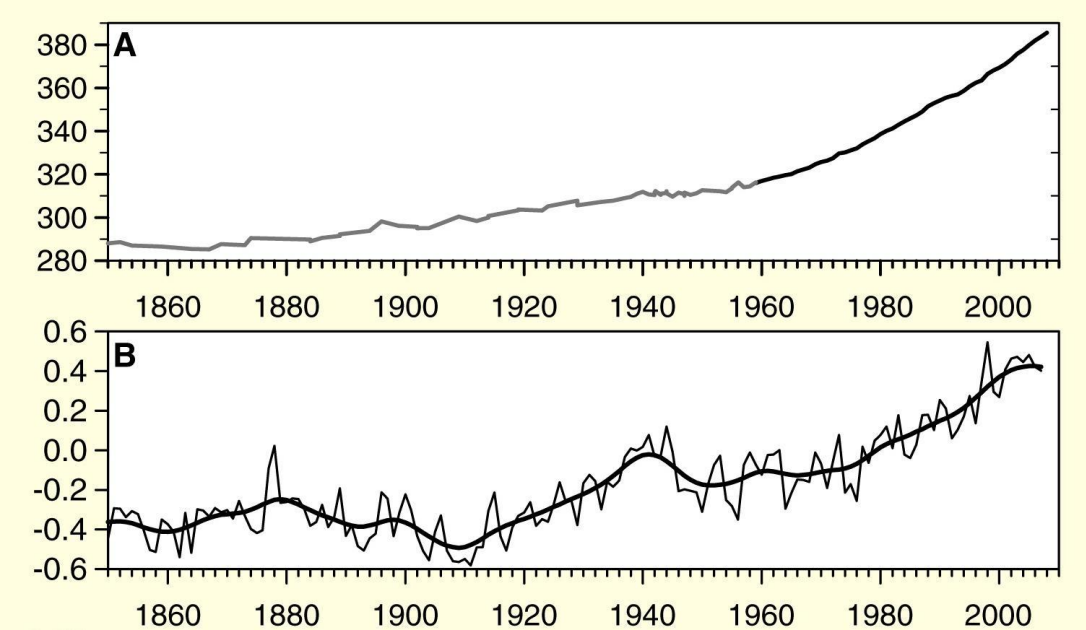

Figure 1. (A) CO_2 from Law Dome ice cores (grey line) and Mauna Loa direct observations from 1960 onwards. (B) Annual and smoothed combined global land and marine surface temperature anomaly. (Brierley & Kingsford 2009)

The increase in atmospheric carbon dioxide levels is connected to the burning of fossil fuels, i.e. coal, natural gas, and oil as well as to cement production. Carbon dioxide is classified the most important green house gas produced by human activities. Harvesting of forests, especially rain forest, has seriously hampered the ecosystem's capacity to store carbon dioxide. Only a small part of the produced CO_2 can be pumped back into the empty oil wells and natural gas mines. Injecting CO_2 into deep oceanic waters only temporarily reduces the atmospheric concentration, but it is not a sustainable solution for longer periods. Carbon dioxide has an ability to react with water, forming carbonic acid, H_2CO_3 (Equation 1). (Marini 2007)

$$CO_2 + H_2O \rightarrow H_2CO_3 \qquad (1)$$

Because the oceanic and atmospheric gas concentrations tend towards equilibrium, increase in atmospheric CO_2 concentration drives more CO_2 in to the oceans, causing oceanic acidification. The pH of the world's oceans has already dropped by 0.1 pH units as a result of the CO_2 uptake. Nevertheless, carbon dioxide emissions need to be

drastically decreased. Reduction of fossil fuel consumption does not seem probable in modern society, so something more needs to be done. One promising solution could be mineral sequestration, in which silica and calcium can precipitate minerals, which together with CO_2 are capable to react into carbonates. The mineral carbonation of calcium silicates yields a geologically permanent solution for CO_2 fixation. (Brierley & Kingsford 2009, Teir et al. 2006)

In this study, oil shale ash (OSA) from oil shale combustion was studied as a primary reactant to capture CO_2. Carbon dioxide emissions into environment from oil shale combustion are considerably high, because of the rock's carbonaceous composition. Oil shale consists of organic and mineral matters, which both form CO_2 upon combustion (Ots 2007). Despite the negative affect of CO_2 emissions, the global need for energy is growing rapidly. Therefore, it is very likely that oil shale will become an important source of energy in the future. All known non-renewable sources of energy will be utilised in a relatively short time period (within a couple of hundred years), so oil shale usage as a significant energy source is simply a matter of time. That is why the refinement of existing processes is important.

Another possible method for reduction of atmospheric carbon dioxide level is the use of bioenergies. Although, for example, combustion of biomass produces CO_2, this CO_2 is initially captured by living plants, and therefore, does not contribute to the release of anthropogenic CO_2 emissions. Bioenergy is considered as renewable energy and it is carbon dioxide neutral. The energy stored in biomass comes from the sun during photosynthesis, in which green plants utilise CO_2 and water yielding oxygen and energy-rich glucose. Therefore, all CO_2 formed in biomass combustion is modified from nature, and in combustion, it is then relieved back into the carbon cycle. (Lepistö 2005)

A significant element of the northern bioenergy sector is the pulp and paper industry. Bioenergy is produced in large scale simultaneously in the pulp industry when lignin in wood is combusted in a craft process. One significant waste product in pulp industry is green liquor sludge (GLS). The aim of this work is to form novel materials of GLS and OSA which could be used for CO_2 capture and storage in gas scrubbing or mineral carbonation. (Nurmesniemi et al. 2005)

2.1 Carbon dioxide and chemical properties

Carbon dioxide is usually considered as a gas, but in chemical compounds, it can be bound to form a solid structure, calcium carbonate for instance. Carbon dioxide constitutes only a small percentage of air, which generally consists of 79% nitrogen, 20% oxygen, and less than 0.05% CO_2. As a gas, carbon dioxide is colourless, odourless, non-flammable, has a slightly sour taste, and is heavier that air. Carbon dioxide is a gas at standard temperature and pressure. At the normal pressure of 1 bar, the melting point of solid carbon dioxide is -78°C. Carbon dioxide can be in liquid phase only above the pressure of 5.2 bar and the triple point of CO_2 is -56.6°C as shown in Figure 2. Carbon dioxide can change directly from solid phase to gas through sublimation. (Topham 1986)

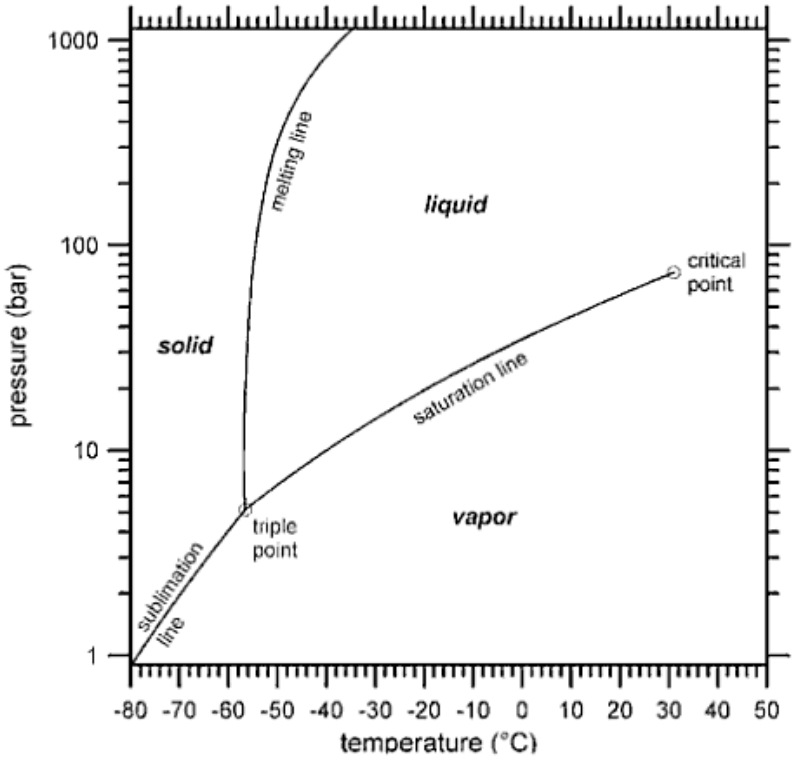

Figure 2. Carbon dioxide pressure-temperature phase diagram (Marini 2007).

At standard temperature, gaseous carbon dioxide is not particularly reactive. The carbon dioxide molecule consists of two oxygen atoms covalently bonded to a carbon atom. Due to the strong covalent bond, CO_2 is relatively stable and does not readily break down into simpler compounds. Reactions between carbon dioxide and other substances are

generally achieved only at high temperature and pressure or by the influence of a catalyst. (Topham 1986)

2.2 Flue gas purification

Biogas is generally produced via anaerobic digestion of natural renewable ingredients such as animal manure, sewage sludge, plant biomass, or other biodegradable feedstock. All these ingredients are rich in chemical energy from their high cellulose content. Biogas is formed when a member of the group of the *Archaea* digests carbohydrates (cellulose, starch, or sugars) under anaerobic conditions. *Archaea* are widely classified as their own group or the group can be classified as a submember of the group *Bacteria* (Schleifer 2009). One group of *Archaea* is called methanogens, because they produce methane as a metabolic by-product (Karakashev et al. 2005). In industrial scale biogas production, the digestion process can be made in anaerobic vessels or digesters, under mesophilic conditions. Mesophilic conditions mean that the temperatures can range between 25°C and 40°C. (Kelleher et al. 2002, Privalova 2010)

Biogas is a gaseous mixture of approximately 60% methane and 30% carbon dioxide. The CO_2 percentage in biogas can be as high as 40%. Biogas also contains a wide variety of trace elements and impurities such as hydrogen sulphide and other sulphur compounds, as well as siloxanes, which are aromatic and halogenated compounds. Equation 2 describes the anaerobic digestion process and its main components. Biogas has high heating value with chemical characteristics close to those of natural gas, therefore, biogas can be used as a substitute for natural gas. (Kelleher et al. 2002, Privalova 2010)

$$\text{Organic matter} + H_2O \rightarrow CH_4 + CO_2 + NH_3 + H_2S + \text{heat} + \text{digestate} \qquad (2)$$

Due to the high CO_2 content, biogas needs to be purified in order to be used in modern high technology solutions. Removal of carbon dioxide is important also, because of its ability to form carbonic acid in wet conditions, which can cause corrosion in pipelines. CO_2 can be separated and captured in many ways, but the problem lies in what to do with

the extracted CO_2. Instead of using real biogas as an adsorbate, in this study CO_2 physisorption is examined by using a gas mixture of 70% pure CO_2 and 30% nitrogen, due to equipment limitations. An important target for further examination would be to extend the study to scrubbing pure biogas stream, because as activated carbon materials, these activated materials may have low selectivity to carbon dioxide over methane. (Hitchon et al. 1999, Privalova 2010)

Biogas purification can be performed in many different ways. Most of the methods for biogas purification have been originated from flue gas purification. The composition of flue gas is somewhat similar to the composition of biogas with respect to carbon dioxide removal. Both of them have CO_2 as a major constituent and nitrogen and methane are unsolvable to the adsorbent. Industrial methods for CO_2 removal from flue gases include chemical absorption, scrubbing, adsorption, and membranes. Green liquor sludge could be used as a biogas adsorbent at integrated pulp and biogas plants and oil shale ash as a flue gas adsorbent in a similar manner. If green liquor sludge and oil shale ash are found to be promising materials for gas purification, they could be used for a number of applications, not only in biogas or oil shale combustion. (Privalova 2010)

Carbon dioxide capture is important for flue gas purification, therefore it is imperative to develop new and more advanced methods. Waste materials such as OSA and GLS have shown promising properties for CO_2 sequestration. Regardless, any carbon dioxide released into the atmosphere, whether it is from fossil or renewable fuels, can have negative effects on the natures balance.

3 CO_2 capture and storage methods

In industrial applications, carbon dioxide can be removed from gases, such as flue gas or biogas, using physisorption. In industrial physisorption processes, the gas mixture flows through adsorbent beds at elevated pressures and low temperatures until the adsorption of the desired constituent reaches equilibrium conditions at the bed exit. The beds can then be regenerated by stopping the flow of the feed mixture, by either reducing the pressure or by raising the temperature, and then flushing the adsorbed constituents with inert gas. Fresh gas mixture is once again flowed through the adsorbent beds, creating an adsorption cycle, which is repeated continuously. These kinds of processes are effective, well understood, and widely used in many industrial applications. It is crucial for the adsorbent to have a high capacity to adsorb CO_2 and to be easily regenerated. (Topham 1986, Meisen & Shuai 1997)

Once all the CO_2 is scrubbed from these gas mixtures, the principal question still remains, how to dispose of the collected CO_2. Today, the main storage methods are subsurface storage such as; saline aquifers, existing oil and gas fields, and unmineable coal seams. However, these methods do not offer solution for the growing need for CO_2 storage. Alternative options for captured CO_2 storage have been examined, but the research is still in early stages (Baines & Worden 2004). Emission trading is one alternative that has already begun possibly making CO_2 emissions even more expensive for industries in the future. Therefore it is important that alternative methods for binding CO_2 be discovered and marketed as soon as possible. (Topham 1986)

In carbon capture and storage, the compounds which bind the CO_2 must be both cost effective and readily available. The products have to stay stable for a long time. There is relatively no desorption in chemisorption, so the most stable long-term storage for CO_2 is the formation of carbonates. This carbonation process is termed “mineral carbonation”. In mineral carbonation, calcium oxide (CaO), for example, either reacts with captured CO_2 or reacts *in situ* with the CO_2 from biogas stream, forming calcium carbonate ($CaCO_3$). The end-products of the mineral carbonation process could be used at landfills or in road

foundations. The basic methods for CO_2 capture and storage are listed in this chapter. (Oelkers et al. 2008)

GLS and OSA are promising precursors, because both of them have a high calcium content. In addition to calcium, OSA also has a large silica content. Furthermore, since both OSA and GLS are waste materials, availability of them is enormous and prices low. The goal of the work is to study if green liquor sludge, or a mixture of the two, could be used as a low-cost material in CO_2 fixation applications and to add value for these waste materials.

3.1 Calcination chemistry

The process for lime burning is called “calcination”. For most people, designation of limestone and its products are not accurate and all these products are called lime. Scientific designation for burnt lime is calcium oxide (CaO), slaked calcium is calcium hydroxide ($Ca(OH)_2$) and limestone consists of calcium carbonate ($CaCO_3$). (Tegethoff et al. 2001)

Calcium carbonate is a simple silvery white coloured alkali metal carbonate that burns to calcium oxide and carbon dioxide when heated. Equation 3 describes how carbon dioxide can be released at the temperature of 842°C (Tegethoff et al. 2001). The melting point of pure calcium carbonate is 825°C.

$$CaCO_3 \rightarrow CaO + CO_2 \quad (3)$$

On the other hand, calcium carbonate can be formed from calcium oxide through reactions with carbonic acid (Equation 1). The production of calcium carbonate via reactions of calcium oxide and calcium hydroxide with carbonic acid, respectively, are shown in Equations 4 and 5. (Tegethoff et al. 2001)

$$CaO + H_2CO_3 \rightarrow CaCO_3 + H_2O \quad (4)$$

$$Ca(OH)_2 + H_2CO_3 \rightarrow CaCO_3 + 2H_2O \quad (5)$$

Calcium carbonate is very difficult to dissolve in pure water, but it reacts with water that is saturated with carbon dioxide to form soluble calcium bicarbonate, Equation 6. (Tegethoff et al. 2001)

$$CaCO_3 + CO_2 + H_2O \rightleftharpoons Ca(HCO_3)_2 \quad (6)$$

Like all carbonates, also calcium carbonate reacts with acids, like hydrochloric acid, to release carbon dioxide (Equation 7). However, according to Teir et al. (2006) carbonate formations can be stored underground for millions of years, which is geologically permanent CO_2 storage method. (Tegethoff et al. 2001, Teir et al. 2006)

$$2HCl_{(aq)} + CaCO_{3(s)} \rightarrow CaCl_{2(aq)} + CO_{2(g)} + H_2O_{(l)} \quad (7)$$

3.2 Scrubbing method

One of the oldest processes for carbon dioxide scrubbing are reactions with alkali-calcium. For example, the “sodasorb” process is a well known and old chemical process used in many fields of industry, especially in medical science. It is mainly used in anaesthesia machines and in gas masks. Chemical absorption of carbon dioxide occurs with alkali metal hydroxides; e.g., calcium hydroxide, sodium hydroxide, lithium hydroxide, and barium hydroxide. In oil shale ash reactions, carbon dioxide can be absorbed into calcium hydroxide where sodium hydroxide (NaOH) and potassium hydroxide (KOH) are alkaline catalysts. In this process presence of water is necessary to form calcium hydroxide from calcium oxide (Equation 8) and to initiate the absorption of CO_2 (Equation 9). Water is also a by-product in the reaction described in Equation 10. Finally, calcium carbonate is formed and the catalysts are regenerated, in Equation 11.

$$CaO + H_2O \rightarrow Ca(OH)_2 \quad (8)$$

$$CO_2 + H_2O \rightarrow H_2CO_3 \quad (9)$$

$$2H_2CO_3 + 2NaOH + 2KOH \rightarrow Na_2CO_3 + 4H_2O + K_2CO_3 \quad (10)$$

$$2Ca(OH)_2 + Na_2CO_3 + K_2CO_3 \rightarrow 2CaCO_3 + 2NaOH + 2KOH \quad (11)$$

Lack of moisture in the incoming gas stream or in the absorbent can prevent the initiation of the reaction. Excess moisture, on the other hand, can coat the surface and pores and cause a blockage which decreases adsorption efficiency. Excess moisture may also inhibit the water produced in the reaction from being carried away. The rate of reaction is dependent on temperature, but the temperature of the incoming gas may dry the absorbent and the initiation of the reaction may be inhibited or the absorbent bed may drain and limit further absorption. When a large amount of moisture is present, attention must be paid to measure absorption of carbon dioxide instead of water (Pinkerton 2000). (Nuckols et al. 1985)

Principal absorption material in the sodasorb process is calcium hydroxide, where NaOH and KOH are catalysts. NaOH is an efficient absorbent, but also other alkaline substances are possible. A large variety of alkaline matter could be used as alkaline. One possibility could be to use trace NaOH of green liquor sludge as a source of alkaline in mineral carbonation. (Nuckols et al. 1985)

Absorption capacity in the sodasorb process is proportional to the fluctuations in temperature. Cooler temperatures provide a better yield. However, water sets a physical limit for the temperature, since it needs to remain in liquid phase during this process. The reaction is exothermic, so sufficient heat transfer has to be calculated. (Nuckols et al. 1985)

3.3 Mineral carbonation

Mineral carbonation is a process where gaseous carbon dioxide reacts with a substrate to form a solid. A variety of raw materials can be used as this substrate for mineral carbonation, such as magnesium and calcium silicates. The substrate material has to have minerals that are able to be carbonated. The minerals suitable for mineral carbonation include alkaline earth metal oxide bearing compounds. The down side with these materials are that alkali metals can dissolve in water and metal oxides are too valuable to be carbonated, such as iron. Principal reactions are to turn silicate minerals into carbonates. The alkaline earth metal oxides, for example MgO or CaO, are turned into $MgCO_3$ or $CaCO_3$ minerals. Today, quite a few minerals as well as methods have been investigated for their use in mineral carbonation of CO_2. (Privalova et al. 2010, Teir et al. 2006)

Mineral carbonation is a promising process for capturing carbon dioxide, and the end product, calcium carbonate, is an inert and non-polluting substance. Since carbonate minerals have a lower energy state than their reactants, silicate and CO_2, at ambient conditions, they are thermodynamically stable. The carbonation reactions are generally exothermic and on an industrial scale, the energy formed in the reaction could be utilised in the processes. For these reasons, the sequestration of CO_2 through mineral carbonation is the process which focuses the largest international research efforts. (Touze et al. 2004)

Worldwide silicate mineral reserves have a potential storage capacity of 10 000 – 1 000 000 Gt of CO_2 storage for 50 000 – 1 000 000 years. Additionally, oil shale ash, for instance, has large quantities of calcium and silica, which have potential to mineral carbonation. (Teir et al. 2006, Reinik et al. 2007)

According to Touze et al. (2004), there are two main processes for mineral sequestration of CO_2, indirect and direct carbonation. The indirect method consists of two stages. The first stage involves the pre-treatment of the mineral with acid and the second stage involves the actual carbonation process. The direct process is a process in which the carbonation is achieved by direct contact between the minerals and CO_2 in a single process. According to Touze et al. (2004), the results of the direct method are promising, unlike those of the indirect method. (Touze et al. 2004, Privalova et al. 2010)

3.4 Other methods

The most common industrial process for CO_2 capture in the petroleum, natural gas, and chemical industries is chemical absorption. Chemical absorption is based on reactions between CO_2 and an aqueous solution of amine based absorbents, like monoethanolamine (MEA) and diethanolamine (DME). In these systems, more than half of the capture costs are created by energy requirements of adsorbent regeneration, and high corrosivity of the amines. In an attempt to avoid these problems, several new and more efficient amines have been developed, like N-methyldiethanolamine (MDEA), (Chowdhury et al. 2009, Meisen & Shuai 1997, Topham 1986)

In other conventional chemical removal methods, a group of alkali and alkaline earth metal hydroxides (calcium hydroxide, for example), peroxides, superoxides, and ozonides can react chemically with carbon dioxide and water, forming carbonates, bicarbonates, or hydrates. These chemical reactions produce minerals that are not easily soluble. Alternately, various metal oxides and organic amines can be regenerated. (Meisen & Shuai 1997, Nuckols et al. 1985)

Physical systems for removal of carbon dioxide include molecular sieves, membrane separation and cryogenic removal. Molecular sieves are formed by using zeolites where pellets are formed and CO_2 is adsorbed into pores. The problem is that while zeolites have a high affinity for CO_2, they have even higher affinity for water. Thus the gas needs to be dried before being introduced to zeolites. Semi permeable membranes can be used to diffuse CO_2 into water, but thin membranes are fragile and the surface area needed is large. However, membranes are still effective in smaller scale solutions and membrane technology is constantly under development. CO_2 can be cold distilled when lowering the temperature below the melting point of CO_2, -78°C (the melting point of methane is -183°C). The drawback for this method is that cold distillation is very energy consuming. The methods listed in this chapter do not offer storage for CO_2, and they are instead only capturing methods. (Meisen & Shuai 1997, Nuckols et al. 1985)

4 Adsorbent materials

Oil shale ash and green liquor sludge are both waste materials and problematic for industry, due to the large quantities formed and the hazardous trace elements such as high heavy metal content. This is why these materials are easily available and novel applications for their utilisation are examined in this study. Oil shale ash is formed when oil shale is combusted or turned into shale oil. Green liquor sludge is a waste fraction from pulp industry and it is currently disposed to landfills. (Nurmesniemi et al. 2005, Ots 2007)

4.1 Oil shale

Oil shale is a yellow-brownish sedimentary rock containing organic compounds that yield oil and combustible gas. Oil shale can also be combusted in power plants to produce electricity and heat. The organic and mineral composition of oil shale is very complicated and varies greatly depending on the area where the oil shale is mined. The main substances are carbonate minerals, like calcium carbonate. Oil shale is a carbonaceous fuel which contains a complicated composition of organic and mineral matter. (Ots 2007)

The most important advantage of oil shale is that there are numerous oil shale deposits all over the world, having been discovered on all continents. In 2006, total deposits of oil shale were estimated to be more than 409 billion tons of shale oil, which is equivalent to 2.8 trillion U.S barrels of shale oil. At the same time, existing resources of crude oil were estimated to be about 1 trillion barrels. When compared to crude oil resources, the oil shale resources are extensive. (Dyni 2006, Maugeri 2004)

4.1.1 Oil shale and oil economics

The world's crude oil consumption was assumed to be around 28 billion barrels a year in 2004. With current oil consumption, crude oil is predicted to be depleted in less than 40 years. The oil reserves probably will not run low in that time, but the level of use is predicted to lower rapidly. There are many predictions for future oil resources and consumption. The most widely accepted prediction is the Hubbert's Peak Oil Curve, which was published already in 1956 but is still approved. The Peak Oil Curve is presented in Figure 3. Peak oil is the point in time when the maximum rate of global petroleum extraction is reached, after which the rate of production enters terminal decline (Hubbert 1956). Timing of the peak is difficult to determine and it is hard to say when it will happen or if it has happened already. Optimistic estimations of peak production forecast that the decline will be in 2020, but more conservative predictions indicate that the peak has already started. (Aleklett et al. 2010, Hubbert 1956)

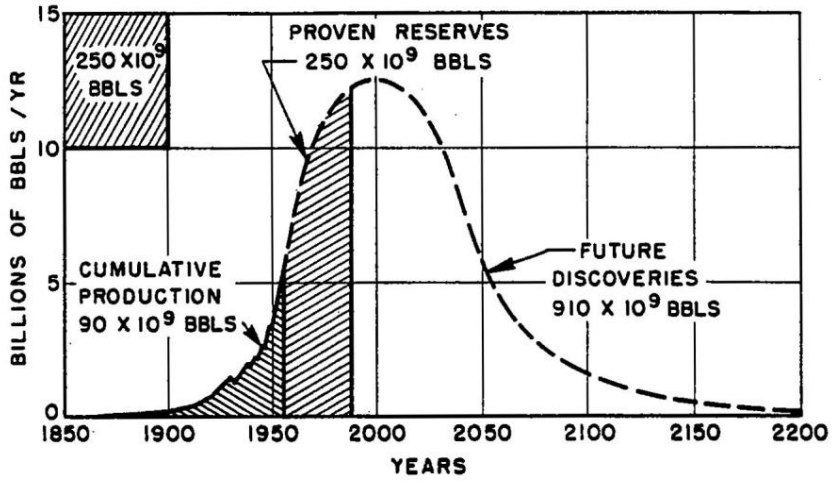

Figure 3. The Hubbert curve – Ultimate world crude oil production based upon initial reserves of 1250 billion barrels (Hubbert 1956).

It is also noteworthy that 35% of all proven reserves of crude oil are located in one place, at the Persian Gulf. Thus, the worldwide need of oil is tremendous while accessibility to the reserves is limited (Maugeri 2004). Shale oil production, however, has not been cost efficient compared to petroleum or natural gas so far. Existing crude oil and natural gas resources are running low, rapidly. So far the potential oil shale resources of the world

have barely been touched. This is why oil shale is expected to become a remarkable source of energy in the near future and the amount of oil shale ash will grow accordingly.

The price of crude oil is fluctuating and the price has risen from 20 USD per barrel to 90 USD per barrel in less than ten years. The highest barrel price so far was reached in 2008, which was 130 USD per barrel. In 2010, Reinik estimated that extracting shale oil is profitable when crude oil price is above 70 USD/bbl (Reinik, private communication 2010). It is very likely that crude oil price will increase significantly in the future.

Oil shale can be produced into gasoline, kerosene, diesel oil, wax, and lubricant oils. To produce one ton of shale oil, 33 tons of oil shale must be consumed. According to Qiang (2003), in 2001 in China the cost for producing 1 ton of shale oil was 1000 yuan RMB, which is equal to 22 USD per barrel. At the same time production costs per barrel of crude oil were only 6 USD. Shale oil production is more expensive compared to crude oil production, but is still notably lower than the retail price of crude oil. (Qiang et al. 2003)

According to these numbers, oil shale utilisation could currently be profitable. The largest drawback for the utilisation of oil shale is that oil shale combustion or oil extraction produces large amounts of ash. In Estonia, 6 million tons of oil shale ash is produced annually and the costs for the ash treatment are high. (Reinik 2010, Shawabkeh et al. 2004)

4.1.2 Estonian oil shale

Estonia, Brazil, China and The United States are the countries that utilise oil shale in their energy production. Production rates of oil shale from countries, for which data is available, are shown in Figure 4. World oil shale production peaked in 1980 when 47 million tons oil shale was mined, mostly in Estonia.

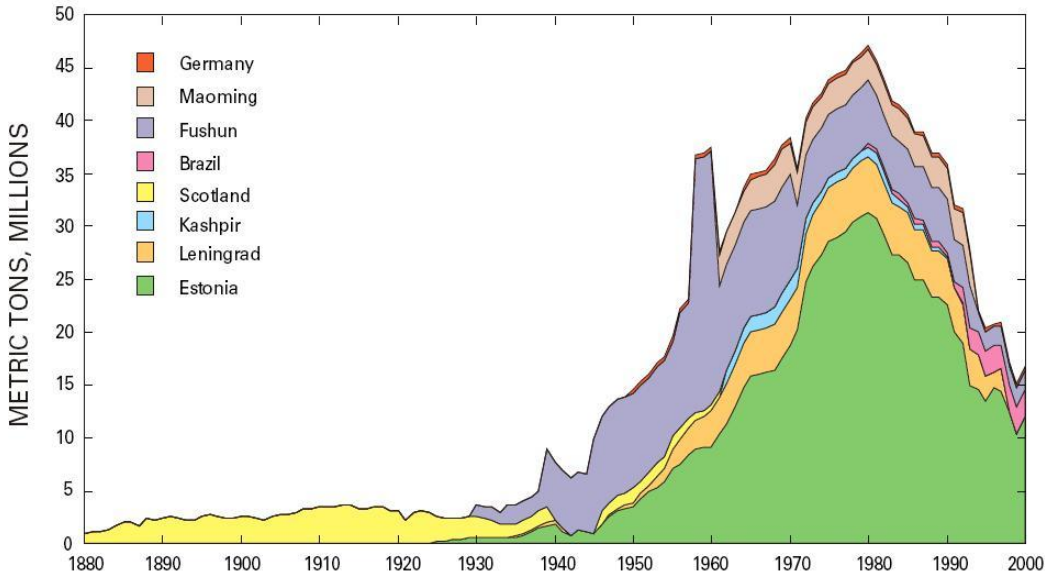

Figure 4. Production of oil shale in millions of metric tons globally from 1880 to 2000 (Dyni 2006).

Estonia is the only country in the world that generates most of its electricity by combusting oil shale. Compared to gasification or shale oil distillation (pyrolysis), combustion is inefficient, but an inexpensive way to turn oil shale into energy. There are still major problems in oil shale usage such as poor reliability in burning processes and the huge quantity of formed ash. The actual amount of heat released in combustion process is influenced by the behaviour of mineral matter and the combustion technology used. There are also several other disadvantages, e.g. sulphur emissions. Oil shale ash causes environmental problems and has high costs of deposal, which is why it is important to find a way to benefit from such a waste material in carbon dioxide sequestration. (Ots 2007, Smadi & Haddad 2003)

The main substance in Estonian oil shale is calcium carbonate. Dry matter of oil shale consists of three parts: organic, sandy-clay, and carbonate. The amount and composition of these parts differs due to the location where it has been mined. Elemental composition of the organic matter consists mainly of carbon, hydrogen and oxygen (Table 1). Among others, the organic matter contains also on average 1.8% of organic sulphur. An important characteristic of the organic matter is the high chlorine content. The mineral matter of oil shale is in two large groups: sandy-clay and carbonates (Ots 2007). The

chemical composition of the sandy-clay part contains SiO_2 (60%) and Al_2O_3 (16%), which are common rock forming minerals. The minerals of the carbonate matter are calcite ($CaCO_3$), dolomite ($CaMg(CO_3)_2$ and siderite ($FeCO_3$). (Ots 2007)

Table 1. Chemical composition of Estonian oil shale (Ots 2007).

Organic matter		Sandy-clay part		Carbonate part	
C	77.5	SiO_2	59.0	CaO	48.0
H	9.7	CaO	0.7	MgO	6.6
O	10.0	Al_2O_3	16.0	FeO	0.2
N	0.3	Fe_2O_3	2.8	CO_2	45.0
S	1.8	TiO_2	0.7		
Cl	0.8	MgO	0.4		
		Na_2O	0.8		
		K_2O	6.3		
		FeS_2	9.3		
		SO_3	0.5		
		H_2O	2.6		
Total	100.1	Total	99.1	Total	99.8

Oil shale composition can vary widely, so Table 1 presents only average composition of Estonian oil shale. The location of the sample mined may affect the composition. (Ots 2007)

4.1.3 Oil shale fly ash

Bituminous shale materials easily yield carbon dioxide when heated, so do oil shale ash. When oil shale is combusted, calcium carbonate reacts to calcium oxide and carbon dioxide. OSA has a very high contend of CaO (50%) and high contend of SiO_2 (22%) and Al_2O_3 (5%) by weight. It is very important to understand that the composition and properties in oil shale ash vary widely. Oymael (2007) has reported different oil shale ash composition all over the world, which are presented in Table 2. Fresh oil shale ash has a large concentration of calcium oxide. Calcium oxide has many promising abilities, for

example an ability to form into tobermorites with silica or to form carbonates with carbon dioxide in wet air conditions. (Smadi & Haddad 2003, Oymael 2007)

Table 2. Different mineral compositions of oil shale ash around the world (Oymael 2007).

OSA	Jordan	China	Germany	Colorado	Estonia CFB*	Estonian PF**
SiO_2	35.4	59.8	12-25	32.0	15.5	21.9
Al_2O_3	3.8	20.5	9-12	7.2	5.2	8.5
Fe_2O_3	2.0	9.9	6-7	2.7	2.9	
CaO	39.7	0.5	16-60	21.8	50.1	50.3
MgO	4.0	2.8	1.4-2.0	7.5	0.9	
SO_3	4.0		9-10		8.3	7.7
LOI***	7.3			20.0	13.1	3.0
Total	96.2	93.5		88.5	96.0	91.4

*Circulating fluidized bed boiler. **Pulverized firing. ***Loss on ignition

Oil shale contains many inorganic plant origin ingredients from the soil. When oil shale is combusted, non-combustible inorganic matter remains and forms ash. The quantity of ash in oil shale combustion is high, because of the large amount of inorganic matter in oil shale. When oil shale is combusted, the heavier fraction of the ash remains in the bottom of a grate and the lighter fraction flies away with flue gas and is collected in electrostatic precipitators. The physical structure of oil shale fly ash is that of a very fine powder. It contains, among other things, sulphur and heavy metals. In this work, the focus is only on Estonian oil shale fly ash, whether the word fly is mentioned or not. (Ots 2007)

Oil shale fly ash has an ability to react with and bind with gaseous sulphur compounds in flue gas. This phenomenon is known as sulfation. Sulfation diminishes SO_2 emissions, but at the same time sulphur is concentrated in ash. The finer the ash particle, the better is the binding with sulphur, due to the particle's increased surface area. The surface area allows the contact between sulphur oxides in flue gas and ash particle. (Ots 2007)

In Estonia, oil shale is combusted in two different burning process, using pulverized firing (PF) technology and circulating fluidized bed (CFB) principle. The operating temperature in PF is around 500°C higher than in CFB. According to Reinik et al. (2007), the physical structure of the resulting ash in CFB is coarser compared to the PF ash. The surface area (0.5 m^2/g) of PF ash is smaller than in CFB ash (6.9 m^2/g). The differences in combusting methods have significant affects to the physical properties of the ash. If the difference in combustion methods has significant consequences, then it makes it difficult to predict the behaviour of different ash samples in CCS. (Reinik et al 2007)

OSA used to be as a fertiliser in the Soviet Union, but due to its high content of heavy metals, the usage has since ended. Since the 1950s, the primary use of fly ash has been in concrete and cement manufacturing and road construction. (Reinik et al 2007)

4.2 Green liquor sludge

Green liquor sludge (GLS), also known as green liquor dregs, is the other interest in this study as a precursor material for carbon dioxide capture or to improve the properties of oil shale ash as a mixture of them.

Green liquor sludge is a remarkable residual product in the causticizing process, which is a part of chemical alkaline pulping process in forest industry. Causticizing is a process which produces white liquor from green liquor. The process is a part of the chemical recovery at a pulp mill, which is a vital process for closed chemical circulation. In chemical circulation, inorganic smelt from the recovery boiler is dissolved in water and the liquor is called green liquor because of its green colour. In the causticizing process,

white liquor, which is the active cooking chemical, is made of green liquor by clarifying it by removing non-soluble waste material. This non-soluble waste material is called green liquor sludge. The simplified flow chart of causticizing process is shown in Figure 5. The process is shown in Equation 12, where inactive sodium carbonate (Na_2CO_3) is converted into sodium hydroxide (NaOH), which is the active cooking chemical. (Nurmesniemi et al. 2005)

$$Na_2CO_3 + Ca(OH)_2 \rightarrow 2\ NaOH + CaCO_3 \quad (12)$$

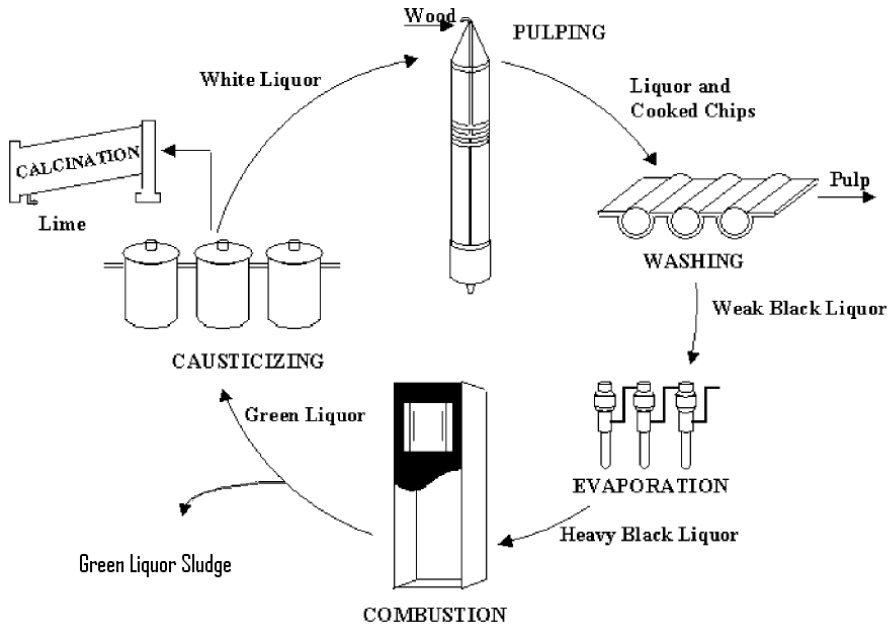

Figure 5. The formation of GLS in chemical recovery circuit (Nurmesniemi et al. 2005, modified).

The exact composition of green liquor sludge changes on a case-by-case basis, but on the whole, GLS contains large amounts of inorganic materials, like calcium, sodium, magnesium, and sulphur. The source of calcium is wood, which is the primary raw material in pulping and calcium is the most common element in wood. Sodium is present in many forms in chemical cooking and magnesium sulphate is used in oxygen delignification. Unfortunately calcium is mainly in the form of calcium carbonate, which is already the favoured end product in mineral carbonation. Green liquor sludge contains

a variety of trace metals. GLS has also traces of NaOH, so it is an alkaline mixture and could be used as a catalyst with OSA. Green liquor sludge contains quite a few different compounds, so activation of GLS and its adsorption abilities need to be studied. (Nurmesniemi et al. 2005)

Environmental legislation classifies the sludge as an industrial waste and the vast majority of the sludge is disposed in landfills. Because of the strict classification, other uses for the material are difficult to determine. Environment regulations have raised the costs of landfill disposal and landfill areas are often overcrowded. In Finland, only 10% of sludge is recycled in the pulp process and it is the biggest single waste fraction in pulp mills. Even one mid-sized pulp mill can produce more than 70 tons of green liquor sludge per year. In total, pulp industries in Finland produces about 100 000 tonnes of green liquor sludge per year. Therefore, a lot has been done to find new solutions for utilisation of the green liquor sludge. Unfortunately, so far not many economic uses have been found. (Nurmesniemi et al. 2005)

5 Hydrothermal activation

The term hydrothermal activation originates from geology, and describes the action of water at elevated temperature, which leads to high pressure. Hydrothermal activation mimics the action of hydrothermal fluids in the earth's crust leading to the formation of various rocks and minerals. Naturally minerals form underground over a long time period in the presence of water (hydro) at high temperature (thermal) and pressure. An understanding of the formation of minerals in nature led to the development of the hydrothermal technique in 1845, when quartz crystals were transformed from fresh silicic acid. The method became popular among geologists and the first commercial application of hydrothermal activation was in ore enrichment in the end of 19th century. The use of sodium hydroxide to leach bauxite was implemented in 1892 to convert pure aluminium hydroxide to Al_2O_3. Synthesis of zeolites was realised during late 1940s by Barrer. (Byrappa & Yoshimura 2001, Teir et al. 2007)

The term hydrothermal activation has not unanimity of its definition. The term refers to any heterogenous reaction in presence of aqueous solvents under high temperature and pressure to dissolve and re-crystallise materials that are insoluble in normal conditions. Byrappa & Yoshimura (2001) agrees with Morey and Niggli's definition about hydrothermal synthesis, and explains it as "...in hydrothermal method, the components are subjected to the action of water at temperatures generally near, though often considerably above the critical temperature of water (370°C) in closed bombs, and therefore, under the corresponding high pressures developed by such solutions". Today, the term is redefined to include milder conditions and there are no lower temperature or pressure limits defined. Pressure inside a closed bomb rises according to the boiling point of water. The temperature-pressure curve for water is presented in Figure 6. (Byrappa & Yoshimura 2001)

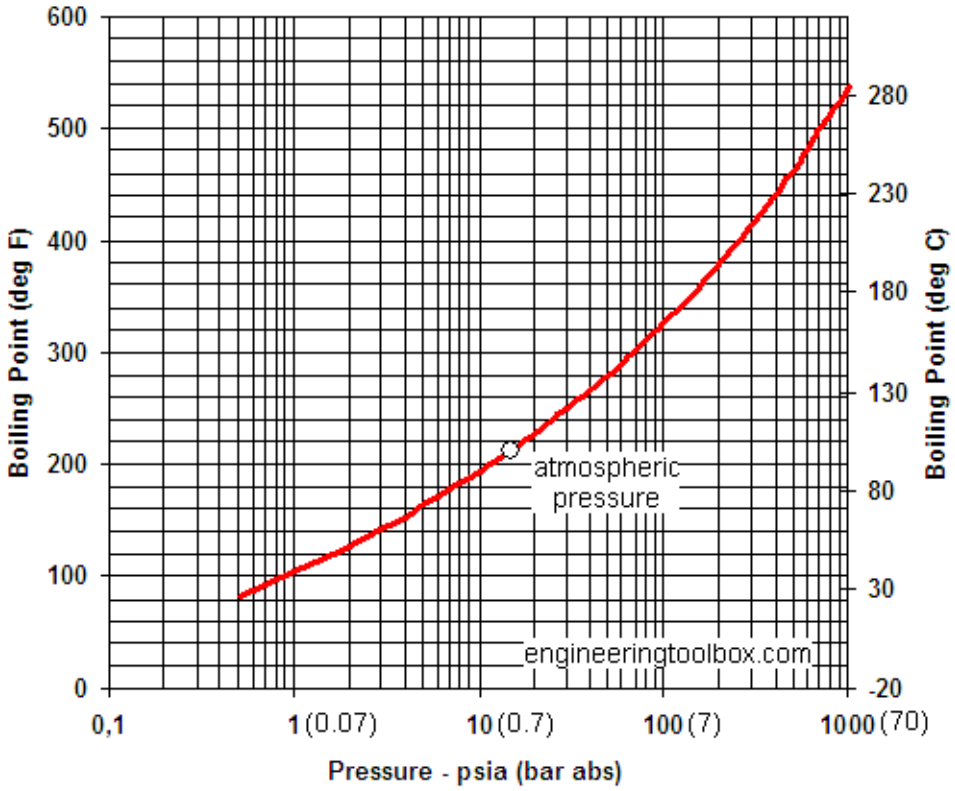

Figure 6. Water boiling point as a function of pressure (The Engineering Toolbox 2011).

5.1 Alkaline hydrothermal activation

Water is the most important solvent and it has been used as a solvent extensively in earlier experiments throughout history. However, several compounds are not soluble in water even at supercritical conditions. A variety of solvents have been researched, for example, many acid and alkaline solvents. Solubility can be increased by using aqueous alkaline solutions as the solvent. This process is called alkaline hydrothermal activation. Alkaline hydrothermal activation is a process where most often either potassium hydroxide (KOH) or sodium hydroxide (NaOH) is used as a solvent in aqueous solution. Byrappa & Yoshimura (2001) refers, that smaller Group I elements Li and Na exhibits a greater tendency for activation than K, Rb and Cs. (Byrappa & Yoshimura 2001, Shawabkeh et al. 2004)

In the early 80's, German scientists found out that coal ash could be turned into zeolites using alkaline hydrothermal activation processes. Coal fly ash and oil shale fly ash have very similar compositions, so using the same activation method, the waste oil shale ash may be converted into zeolite-like calcium silicate hydrate minerals or possibly to tobermorites and katoite. These new minerals are environmentally friendly and valuable products. Oil shale fly ash is not very reactive without the activation process. The activation process obtains higher surface areas and higher micropore volumes. At the same time, new minerals, as tobermorites and katoite are formed when calcium and silica reacts. (Reinik 2010)

5.2 Cation exchange reaction

Under hydrothermal activation the reactants, which would otherwise be difficult to dissolve, go into solution as complexes under the action of mineralisers or solvents. Alkaline hydrothermal activation follows a reaction called a cation exchange reaction, in which the calcium oxide (CaO) and silicon dioxide (SiO_2) and aluminium oxide (Al_2O_3) of the fly ash are dissolved into their ions Si^{4+}, Al^{3+}, Ca^{2+} and O^{2-}. Sodium hydroxide solvent is dissolved to Na^+ and $(OH)^-$ ions. The covalent bonds break and acid cations can be replaced with an alkaline $(OH)^-$ group or substituted with aluminium. Negative charge remains in the zeolite-like structure and the formed ion is replaced with new group which forms a new mineral structure. The exact reaction mechanism is not known and in real world situations, many different reactions occur at the same time. A sketch of the reaction is presented in Figure 7. (Byrappa & Yoshimura 2001)

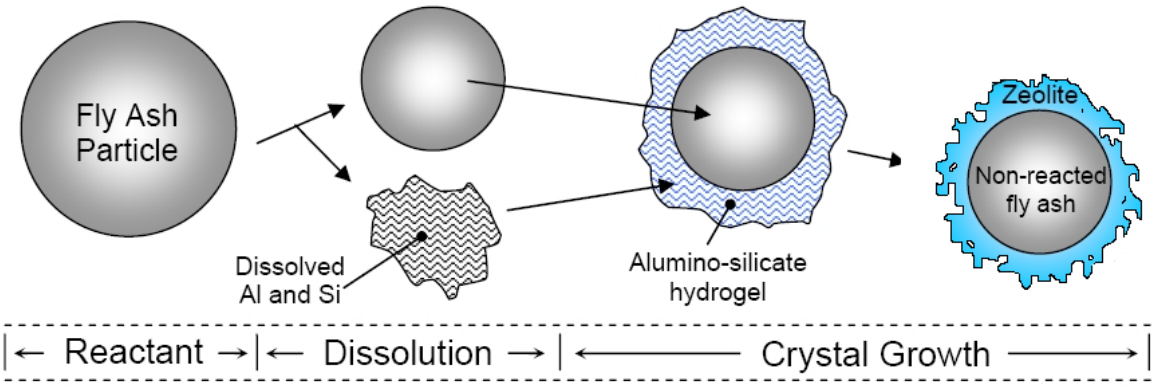

Figure 7. Sketched reaction mechanism for the hydrothermal conversion of fly ash to zeolite-like structures (Reinik, private communication in 2010).

Shawabkeh et al. (2004) expected that the activation reaction between the ash and sodium hydroxide solution was carried out in a two phase reaction (Equation 13), in which a hydrous aluminosilicate gel formats. This gel then carefully cures at high temperatures to obtain maximum crystal growth of minerals.

$$NaOH + ash \rightarrow Na_a(AlO_2)_b(SiO_2)_c \cdot NaOH \cdot H_2O \rightarrow Na_j(AlO_2)_j(SiO_2) \cdot 2H_2O \qquad (13)$$

The concentration of the solvent ensures that there are a sufficient number of molecules to react and raise the rate of the molecules to collide in the solution, which affect the reaction kinetics. Concentration also affects the reaction paths, offering various end products. The reaction can be a first or higher order reaction, in which the concentration of the solution has a significant importance. Laboratory scale experiments are generally performed in deionised water solutions, which are unlikely to represent the processes occurring in the complex fluids of natural systems, which contain numerous dissolved ions. These constituents have both significant rate-inhibiting and enhancing effects on reaction behaviour, even when they are present only in very small quantities.

5.3 Hydrothermal minerals

According to Reinik et al. (2007), Estonian oil shale has naturally an optimal Ca/Si ratio and silicon in the oil shale ash is possible to convert completely into calcium silicate hydrate minerals in alkaline hydrothermal activation process. The main product of the activation process is aluminium substituted 11Å tobermorite $Ca_5Si_5Al(OH)O_{17}*5H_2O$. The other calcium-silicate mineral formed in the activation is katoite ($Ca_3Al_2(SiO_4)_{1.5}(OH)_6$) (Reinik et al 2007, Krivovichev 2008)

5.3.1 Tobermorites

Tobermorites were firstly discovered in Tobermory area, on the Isle of Mull in Scotland in 1880. Today, tobermorites are mostly used as core binding materials in concrete and cement. Zeolites and tobermorites have similar properties and structures, and they are, in general, used in waste water treatment, nuclear waste treatment, and in heavy metal purification. Tobermorites could have advantages as being catalysts in chemical reactions. Novel applications to utilise tobermorites have been extensively investigated. Some promising solution for tobermorites use could be CO_2 capturing, in laundry detergents, and in lactose isomerisation. Tobermorites are naturally rare, layered calcium-silicate hydrate minerals which are readily synthesised from a variety of parental materials under hydrothermal conditions. (Coleman 2006)

The tobermorite group of hydrated calcium silicates includes a variety of minerals with different crystal structures and chemical compositions. The three main phases of tobermorites exist corresponding to their degree of hydration. The most hydrated form is 14Å tobermorite, the second hydrated is 11Å tobermorite and the least hydrated form is 9Å tobermorite. Nomenclature of the compound is related to the distance between the elementary layers in its crystal structure. The thickness of the layer in 14Å (Ångström) tobermorite is 1.40 nm. For 11Å and 9Å tobermorites the thicknesses of the elementary layers are 1.13 nm and 0.93 nm, respectively. The thickness of the layer is related to the water content in the structure. The layers are separated by water-rich sheets. 14Å tobermorite transforms to 11Å tobermorite by heating to 100°C; subsequent heating at

280°C for a few hours, drives off the water and gives rise to 9Å tobermorite. Finally, the heating above 880°C results in fully dehydrated phases. (Al-Wakeel et al. 2001, Krivovichev 2008)

Tobermorites have a unique and very complex crystal structure. The basic layer consists of a central sheet of CaO which is sandwiched by rows of $SiO_2(OH)_2$ tetrahedra. (Al-Wakeel et al. 2001, Tunega & Zaoui 2010) In nature, the crystal structure is often poor and disordered, but the orientation in synthetic tobermorites is typically good. The structure of 11Å tobermorite is shown in Figure 8. Cations and water molecules are located in various structural sites. Several different structures have been found for the same tobermorite. For example, there are at least three possible chemical structures for 11Å tobermorite, which are $Ca_4Si_6O_{15}(OH)_2 \cdot 5H_2O$ (found from Wessels mine in South Africa) and $Ca_{4.5}Si_6O_{16}(OH) \cdot 5H_2O$ (from the Urals). Al-Wakeel et al. (2001) present a structure of $Ca_5Si_6O_{16}$ $(OH)_2 \cdot 4H_2O$. For industrial applications, it is possible to produce synthetic tobermorites from various starting materials. One of the most widely used procedures to synthesise tobermorites has been the hydrothermal activation of pure CaO and quartz. New synthesis methods involve the replacements of pure CaO and quartz with various fly ashes. (Krivovichev 2008, Merlino et al. 2001)

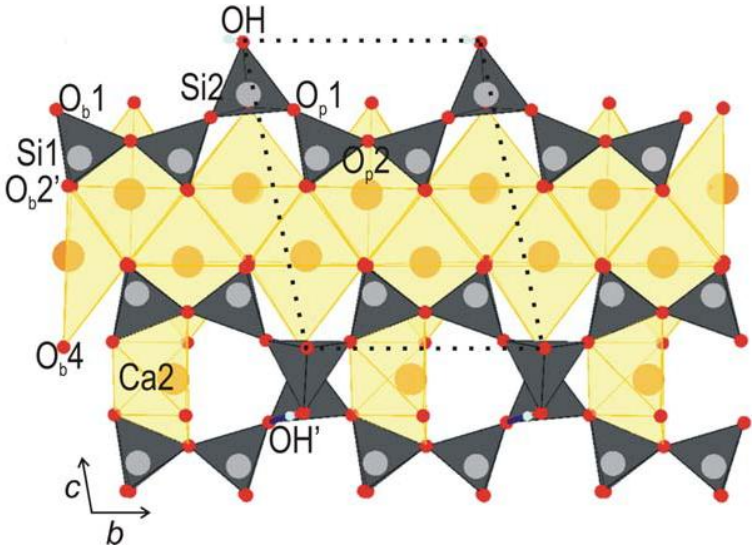

Figure 8. Structure of 11Å tobermorite. Silicon tetrahedra are in dark gray, Ca-polyhedra are in light yellow. Dotted lines represent structural unit cell. (Tunega & Zaoui 2010)

Hypothetical values for mineral sequestration have been calculated for a number of minerals, including the reactions between CO_2 and tobermorites. Touze et al. (2004) has listed possible reaction equations (Equations 14, 15 and 16) for tobermorite reactions with CO_2 beneath.

9Å tobermorite:

$$Ca_5Si_6H_6O_{20} + 5CO_2 \rightarrow 5CaCO_3 + 6SiO_2 + 3H_2O \quad (14)$$

11Å tobermorite:

$$Ca_5Si_6H_{11}O_{22.5} + 5CO_2 \rightarrow 5CaCO_3 + 6SiO_2 + 5.5H_2O \quad (15)$$

14Å tobermorite:

$$Ca_5Si_6H_{21}O_{27.5} + 5CO_2 \rightarrow 5CaCO_3 + 6SiO_2 + 10.5H_2O \quad (16)$$

The reactions above are calculated under standard temperature and pressure (25°C, 1 bar). The reactivity of tobermorites is also calculated at 150°C with pressures studied at standard pressure (1 bar) and 100 bar. Touze et al (2004) have pointed out that the pressure has more important role for reactivity than temperature. For example, in conditions of 150°C and 100 bar, reactivity of tobermorites is high, unlike at 150°C and 1 bar, where reactivity does not occur. Direct carbonation can be performed under many conditions, but yield is low and the kinetics can be very slow in low temperatures. The conclusion of Touze's report is that the carbonation process has potential, but it is unclear how or under which conditions it would be possible. (Touze et al. 2004)

Today, tobermorites are most often used in cement manufacturing. Other applications include adsorption agents for heavy metal removal and nuclear waste disposal. (Al-Wakeel et al 2001, Tunega & Zaoui 2010)

6 Adsorption

Adsorption is a phenomenon where molecules are accumulated on the surface of a material. More accurate definition for the word adsorption is enrichment of one or more components on an interfacial layer of porous solid, *adsorbent*. The adsorbed molecule (*adsorptive*) comes into a contact with the adsorbent material and when the molecule is attached on the adsorbent it is called *adsorbate*. When the adsorptive molecules penetrate into the surface layer and enter in the structure of the bulk solid, it is termed *absorption*. It is sometimes difficult to distinguish between adsorption and absorption, so it is then convenient to use the wider term *sorption* which covers both phenomena. (Sing et al.1985)

Early in the 20th century, studies of gases which were first adsorbed to a substrate and then removed by heating revealed that more gas was removed from the experiment than could be explained by physical adsorption alone. Oxygen gas removed from carbon substrate was found not to be pure oxygen, but to contain oxides of carbon. This suggested that two processes were involved in gas uptake on solids; physical and chemical adsorption. Adsorption mechanisms can therefore be divided into two fundamental groups. Chemical adsorption is simply referred to as chemisorption and physical adsorption as physisorption. Chemisorption is a process where the adsorbate and adsorbent have a chemical surface reaction between the gas atoms and the adsorption site with chemical bonds. These bonds can be either ionic, metallic, or covalent bonds. Due to the formation of these bonds, stability of chemisorption is very high. The reactants actually form a thin, one molecule deep layer of the new chemical compound. Chemisorption takes place only on accessible active sites, so to fully understand the chemisorption properties, the active specific surface area must be known. Physisorption is based on the physical blocking of atoms and gas bubbles inside holes, cracks and cavities of porous adsorbent. In physisorption, intermolecular forces are minimal. Forces to keep the adsorbate in place are weaker, mostly through van der Walls forces and the electronic structure is barely perturbed upon adsorption. (Webb & Orr 1997)

Desorption is converse to the process of adsorption. Desorption occurs when the adsorbate detaches from the adsorbent material. Desorption is generally present in physisorption (Sing et al. 1985). At some temperature the heat energy is greater than van der Waals force, causing the breakage of the bond and allowing desorption to occur. The sorption mechanisms of chemisorption and physisorption are presented in Figure 9. (Webb & Orr 1997)

Figure 9. Sorption mechanisms of chemisorption and physisorption.

Unlike chemisorption, physisorption is a common phenomenon and it occurs whenever an adsorptive is brought into contact with the surface of a solid material (adsorbent). Physisorption capacity is a function of both temperature and pressure. The colder the system, the larger the adsorptive load. This is why many fine particle measurements are made under liquid nitrogen temperature, -197°C. Pressure is the other notable factor. Adsorbate uptake is greater at high pressures. Adsorption is usually an exothermic process so energy is released in the process. The importance of temperature and pressure for adsorbate uptake is presented in Figure 10. (Beruto et al 1984, Webb & Orr 1997)

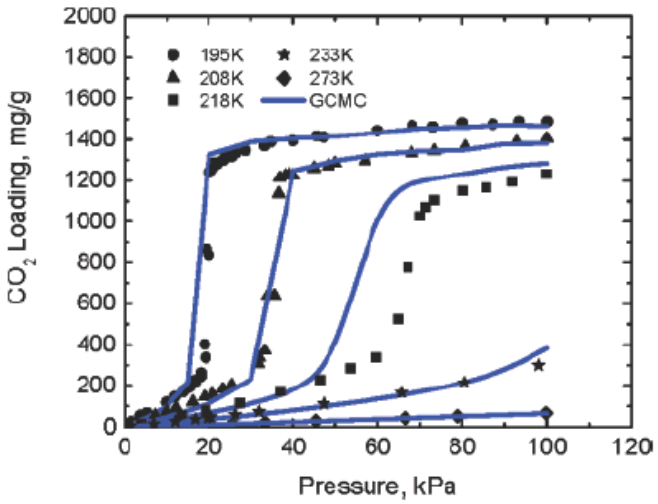

Figure 10. CO_2 physisorption as a function of pressure at different temperatures (Walton et al. 2008).

Contrary to physisorption, chemisorption favours higher temperatures. Reaction kinetics increase and the yield is greater at higher temperatures. Activation energy is the amount of energy that the reaction requires in order for the chemical reaction to occur. The activation energy for chemisorption is much higher than for physisorption. The activation energy for chemisorption is usually between 80 and 800 kJ/mole. If the heat of adsorption is less than 80 kJ/mole, the sorption is usually due to physisorption. Activation energy depends on the reaction itself, but in most cases it can be lowered with the use of catalyst. Chemisorption is commonly related, for example, to carbon dioxide fixation. Carbon dioxide fixation is a process where gaseous carbon dioxide is converted into a solid. (Beruto et al 1984, Webb & Orr 1997)

The interfacial layer of material can be divided in two regions: the surface layer of the adsorbent and the adsorption space in which enrichment of the adsorbate can occur. These two regions are called surface area and pore volume. (Webb & Orr 1997)

6.1 Surface area and pore volume

In adsorption, the mechanisms between adsorbate and adsorbent are all surface reactions. That is why the magnitude of the surface area and pore structure are the most important variable to determine. In many cases, it is important to understand the surface structure of a material. For instance, when comparing two absorbents together, quantity of the surface area is in almost as important as knowing which material it actually is. A relatively large proportion of the atoms of a fine powder are on or near the material surface. Small particle size and porosity of a material are essential for larger surface area. Cracks, cervices or pores in the powder's structure are necessary. The surface area in porous material can be hundreds of times larger compared to the surface area of a sleek material. For an adsorbent material, the specific surface area is usually between 100 and 3000 m^2/g. An absorbent with large surface area has a better ability to make connections and bindings. Additionally. the larger the surface area, the more molecules can be adsorbed on the surface. Surface molecules are bound on only one side to inner molecules, leaving bare atomic and molecular forces at the surface. The size distribution for natural materials is also wide. (Webb & Orr 1997)

The relationship between particle size and surface area is inverse, so the smaller the particle size the larger is the surface area. Definition of the word 'size' is not that easy as it seems at first, since most of the particles are irregular shaped. That is why equivalent size is commonly used. The equivalent size means, that the diameter of irregularly shaped particle is the same as that of a sphere, which will behave identically when both are exposed to the same process. (Webb & Orr 1997)

The volume of all cracks, fissures, holes, and chambers within the body of a particle or layer is the total pore volume. Process for measuring pore volume size and volume is similar to that for determining surface area. Pore volume is measured when several layers of gas molecules reach the infinite thickness and saturation vapour pressure. Gas adsorption measurements are widely used for determining the surface area and pore size distribution of a variety of different solid materials, such as industrial adsorbents. Nitrogen adsorption is the most used method for determining the surface area. (Webb & Orr 1997)

Small pore sized material needs higher gas pressure to fill all micro pores. Ravikovitch et al. (2000) have detailed in their research that CO_2 adsorption measured below 1 atm is not suitable for characterisation of carbon fibre because approximately 3/4 of pores would not be filled with CO_2 at atmospheric pressures, making high-pressure CO_2 experiments required for proper measurement. In general, the smaller the pore size, the higher pressure needed. Microporous material needs significantly higher pressures to fill all the pores. Pore sizes are classified in three sections, micropores, mesopores and macropores. Pores of widths less than 2 nm are called micropores. The second smallest pores are called mesopores when the pore width is between 2 nm and 50 nm. When the pore width is larger than 50 nm they are macropores. (Ravikovitch et al 2000, Webb & Orr 1997)

There are numerous modelling and simulation methods to characterise porosity, but reliability of the methods to characterise porosity in materials is weak. Development of reliable methods for characterisation of porous materials remains a problem, especially for materials with a wide range of pore sizes. The influence of neighbouring pores and pore geometries, i.e., random oriented crystallites, rectangular and square pores, also have affected the results. The range of material properties makes it difficult to predict the adsorption of gases, and the results depend on mathematical modelling. More sophisticated models of material structure are needed for a better understanding of the different factors involved. From a practical point of view, the simplest models have the advantage of being free from additional assumptions and parameters that are often difficult to justify. (Ravikovitch et al 2000)

6.2 Surface property measurements

The adsorption theory states that molecules, applied under increasing pressure, to a clean, cold surface form a layer one molecule deep monolayer on the surface, before beginning the second layer. Data treatment techniques find the quantity of gas forming this first layer and then the area is calculated from the number of molecules of the gas adsorbed and gas molecule dimensions. (Webb & Orr 1997)

Surface properties are measured generally with a sorptometer, which is a device for determining surface structure, specific surface area and porosity of a solid material. The measurement is based on nitrogen adsorption on the surface. That is why the process is often called BET N_2 process (BET refers to the BET theory, which is explained later). The amount of nitrogen molecules on the surface is calculated and the surface properties are defined. The measurement is usually made in nitrogen adsorption, but other gases, such as helium, are possible to use as well. (Webb & Orr 1997)

The first step in determining the surface area is to rid the sample of moisture and atmospheric vapours, this phase is called degasification. The degasification phase can be performed in vacuum or by evacuating with a non adsorbing gas, usually nitrogen. Nitrogen evacuation is done at high temperatures, usually over 100°C for a couple of hours. The second step is to weight the sample and lower the temperature of the sample to that of liquid nitrogen (temperature is -197°C) at normal pressure. The adsorbed gas is then injected onto the sample in small doses. The gas adsorbs on the surface and the accumulated gas quantity adsorbed versus gas pressure data at one temperature are then graphed to generate a curve that is called an adsorption isotherm. The adsorption isotherm is then treated in accordance with gas adsorption theories to arrive at a specific surface area (S_p) and pore structure. The unit for the value for specific surface area is given in square meters per gram (m^2/g). (Webb & Orr 1997)

6.3 Adsorption isotherm and adsorption theories

When the quantity of molecules adsorbed on the surface has been measured, sorptometer determines a curve called adsorption isotherm. The adsorption isotherm is a measurement of the molar quantity of gas uptake at constant temperature on clean solid surface as a function of gas pressure. Adsorption isotherms commonly follow one of the basic forms for isotherms, which are presented in Figure 11. The shape of the graph predicts the structure of the sample material via adsorption and desorption curves. (Webb & Orr 1997, Sing et al. 1985)

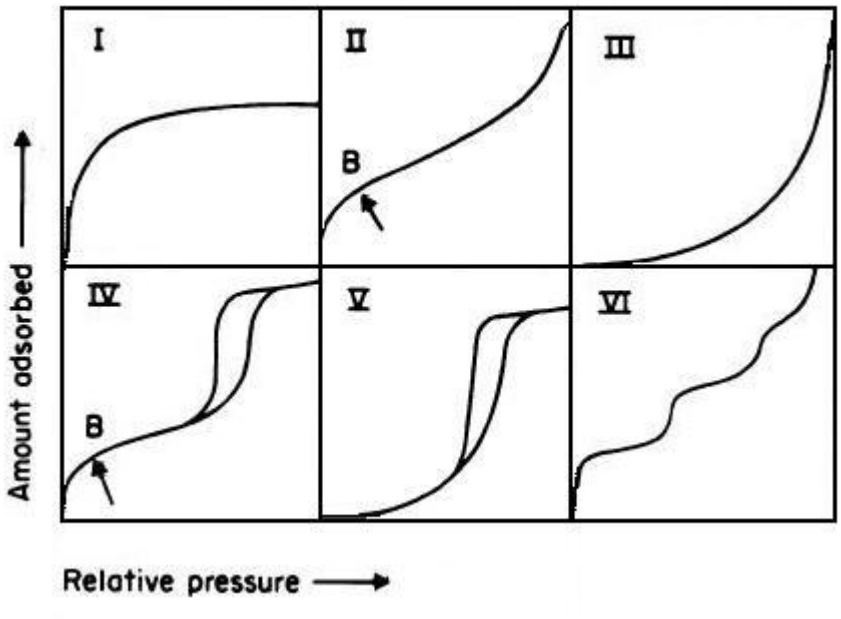

Figure 11. Adsorption isotherms for physisorption (Sing et al. 1985).

Type I adsorption isotherm presented in Figure 11 represents material with extremely small pores. Types II and IV indicates non-porous material or material with very large pores. Types III and V are valueless for surface and pore analysis, because the adsorbate molecules have greater affinity for each other than for the solid. Type VI indicates non-porous material with uniform surface. Only isotherm types I, II and IV are useful for surface area characterisation. (Sing et al. 1985)

When the adsorption isotherm is measured, the information about the surface characteristics of the sample material is extracted with some of the many adsorption theories. There are a variety of adsorption theories depending the surface structure of the material. Some of the theories are simple to use and some are suitable only for specific solutions. Today, all calculations are solved with computers, so even complex systems can be calculated quickly and accurately. The most common difference between utilisation of the methods is the pore size variation of the sample. In most cases, the surface area characteristics for microporous and mesoporous material are not possible to calculate with the same methods. Also some methods are more capable for determining the pore volume than the others. The two most commonly used methods in literature are BET theory and Dubinin's analysis for mesoporous and microporous material,

respectively. These two and some other useful methods are explained by Webb & Orr (1997) and Sing et al. (1985). (Webb & Orr 1997, Sing et al. 1985)

6.3.1 Langmuir theory

The oldest adsorption theory is the Langmuir theory, which was developed to achieve the maximum effectiveness for CO_2 adsorption for activated carbon in gas masks. Langmuir theory is adequate for chemisorptions, because its first assumption is that gas form only one molecular layer on a solid surface and the gas molecule remains in contact with the solid for a time before released to the gas phase. Adsorption is derived from the delay. Langmuir theory is still useful for both chemisorption and physisorption. (Webb & Orr 1997)

6.3.2 BET theory

The Brunauer-Emmett-Teller (BET) gas adsorption theory is the most commonly used adsorption theory. The theory is usually used to determine the surface area and pore volume of a solid porous material. The theory can predict multilayer adsorption, by calculating the rate of adsorption and evaporation of gas molecules on an already adsorbed layer, therefore, it is convenient for adsorption to mesoporous materials. The theory is rather simple and it is easy to use. The BET equation in the linear form is:

$$\frac{P}{V_a(P_0-P)} = \frac{1}{V_m C} + \frac{C-1}{V_m C}\left(\frac{P}{P_0}\right) \qquad (17)$$

where V_a is the quantity of gas adsorbed at pressure P

P is the gas pressure

P_0 is the saturation pressure of the gas

V_m is the quantity of monolayer capacity

C is the related exponentially to the enthalpy of adsorption in the first adsorbed layer. (Webb & Orr 1997)

BET theory determines a variable, which is known as C-value. In the literature it is said that the C-value should be between 0 and 300. If the value is either bigger or smaller the results of the method are not trustful. Negative C-value is a sign of microporous material, and it is not possible to define accurately with BET theory. (Webb & Orr 1997 p. 143)

The biggest shortcoming in BET theory is that the theory assumes uniform surface coverage with no favoured adsorption sites and it assumes that gas is strongly attracted to the surface than to other gas molecules. The second problem is that the theory is not very accurate when microporous material is present. However, the theory is the most commonly used method among all adsorption methods in the literature.

6.3.3 t-Plot theory

The t-Plot theory is one of the standard isotherm theories, where t stands for thickness of molecules adsorbed. Every adsorbate-adsorbent system yields a unique adsorption isotherm curve, but a variety of materials with different total surface area have otherwise alike isotherm curves of similar shape when analysed with the same adsorbate at the same temperature. These isotherms can be superimposed simply by normalising the vertical scale. The theory predicts the surface characteristics by standardising the isotherms semi-quantitatively. In other words, the theory calculates the microporous area from reference adsorption isotherms. (Webb & Orr 1997)

6.3.4 Dubinin's theory

Phenomenological models of adsorption based on Dubinin's theory of volume filling of microporous material have found a great utility in describing adsorption equilibrium of various gases and vapours. The Dubinin-Radushkevich, Dubinin-Astakhov, and Dubinin-Stoeckli equations have become widely accepted practical methods for calculating the micropore volume, characteristic energy of adsorption, and distribution of micropore

sizes. The latter involves postulated forms of the adsorption energy distribution and empirical correlations between the adsorption energy and the pore size. (Ravikovitch et al 2000)

Dubinin theory differs from the other methods, since instead of measuring a load of molecules on the pore wall, the theory measures single pores only a little wider than the nitrogen molecule itself. Dubinin theory needs information of pore filling and evacuation in micropores, which are not possible to determine with all types of sorptometers that does not generate high enough vacuum. (Ravikovitch et al. 2000, Webb & Orr 1997)

6.3.5 BJH method

The method is named after its developers Barrett, Joyner and Halenda. The BJH method is a method for calculating pore size distributions for mesoporous material. Mesopores are commonly defined as materials having pore widths between 2 nm and 50 nm, but the method is usable for a little wider variation. In this work, variation between 1.7 nm and 300 nm is calculated. The method is based on Kelvin equation, which is usually written as: (Webb & Orr 1997)

$$ln\left(\frac{P^*}{P_0}\right)=\left(\frac{2\gamma v\cos\theta}{RTr_m}\right) \quad (18)$$

where P* is the critical condensation pressure,
γ the liquid surface tension,
v the molar volume of the condensed adsorbate,
θ the contact angle between the solid and condensed phase,
r_m the mean radius of curvature meniscus,
P^*/P_0 the relative pressure,
R the gas constant,
T the temperature.

Kelvin method measures emptying of condensed adsorbate in the pores in stepwise manners as the relative pressure decreases. Barrett, Joyner and Halenda set the limit of conditions, when all pores are considered to be fulfilled. The limit is set to be the relative pressure of 99.5%. (Webb & Orr 1997)

Experimental part

7 Experimental procedures and set-up

In this work, two kinds of fly ashes and green liquor sludge were studied as CO_2 capture and storage materials. One of the ash materials studied in this work is called “old ash”, which was collected in 2004 and the second ash is called “new ash”, collected in 2010. The ash samples were collected from the same combustor, but the time between the sampling was six years. Old ash was collected from the 1^{st} and new ash from the 4^{th} electrostatic precipitator of the gas flow duct of Estonian power plant (Narva Power Plants Ltd). The boiler of the plant operates on the principle of circulating fluidized bed (CFB) technology. The location of the oil shale mined may have changed during the time, which also means that the compositions of the raw materials are different. The colour of new ash, for instance, was slightly pink after the activation process when old ash remained sandy gray. The colour difference was probably caused by a high content of iron or some other trace metal. Green liquor sludge was studied as an individual compound and also a mixture with OSA for CO_2 capture. All precursors in this work were as very fine dry powders.

The goal of the work was to determine how these low cost materials could be utilised in carbon dioxide capture and storage. For that purpose, in the experimental part of the work, reactivity of oil shale ash in carbon dioxide storage was evaluated and the actual CO_2 physisorption capacities of green liquor sludge, fresh oil shale ashes, activated oil shale ash and an optimal mixture of all previous materials were measured. The work was divided into two phases. The first phase was chemisorption and the second phase studied was physisorption. The precursors are naturally not very reactive, so they were hydrothermally activated before each process.

In the activation process, the precursors were activated using alkaline hydrothermal activation with aqueous sodium hydroxide solution under high temperatures and pressures. The purpose of the activation was to generate hydrothermal minerals, specifically tobermorites. These hydrothermal minerals were used as a base for later reactions in chemisorption or to raise specific surface area and porosity of a material for physisorption.

In the first phase of the project, chemisorption was carried out with the direct method, where dry activated ash was reacted with carbon dioxide above the critical point of CO_2 under high pressure and temperature. Chemisorption was studied to examine whether carbon dioxide reacts with the hydrothermal minerals, forming calcium carbonate as the main end product. The reaction mechanism and conditions of the experiment were modelled according to those of Touze et al. (2004).

The second phase studied in the project was physisorption, which means that carbon dioxide molecules are attached on the surface of the particles and are removed in desorption phase. If the material has presumptions for CO_2 physisorption, it could be used, for example, in gas purification.

Dr. Janek Reinik from the National Institute of Chemical Physics and Biophysics in Estonia has studied Estonian oil shale ash and its utilisation as a parental material for novel applications (Reinik et al. 2007, 2008, 2010). Reinik has produced a set of activated oil shale ash samples, which have been used as reference materials in this work. Valuable information about the reaction conditions was studied with the same activated ash. Also, preliminary tests for physisorption were conducted in co-operation with Reinik.

Water is present in numerous calcination reactions, but in this work, the effect of water was not taken into consideration in either of chemisorption or physisorption studies. The main reason to exclude water in this work was that the tobermorite reaction (Equation 15) was evaluated as the primary reaction and water is not present in that reaction. The presence of water would have made this work significantly more broad, while approach is more in the use of the waste materials. To minimise the effect of water, all samples were dried and degassed before and after each chemisorption and physisorption experiments. This was done also to get rid of the moisture before weighting the samples to guarantee similar conditions.

Reaction kinetics, mechanisms, rate, liquid-solid ratio, temperatures, pressures, and yields were the factors which were in the focus. There were many uncertainties about these factors, and all the factors were not studied, but some answers were expected.

7.1 Sorptometer measurements

The primary machinery used to determine the surface area and porosity was a sorptometer. Sorptometer analysis is a good method to gather information on surface structure and surface characteristics. In this work, the sorptometer has been used for several analyses during the experiments. All oil shale ash and green liquor sludge samples were analysed before and after each experimental step. Surface analyses were made of the reference samples as well. Surface analysis can reveal whether the activation process is not successful, or when comparing different activations in similar conditions. Sorptometer analyses were also used to find the best reaction conditions in chemisorption or the most suitable candidates for physisorption.

The surface structures were determined using various adsorption theories; BET surface area, t-plot microporous area, BJH surface area, and BJH pore diameter methods. The materials studied had microporous characteristics. Unfortunately, Dubinin's theory for microporous surface was not possible to use, since the sorptometer used in this work was not able to measure microporous area due to a lack of high vacuum pressure. Therefore the microporous area values presented in this work are only estimations.

The model of the sorptometer used in this work was a Micromeritics Tristar 3000 and was equipped with automatic degasser. The equipment was capable of measuring three samples at a time. The adsorptive gas was nitrogen and the measurements were performed in liquid nitrogen bath. The sorptometer was fully automated, so the operator only needed to measure a sufficient amount of sample material in a glass tube, mount the tube into the equipment and fill up the nitrogen thermo bath and define the setting for the computer and the computer performed all calculations.

In Figure 11, adsorption isotherms were defined by their shape. Only type I, II and IV adsorption isotherms were possible for surface analysis. In Figure 12, an example adsorption isotherm of an activated oil shale ash sample is presented, but the shapes of the other samples were almost identical. The shape of the figure shows that the material has either no pores or the pores are relatively large. Knowing the surface structure is in important role in this work, despite the margin of errors for the surface areas and porosities are not known. For example, BET C-values were outside the suggested range

of 0 and 300 for most of the samples. However, the values measured seem reasonable and fit the similar values presented in the literature.

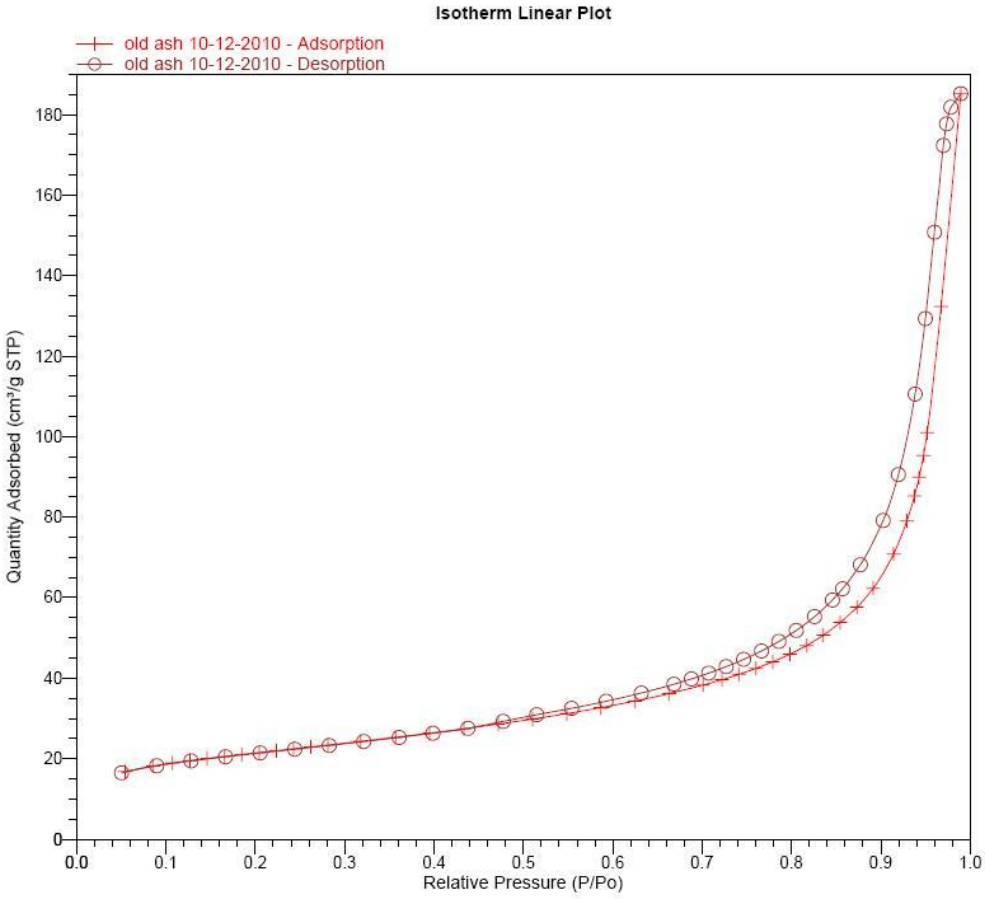

Figure 12. Adsorption isotherm of 4M140 activated old ash sample

7.2 Hydrothermal activation process

All activations presented in this work were performed by implementing similar activation processes. The variables of the processes were activator concentration, temperature, and time. Reaction conditions were alternated to find the critical limits and the best conditions for the activation reaction. In the literature, the same kinds of ash activations are examined under different temperatures and concentrations. Sodium hydroxide solutions with concentrations between 1M and 10M and temperatures from room temperature up to 160°C and time from 5 hours to 28 days are reported. (Al-Wakeel et al. 2001, Puertas et al. 2000, Reinik et al. 2007, 2008, Shawabkeh et al. 2004). According to Shawabkeh et al. (2004), an increase in activation time from 5 to 24 h does not have significant effect on the rate of activation in alkaline activation processes, so the 5 h reaction is considered an optimal time from an economical point of view. In nature, the same reaction would take hundreds of thousands years. In this work, the raw materials were activated in NaOH solution for 24 hours and in constant temperature. (Shawabkeh et al. 2004)

In the first step of the hydrothermal activation process, the reference samples were analysed with sorptometer to find the possible range of temperatures and concentrations. The best conditions were assumed to be the conditions in which the ash had gained the largest specific surface area and microporous area. This was based on an assumption that calcium silicate minerals have naturally high specific surface areas, and the sample with the best surface characteristics had developed the most minerals, hopefully tobermorites.

Sorptometer analyses of the reference samples showed that the concentration of 1 M was too low to gain specific surface area growth. Specific surface area and microporous areas are listed on Table 3. Sample 8M130had the highest surface area, but X-ray diffraction analysis performed earlier showed that the sample contained a mineral other than tobermorites (Reinik, private communication in 2010). That was why 4 M and 5 M NaOH solutions were selected for the further hydrothermal activations. The reference samples were produced at 130°C and 160°C. In this work, activation temperatures were 130°C and 145°C, due to material limitations of the reactor vessel. (Puertas et al. 2000)

Table 3. Surface properties of Reinik's samples.

Sample name	BET-surface area [m^2/g]	t-Plot Micro area [m^2/g]	t-Plot External area [m^2/g]	BJH surface area [m^2/g]	BJH average pore diameter [nm]	BET C-value
Old ash	7.1	0.6	6.5	8.4	18.1	160
1M130	37.5	4.6	32.9	38.3	14.9	236
1M160	57.9	11.2	46.6	58.8	16.0	990
3M130	58.7	13.6	45.0	57.8	18.2	-1483
3M160	49.9	11.2	38.7	49.2	15.9	-6424
5M130	60.7	13.6	47.2	60.5	17.8	-2779
5M160	46.5	10.4	36.2	45.2	22.1	-6203
8M130	70.1	18.1	52.0	67.1	21.4	-636
8M160	58.5	141.1	44.4	56.2	16.6	-1243

The activations were initially meant to be run in 100ml VWR borosilicate glass 3.3 flasks, inside a temperature controlled Parr 4841 pressure reactor, shown in Figure 13. The reactor is a rocking-type reactor used to guarantee continuous homogenous stirring in the reactor bomb. The bomb was pressure proof to insure a desired temperature in the water solutions. The pressure of water at its boiling point at temperature of 150°C is around 6 bar. The curve of the boiling point as a function of pressure was showed earlier in Figure 6 in Chapter 5. The temperature was measured from the bottom of the bomb with a thermo sensor, but the exact temperature inside the bomb is not known. A small amount of water was added inside the bomb to generate equal pressure inside the bomb and the reactor vessels. Three samples were prepared in the reactor bomb at once and quantity of a sample was approximately 12 g of activated material.

Figure 13. On the left the bomb and three samples opened. On the right, Parr pressure reactor 4841 assembled.

Early in the activation process, corrosion in the borosilicate glass bottles was detected. Borosilicate glass is not resistant to temperatures over 100°C in highly alkaline conditions. 5 M NaOH solution and 150°C temperature are strong enough to corrode the flask. Corrosion was noticed when comparing weights of new and used flasks. The difference in the total weights was as great as 25 g, which was more than double compared to the weight of a sample (12 g). Borosilicate glass has silica and boric oxide as the main constituents. Silica is also the other main compound in oil shale ash. Silica in the glass likely dissolves in sodium hydroxide solutions as following: (Molchanov & Prikhidko 1956)

$$SiO_2 + 2NaOH \rightarrow SiO_3 + 2Na + H_2O \quad (19)$$

New reactor vessel materials were searched and quartz glass and Teflon® were selected to be the most promising materials. Availability of Teflon® vials made it the new vessel for further experiments. The Teflon® vials chosen were 150 ml VWR bottles with

Teflon® lids. The manufacturer ensured that the vials are durable up to 200°C and are highly chemical resistant.

The activation process was conducted by adding 12 grams of raw material (oil shale ash or green liquor sludge) in the Teflon® vial and an appropriate amount of sodium hydroxide pellets (Chempure®). Distilled water was added, depending the desired molarity of the solution. Molarity is the number of moles of solute dissolved in one litre of solution. The formula for calculating the amount of NaOH needed in the solution is presented in Equation 20.

$$m = \frac{c\, M_{NaOH}\, V_S}{V} \tag{20}$$

where m is the mass of NaOH,
c the desired concentration,
M_c the molar mass of NaOH,
V_S the total volume of the solution [ml]
V the volume of the mixture [ml].

The Teflon® lids were then closed and the vials were shaken well. The third step was to insert all three vials into the bomb. Water was added in the bomb to ensure back pressure, which prevented the Teflon® vials from breaking. The bomb lid was closed and sealed with a copper ring, and stainless steel bolts were tightened into a right moment. The thermo cable was connected and the bomb mounted in the reactor. The temperature was set to 105°C, slightly over the boiling point of water in atmospheric pressure, and heating and stirring were started. The heat was kept in 105°C for an hour to ensure proper heat exchange between the bomb and the solution inside the Teflon® vials. After that the temperature rose to 130°C and another hour was waited before the temperature had risen to the desired activation temperature.

After the 24 hour treatment, heating was turned off and the reactor was slowly cooled down to room temperature. The bomb was disassembled and the Teflon® vials were emptied and rinsed through a filter paper. Filtration proved to be a bad method for rinsing

the sample because a lot of the finest material stayed in the filtration paper. A better method could be a centrifugal method. The samples were cleaned of sodium hydroxide when pH of the sample was seven. The pH was determined using indicator paper. The cleaned sample was dried in an oven for 24 hours in 105°C and finally ground in a mortar.

Naming of the activated samples follows a simple system, where the first letter represents the concentration and the second stands for the activation temperature. For example, 5M145 means that the sample was activated in 5 M sodium hydroxide solution and in 145°C temperature. Higher than 145°C temperature were not possible to use using fragile Teflon® vials in Parr Reactor bomb. Early during the experiments, one of the Teflon® vials were broken, because the pressure rose too high, when the activation temperature was 150°C.

11Å tobermorite was the mineral expected in the activation process. As was mentioned earlier, 14Å tobermorite transforms to 11Å tobermorite in the temperature of 110°C. The lowest activation temperature used in this study was 130°C, therefore the presence of 14Å tobermorite was not expected. Other mineral expected to be formed in the activation process was katoite. Depending of the nature and elemental composition of the raw materials activated, different reactions can take place and minerals formed can have diverse microstructures.

7.2.1 Green liquor sludge activation

Green liquor sludge was activated in three samples to be used mostly in physisorption. The first sample activated was pure GLS, the second with 50:50 mixture of GLS and OSA and the third with 70:30 wt.-% of GLS and OSA, respectively. The activation processes for the samples containing GLS were performed in a similar way to the oil shale ash activation. The GLS activations were all performed in 4 M sodium hydroxide solution in 130°C temperature for 24 hours.

7.3 Chemisorption

According to Touze et al. (2004), mineral carbonation of CO_2 onto tobermorites could be made under high pressure and in elevated temperature. Tobermorites should be reactive in arbitrary conditions in 150°C and 100 bar. All the experiments for studying chemisorption in this work were carried out in the same conditions.

Chemisorption experiments were conducted in a Parr 4848 pressure reactor. The reactor was connected to an AGA CO_2 gas bottle. The reactor setup is presented in Figure 14. The maximum pressure of the gas reached at room temperature was the vapour pressure of liquid CO_2. At room temperature, the vapour pressure of CO_2 is around 57 bar. According to the ideal gas law, the pressure inside the closed reactor increase when heated. At 150°C, the calculated pressure of CO_2 is around 100 bar, which proved to be the same as in real experiments. There was no compressor used in the reactor, but the reactor was equipped with cooling, so higher pressures could have been possible to reach, but the gas would have transformed into liquid phase. Reactivity of supercritical CO_2 was studied in this work, so the CO_2 liquefaction was not desired.

Figure 14. On the left, Parr pressure reactor 4848 and its controller unit. On the right, ash sample in the glass vessel in Mettler electronic balance.

Chemisorptions were carried out in a glass vessel, which is shown in Figure 14. The first step was to weight the vessel and the activated ash dose with Mettler 168 analytical balance. After the weighting, the vessel was put into a Carbolite tube furnace, where the sample was dried and degassed in nitrogen atmosphere in 180°C for 4 hours. Drying in that condition removes crystallised water and physisorbed molecules. The temperature was still lower than the temperature in which 11Å tobermorite transforms to its less hydrated state. After the 4 hour drying, the furnace was turned off, and the vessel was taken out, when the temperature in the furnace was under 36°C. Cooling the furnace down was a slow process, even with external air cooling. The samples were taken out from the furnace at the same temperature, in order to minimise the moisture effect in weighting. The sample was weighted immediately after its removal.

After the weighting, the vessel was put into the reactor bomb. An aluminium foil cover was used on the vessel to avoid static electricity from sucking up the fine ash particles from the vessel. When the reactor bomb was closed carefully, the bomb was flushed using pure carbon dioxide stream to remove air and to secure pure CO_2 atmosphere in the reactor. The reactor was pressurised up to 56 bar and possible leakages were checked up. Heating was increased to 150°C when the pressure inside the reactor started rising up to 100 bar. The reaction was run for 24 hours.

After the 24 hour reaction, heating was turned off, pressure lowered and the vessel was taken out. Since water was an end product in the desired reaction and CO_2 is able to physisorb on the ash in high pressure, the sample was dried and degassed the same way it was dried before the reaction, after which the final weighting was performed. The mass change was calculated and evaluated.

The chemisorption processes were conducted for three sets of samples. Each set included three samples. The samples analysed are shown in Figure 15.

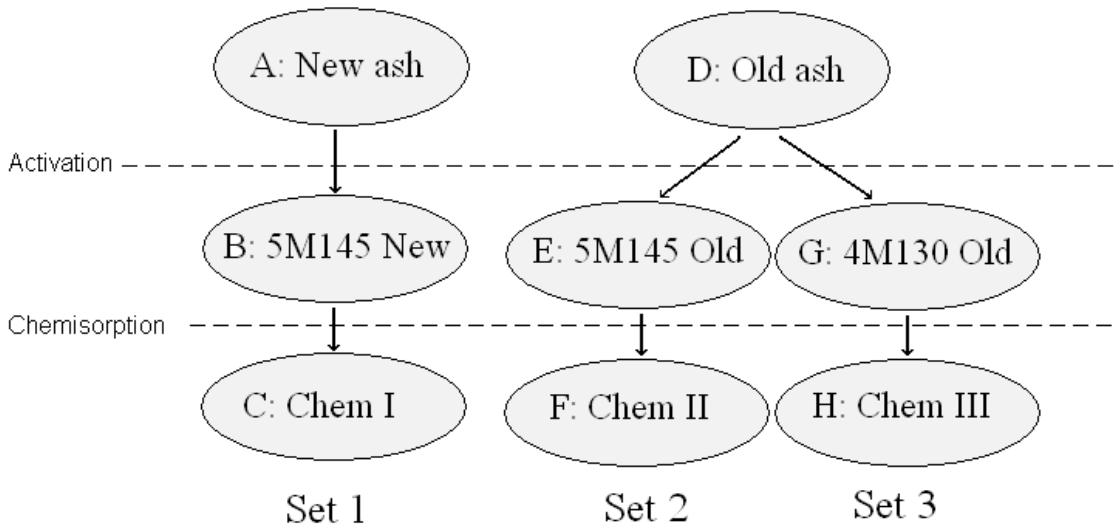

Figure 15. Chart of chemisorptions.

All the three sets had three samples in each. The first sample in a set was original, untreated ash, the second sample was activated ash and the third sample was chemisorbed ash. Set 1 was made of new ash and sets 2 and 3 were produced of old ash. All the samples in a set followed their production lines from original ash to chemisorbed material. During the experiments, a number of chemisorptions were conducted, and the results showcased in this work were for the most representative samples of all chemisorption.

After the chemisorption, the samples were analysed. Analyses were performed comparing their weights and surface characteristics. Other analysis methods were imaging using field emission scanning electron microscope (FESEM) and energy filtered transmission microscope (EFTEM), nuclear magnetic resonance (NMR) and X-ray diffraction (XRD) analysis.

7.3.1 Mass comparison

When activated OSA reacts with carbon dioxide, the mass of the sample increases. All the samples were weighted using Mettler AE 163 electronic balance before and after each chemisorption to determine whether the chemical reaction occured. The reaction

equation for the tobermorite reaction with CO_2 is presented in Equation 15 in Chapter 5, in which an 11Å tobermorite molecule and five CO_2 molecules reacts forming five calcium carbonate, six silicon dioxide and 5.5 water molecules. The reaction can be determined via mass analysis. When water formed in the reaction is evaporated and the dry masses before and after the reaction are compared. Some part of the mass of reacted CO_2 molecules stay in the compound, while the mass of formed water molecules will be lost. Therefore, the increase in mass is directed in solid residues. Due to the reaction equation, increase in mass was expected.

It was uncertain how much of the tobermorites actually were able to react in the experiment. Chemisorption is a surface reaction, so the reaction can take place only on the surface, and more importantly, on the active sites. It is unsure how much of the tobermorites were on the surface and were able to react. The approximate particle size for activated oil shale ash was around 10 µm, which is relatively large, and the specific surface area was around 60 m^2/g, so the vast majority of the minerals are not able to take part in the reaction. The reaction equation predicts 16% mass increment, when one tobermorite molecule reacts with CO_2. This is the upper limit for possible mass increment caused by chemisorption. 16% mass increment would be possible only if the reaction follows the reaction equation and all tobermorite minerals in the material react in the reaction. It is important to note, that even the activated oil shale ash has many other minerals as well, for which the reactivity is not determined. As was mentioned earlier, water formed in the reaction was evaporated, and a portion of reacted CO_2 goes to the water, so all adsorbed CO_2 is not visible in mass analysis. To get one unit mass increment for a sample, 1.8 times the mass CO_2 must be adsorbed onto the material.

The samples were dried and degassed before each weighting. The amount of moisture in the sample under normal conditions can be as great as 10% of the mass (determined using sorptometer). Dry, porous material easily takes up moisture from the air, which affects the precision of weighting the samples. It was not possible to weight the samples in room humidity, because after chemisorption a large amount of CO_2 and water formed in the reaction and were then physisorbed onto the material. Excess CO_2 and moisture needed to be removed before weighting, so degassing and drying were compulsory processes.

Weighting is an indirect method to study the chemical reaction, so there is always some level of inaccuracy in results and reliability. The accuracy can be monitored by determining the relative error in the weighing process. The relative error is the total amount of error in all measurements. Both measurements have a margin of error, which can be caused by the error in balance, by humidity, or by human error. The mathematical expression of the relative error is:

$$\Delta m = \left|\frac{\Delta x_1}{x_1}\right| + \left|\frac{\Delta x_2}{x_2}\right| \quad (21)$$

where Δm is the maximum measured mass difference
Δx_1 and Δx_2 are the precisions of measurements 1 and 2
x_1 and x_2 are the masses in measurements 1 and 2

And the percent error is:

$$\delta = \left|\frac{\Delta m}{m}\right| * 100\% \quad (22)$$

where δ is the percent error
Δm is as above
m is the final mass

Precision of the balance was 0.0001, which is significantly smaller than the error caused by moisture change in the sample, which was approximately 0.002. If the mass of the sample is 1g, it can be assumed that the percent error is around ±0.4%. If the weight increment predicted is a couple of percents, the error due to moisture content in the sample would be smaller than the mass change, but the error would still exist.

7.3.2 Imaging methods

Field emission scanning electron microscope (FESEM) is a machine which takes close up images of the material surface. The principle is that an electron beam reflects off of the surface, drawing a black and white image of the sample. FESEM is principally similar to a light microscope, except the light is replaced with high energy electron beam. Magnification of FESEM is usually from 12 to 100 000 times, so it is designed to view in micrometer scale. The model of the equipment used in this work was Zeiss FE-SEM Ultra Plus, Figure 16. (Carl Zeiss 2011)

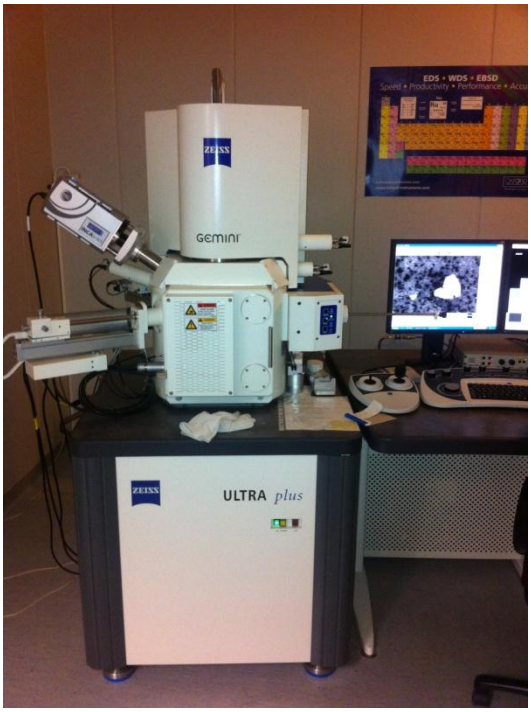

Figure 16. Zeiss FE-SEM Ultra Plus.

The other microscope was an energy-filtered transmission electron microscope (EFTEM), which is an electron microscope, but it is capable of imaging at higher resolution than FESEM. The maximum magnification for EFTEM is 500 000 times and resolution is in the nanometre scale. The electron beam does not reflect off of the surface as in FESEM, but it passes partially through the sample. The model of the EFTEM used was Zeiss EFTEM (energy filtering transmission electron microscope) (Carl Zeiss 2011)

Energy-dispersive X-ray spectroscopy (EDS) is a feature to determine elemental compositions. EDS uses the same Zeiss FE-SEM to analyse the X-ray diffraction from the surface. The analysis yields a semi-quantitative approximation of the sample composition. The determination was made on a small part of the sample, so regional variations in elemental composition occur. Therefore, the sample was analysed at many different spots and the average elemental composition was calculated. (Carl Zeiss 2011)

7.3.3 Nuclear magnetic resonance analysis

Magic Angle Spinning - Nuclear magnetic resonance (MAS-NMR) analysis was performed to reveal how the mineral compositions had changed during the activation and chemisorption processes. NMR analysis is based on the study of atomic nucleus in radio frequency magnetic field. The atomic nucleus is normally described as having mass and charge. Moreover, the nucleus has angular momentum, spin, and magnetic moment (μ). In the absence of an external magnetic field, the spin states all possess the same potential energy. However, they have different energy values if a magnetic field is applied. The principal of the NMR technique depends on these energy differences. (Akitt & Mann 2000)

Electrically neutral atoms have the same number of electrons and protons, but the number of neutrons can differ. Atoms with different number of neutrons but the same number of protons are called isotopes. The isotope number is a sum of protons and neutrons in the nuclei and it is written with a superscript at the upper left of the chemical symbol. There are several nuclei studied for NMR spectrometry, and the most commonly used are ^{13}C, ^{1}H, ^{11}B, ^{19}F, ^{31}P, ^{27}Al and ^{29}Si. ^{29}Si is studied especially in a wide range of inorganic and organic compounds. Oil shale ash has silica as a main constituent and that is why the NMR spectrometry was used in this work using ^{29}Si isotope analysis. (Akitt & Mann 2000)

The ideal structural unit of 11 Å tobermorite is presented in Figure 17. The unit has a double Ca-O sheet between wollastonite and silicate chains in parallel arrangement to the

b-axis direction. The latter creates an interlayer region, which accommodates for the labile Ca-ions and water molecules. (Reinik et al. 2007)

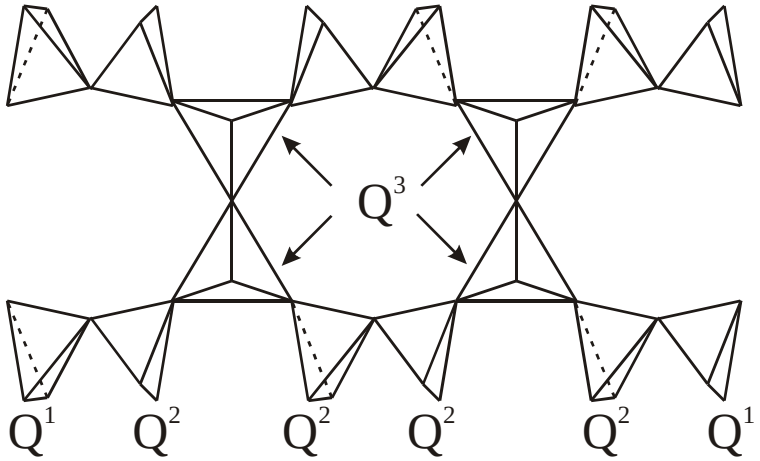

Figure 17. Structural unit of 11 Å tobermorite

In the SiO_4/AlO_4 tetrahedron chains ("dreierkette") the site Q^1 is the silicon site at the end of the polymeric silicate chain, Q^2 is the silicon site in the chain middle groups, Q^2(1Al) is the chain middle group site, where one of the two neighbouring tetrahedra contains an aluminum ion. Q^3 is the silicon site with three nearest neighbour SiO_4 tetrahedra, the branching tetrahedron which links together two chains, and Q^3(1Al) is the site, where one of the three nearest neighbour tetrahedra contains an Al ion. (Reinik et al. 2007)

7.3.4 X-ray diffraction analysis

X-ray diffraction analysis (XRD) is a commonly used diffractometric method for the characterisation of crystalline structures. This is due to the relative ease of application of the method as well as the fact that the samples do not need complicated pre-treatment. In this work, mineralogical composition and proportions of OSA in different phases of the chemisorption process are expected. (Drits & Tchoubar 1990)

In XRD analysis, the first step is to define all the structural models in the crystallo-chemical family in which the material belongs. The second step is the calculation of synthetic diagrams corresponding to each of the structural models. Finally, the model producing synthetic diagrams closest to the experimental spectrum is determined. The similarity of the two spectra justifies the adequacy of the calculated spectra. (Drits & Tchoubar 1990)

7.4 Physisorption

The feasibility of the physisorption of the precursor materials for gas purification was studied using a sorptometer for surface structure analysis and thermogravimetric analysis (TGA) for measuring the actual CO_2 physisorption uptake. Physisorption was studied for a variety of OSA and GLS samples. The set of samples studied contained 6 activated and 2 original, unactivated samples. All the activations were performed in the same reaction conditions (4M and 130°C). The eight samples consisted of four oil shale ash and four green liquor sludge samples. The ash samples studied were the both of the fly ashes, old and new, as well as activated samples of both. Green liquor sludge was studied in its pure and activated form. Also two mixtures of GLS and OSA were activated and analysed. In GLS mixture samples, the precursors were mixed before the activation process to provide new possible reaction mechanisms and new materials.

The procedures for determining the amount of gas adsorbed may be divided into two groups: those which depend on the measurement of the amount of gas removed from the gas phase and those which involve the measurement of the uptake of the gas by the adsorbent. The objective of this work was to determine the gas uptake by the later method, where mass increase in adsorbent was measured by gravimetric methods.

The physisorption experiments were conducted in TGA streaming carbon dioxide on the surface of sample materials, and measuring the mass change in different temperatures. TGA is a method to evaluate how temperature affects the physical and chemical reactions in a material. A range of materials can be studied by thermogravimetric analysis, in which the weight change of a sample is measured when heated at a constant

rate of heating. In thermogravimetric analysis, two curves are constructed, one for mass and one for temperature change. For example, TGA can be used for measurements in gas uptake and storage for various materials. TGA is a very accurate method when compared to heating with constant temperature, because TGA does not cause changes in the sample. However, it is very important to be careful when analysing the results, as impurities in inlet gas flow can act even more significant role in the adsorption than the investigated reaction itself. (Pinkerton et al. 2000)

Physisorption favours low temperature, therefore the measurements were performed by examining carbon dioxide adsorption at near room temperatures. Also elevated pressure causes an increase in the gas uptake. The TGA device used did not have option to raise the pressure, so all the runs had to be performed under atmospheric pressure. Desorption was conducted in elevated temperature under inert nitrogen atmosphere. Relatively pure CO_2 was used as a flux gas and nitrogen was used as a carrier gas. The TGA used in this work needs to have a flow rate of base gas, so pure CO_2 was not possible to use. The flow ratio was 70 wt.-% of CO_2 and 30 wt.-% of N_2. The goal of the physisorption experiments was to study how these waste materials could be utilised in biogas purification, but in the early phases of the study, only CO_2/N_2 gas mixture was used. (Sing et al. 1985)

CO_2 physisorption onto sample materials was measured using TA Instruments Q5000 analyser, which is shown in Figure 18. 6 mg of the examined material was set on a scale plate and a prepared carrier gas (nitrogen) was streamed over the sample at high temperature (180°C) for 90 minutes to be sure that the sample is completely dry and degassed. After the drying phase, the CO_2 valve was opened and the adsorption was measured near room temperature. 40°C was used due to equipment limitations. TA Q5000 does not have cooling and it was difficult to reach lower temperatures than that. Adsorption phase was followed by desorption phase, where temperature was brought back up to 180°C and the gas valve was returned to nitrogen. The total running time for one sample was almost 6 hours and nine samples were analysed in total.

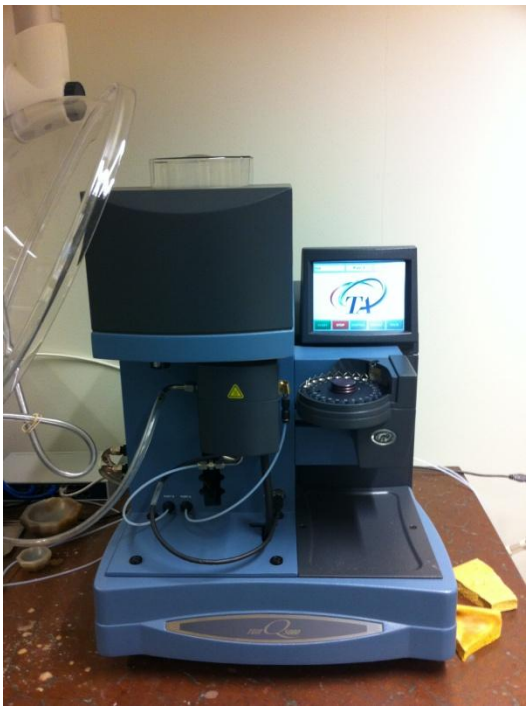

Figure 18. TA Instruments Q5000 thermogravimetric analyzer.

After the completion of the TGA experiments, it was noticed that the sensor in the device was broken. The device was used also for other measurements containing CO_2 after these experiments. According to the manufacturer, carbon dioxide is corrosive in these conditions and purities. That is why CO_2 is not suitable for the equipment. It is unclear whether the sensor was already broken when the TGA analyses were performed. The possibly broken sensor may have had an affect for the results and decrease the reliability of the measurements.

8 Results and discussion

The experimental part of the work was divided into two branches. In the first branch, chemisorption abilities for two batches of activated oil shale ash were characterised and their surface features were studied. The second branch was physisorption in which CO_2 uptake was measured for pure and activated OSA and GLS materials. The most representative samples were selected for analyses.

8.1 Chemisorption

The samples studied in chemisorption were divided into three sets, shown in Figure 15 in Chapter 7.3. Each set represented the whole production chain from original fly ash to end products. The results of chemisorption presented in this chapter are mainly for the set 3 samples, when the rest of the results (set 1 and 3) are showed in the Appendices. The results were evaluated by analysing the materials using several analysing methods, such as mass increment comparison, surface characteristics comparison, imaging methods, nuclear magnetic resonance analysis and X-ray diffraction analysis.

Green liquor sludge chemisorption was studied using an activated sample that was a mixture of 50% green liquor sludge and 50% oil shale ash. The chemisorption of the GLS sample did not indicate practical chemisorption capabilities when the mass increment was measured (the increment was 0.4%). Due to the weak results of GLS chemisorption experiments, most of the chemisorption experiments focused on the OSA.

8.1.1 Results of chemisorption

The actual mass increment for set 1 of chemisorbed sample (sample C) was 0.05% ±0.4%, which does not predict any reaction. For set 2 (sample F), the mass increment was 2.2% ±0.4% which is a promising result. For set 3 (sample H), the mass increment

was as high as 5.6% ±0.4%, which indicates very good chemisorption abilities. The mass change analyses are showcased in Table 4. Entire list of chemisorptions and their reaction conditions and carbon dioxide uptake are showed on Appendix 3.

Table 4. Mass change weighted in chemisorption.

Set	Before [g]	After [g]	Difference [%]
1	1.0278	1.0283	+0.05 ±0.4%
2	1.0391	1.0622	+2.2 ±0.4%
3	0.8983	0.9485	+5.6 ±0.4%

8.1.2 Surface characteristics

It was important to study whether the activated material had the prerequisites for chemisorption. The only possible method to study that in this point of work was to clarify how the surface characteristics had developed. The activation process was reviewed by comparing surface areas and average pore diameters. Initially, original ash samples had the specific surface areas of 6.3 m^2/g for new ash and 7.1 m^2/g for old ash, listed in Table 5. After the activation, the surface area for new ash had increased to 64.6 m^2/g and 67.9 m^2/g and 74.3 m^2/g, samples E and G, respectively, for the old ash. Comparing these values to those of the reference samples (Table 3), it was noticed that the magnitudes were about the same and it was predicted that the difference in porosity is mainly due to minerals formed during the reaction.

It is possible to reveal information of the chemisorption process by studying the specific surface area. If the reaction occurs, it would affect the surface properties, such as specific surface area. The hydrothermal minerals have higher specific surface area than the end product of the reaction, calcium carbonate, so the specific surface area should diminish. The surface properties for the group chemisorbed are listed in Table 5. It is important to note in Table 5 how the surface structures are changed between activated and chemisorbed samples in sample pairs B-C, E-F and G-H. For example, set 1 has activated

ash (sample B) and chemisorbed ash (sample C). In the chemisorption process, BET-surface analysis showed a decrease from 64.6 m^2/g to 62.6 m^2/g. Likewise BJH average pore diameter analysis showed an increase from 15.6 nm to 18.5 nm. This could indicate that the microporous materials on the surface had transformed into new materials with larger pores.

For set 2, the BET analysis showed surface area decreasing from 67.9 m^2/g to 65.7 m^2/g, and the change had happened in t-Plot microporous area, which had decreased from 13.1 m^2/g to 10.2 m^2/g. BJH average pore diameter increased from 16.1 nm and 16.7.

Set 3 had a change in BET surface area as well. The area had diminished from 74.3 m^2/g to 60.7 m^2/g. Also t-Plot microporous area had almost halved from 14.3 m^2/g to 7.4 m^2/g. BJH average pore diameter, on the contrary, had decreased from 15.9 nm to 14.6 nm, which could indicate that the largest pores were filled up with physisorbed CO_2.

Table 5. Surface characteristics for chemisorbed samples.

Sample	BET-surface area [m^2/g]	t-Plot Micro area [m^2/g]	t-Plot External area [m^2/g]	BJH surface area [m^2/g]	BJH average pore diameter [nm]	BET C-value
Set 1						
A: New ash	6.3	0.8	5.6	7.3	20.0	244
B: 5M145 new	64.6	12.2	52.3	58.6	15.6	786
C: Chem I	62.6	12.1	50.5	57.0	18.5	749
Set 2						
D: Old ash	7.1	0.6	6.5	8.4	18.1	160
E: 5M145 old	67.9	13.1	54.8	63.5	16.1	992
F: Chem II	65.7	10.2	55.5	63.1	16.7	336
Set 3						
D: Old ash	7.1	0.6	6.5	8.4	18.1	160
G: 4M130 old	74.3	14.3	60.0	71.7	15.9	930
H: Chem III	60.7	7.4	53.3	62.0	14.6	224

Comparison of the surface characteristics does not necessarily indicate whether or not the reaction had occured, nor does it indicate what kind of reaction had ensured. This kind of comparison of surface characteristics still gives an indication that something had changed in the chemisorption process.

8.1.3 Imaging method results

The samples were imaged using FESEM and EFTEM to detect, how hydrothermal activation and chemisorption had affected the surface structures of the samples. FESEM images were taken of each sample at two magnifications, 5 000 and 25 000 times. EFTEM analysis was executed only for the set 3 samples at 100 000 and 250 000 times magnifications. The FESEM and EFTEM images of the set 3 are presented in Figures 19 – 21. The rest of the FESEM images of the sets 1 and 2 are showcased on Appendix 4.

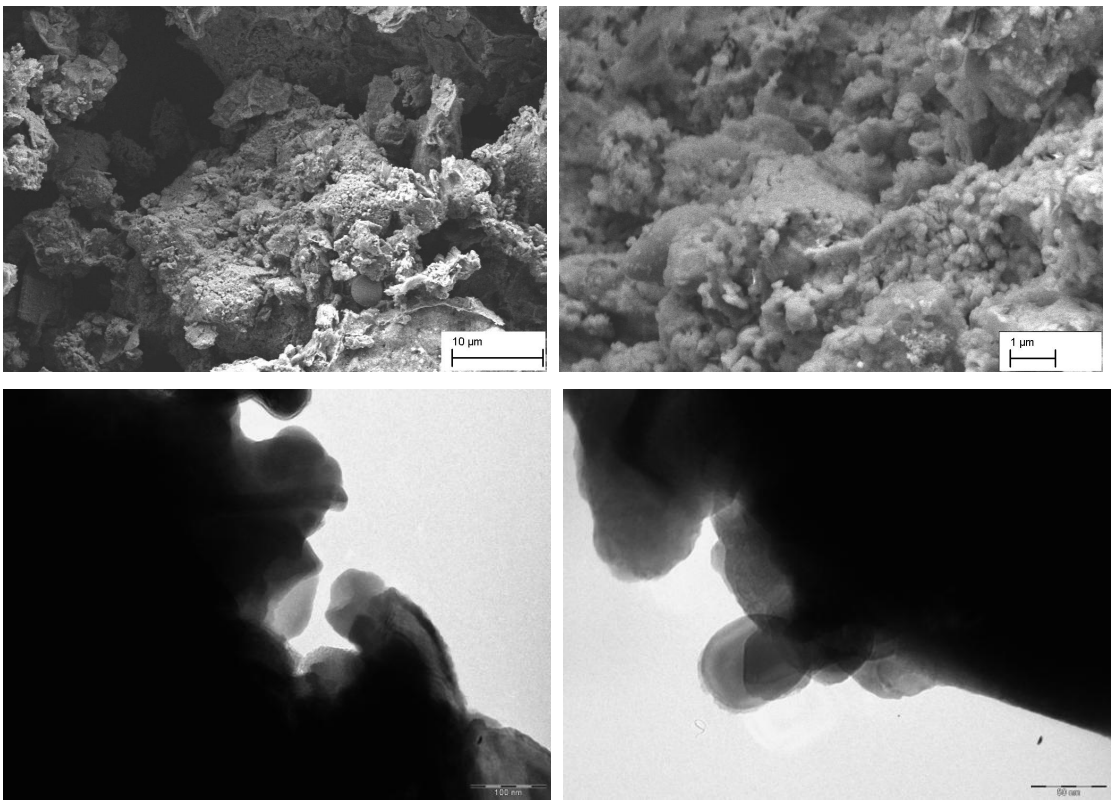

Figure 19. FESEM and EFTEM pictures of sample D. On the upper left, 5k x and 25k x on the right. EFTEM pictures of sample D at 125k magnitude on the bottom left and at 250k magnitude on the right.

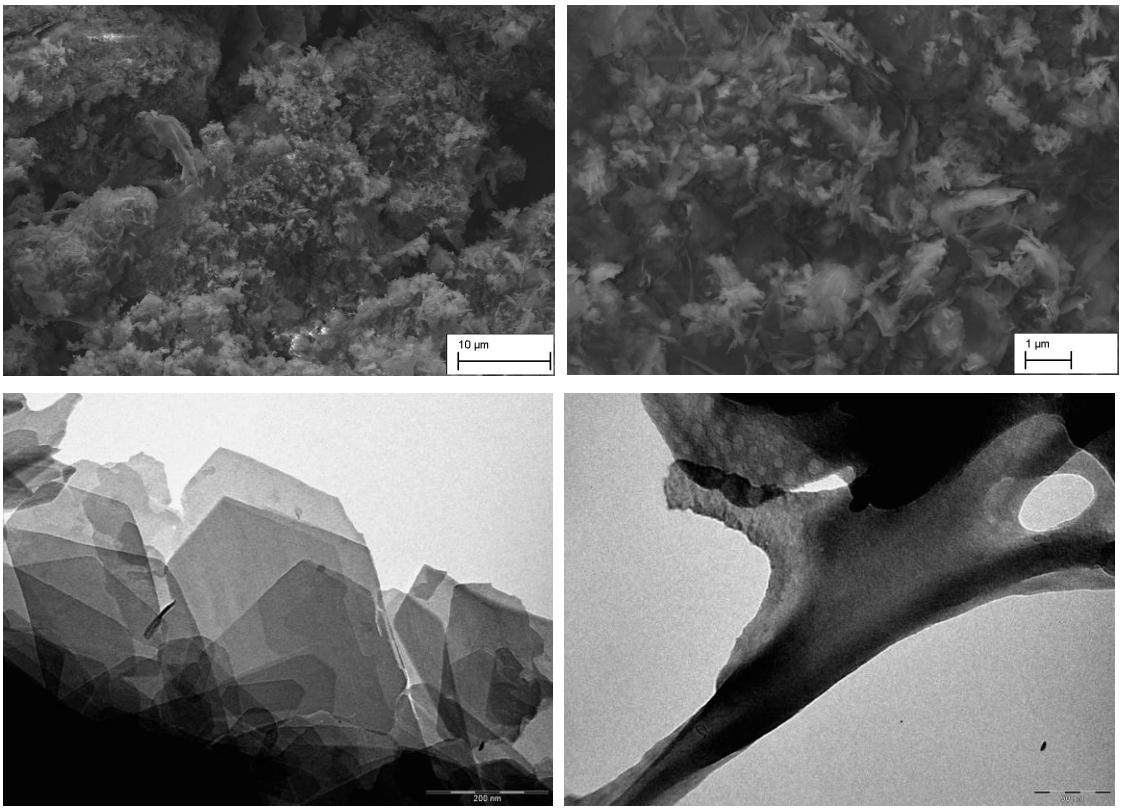

Figure 20. FESEM and EFTEM pictures of sample G. On the upper left, 5k x and 25k x on the right. EFTEM pictures of sample D at 125k magnitude on the bottom left and at 250k magnitude on the right.

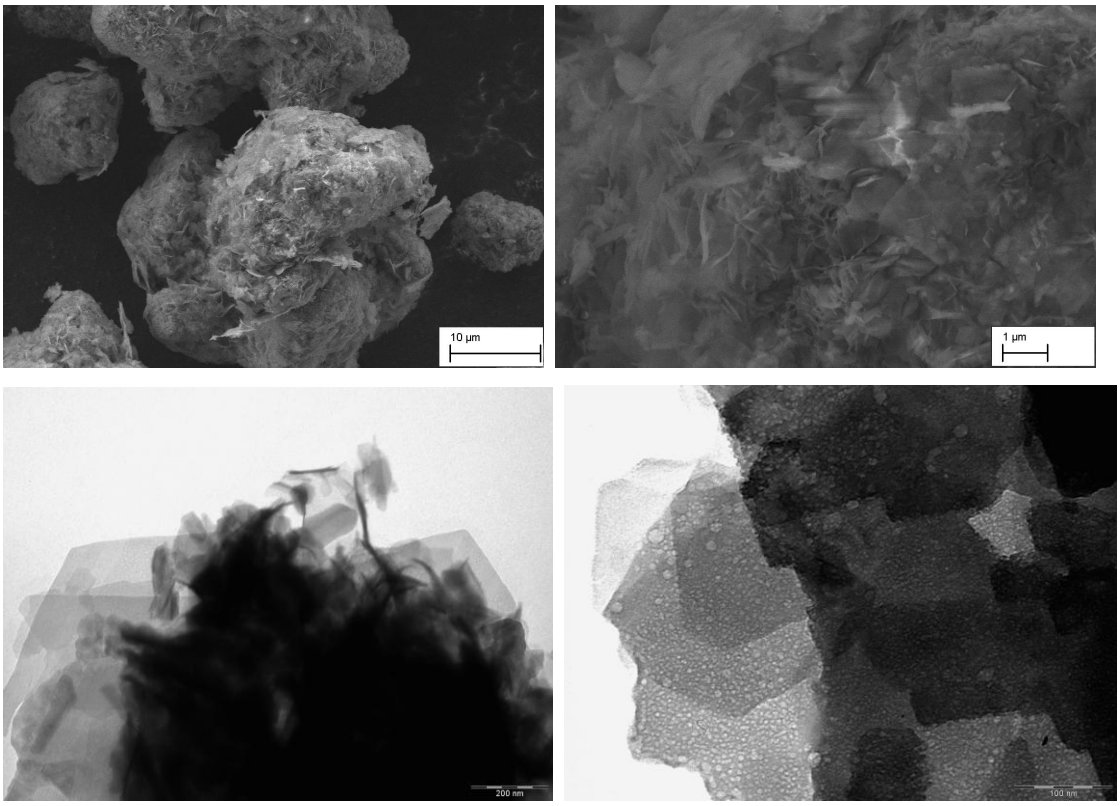

Figure 21. FESEM and EFTEM pictures of sample H. On the upper left, 5k x and 25k x on the right. EFTEM pictures of sample D at 125k magnitude on the bottom left and at 250k magnitude on the right.

FESEM analysis showed that in the beginning of the experiments, the original ashes (Figures 19 and Appendix 4 Figure 1) had smooth surface structures and particles had spherical shapes. The particles were loose and separate. After the activation process, the textures of the ash had transformed into more cracked and the particle size had increased (Figure 20). The average particle size seems to be around 10 µm, which were attached to each others. The images show that the surfaces had holes and cavities with visible spikes. Figure 21 presents the situation after chemisorption, where it seems that the surface had not visibly changed compared to Figure 20. Only the sharpest edges were possibly cut off. FESEM images also reveal that the old untreated ash had slightly more diverse structure than untreated new ash. Old ash had larger particle size and greater texture. FESEM is not capable of showing differences in chemisorption when only a thin layer of material has reacted.

EFTEM images showed that original old ash had rather straight lines and simple surface structure, as can be seen in Figure 19. The activation process had changed the surface to coarse and rough (Figure 20). The most interesting point was that the mineral structure on the sample G is notably visible and well formed. The same mineral structure is visible also in sample H in Figure 21. These EFTEM images prove that activation process had successfully turned calcium and silica to hydrothermal minerals.

Average elemental compositions of the all the samples measured with EDS are listed in Table 6. New ash and old ash (samples A and D, respectively) had similar compositions. Only Ca content in original ashes differed 3.6 percentage points and other elements were within 2 percentage points. For example, sample A had 3.5 wt.-% of iron and sample D only 2.7 wt.-%, which explains the pink colour of the new ash.

Table 6. SEM-EDS elemental composition for the ashes studied in chemisorption.

Element	Set 1 [wt.-%]			Set 2 [wt.-%]			Set 3 [wt.-%]	
	A	B	C	D	E	F	G	H
O	42.9	45.6	45.5	44.0	46.6	44.4	41.8	43.6
Ca	25.6	23.6	23.9	29.2	24.3	23.7	26.8	26.6
Si	12.7	14.4	14.7	11.0	19.3	17.8	18.6	18.6
Al	4.7	4.5	4.6	4.3	4.2	4.2	4.1	4.0
K	2.8			3.4				
S	3.3			2.5				
Fe	3.5	2.8	3.1	2.7	1.5	2.1	2.3	1.8
Mg	3.5	3.0	3.8	1.9	2.0	2.7	2.4	1.5
Cl	1.1			0.6				
Na		1.1	0.9		1.9	1.8	1.6	1.7
C*		4.5	3.3			2.9	2.4	2.0
Total	100.1	99.5	99.7	99.7	99.7	99.5	99.9	99.7

Hydrothermally activated samples that were not chemisorbed (samples B, E and G) did not have any potassium, sulphur, or chlorine remaining in the ash. These elements were dissolved and then flushed away in the activation process.

The EDS analyses were performed on a carbon tape to keep the samples from moving and to provide a solid, homogenous background which is conductive. The drawback of the use of the carbon tape is that elemental analysis is not reliable when measuring the concentration of carbon. The measurement will, therefore, predict carbon even if carbon is not present in the sample. Two of the activated ash samples, samples B and G, had 4.5 % and 2.4 % by weight carbon, respectively, even when carbon was not a precursor in original ash and it was not added during the activation. In that case, carbon probably is a reflection from the tape instead of being an existing element. Chemisorbed samples (C, F and H) otherwise did not predict high quantities of carbon. All of the samples had only 2-3 % of carbon by weight after chemisorption process. The EDS analysis of carbon showed opposite progress in chemisorption process, but the method is not reliable for evaluating the chemisorption process. The EDS analysis is not capable of analysing carbon, but it predicted that CO_2 had not chemisorbed on the ash in the reactions.

8.1.4 Nuclear magnetic resonance

NMR spectra of the set 3 are shown in Figure 22. The results of the sets 1 and 2 are presented on Appendix 5. The first curve of a graph presents NMR spectrum for original ash, the second line is for activated ash and the bottom line correspond the situation after chemisorption.

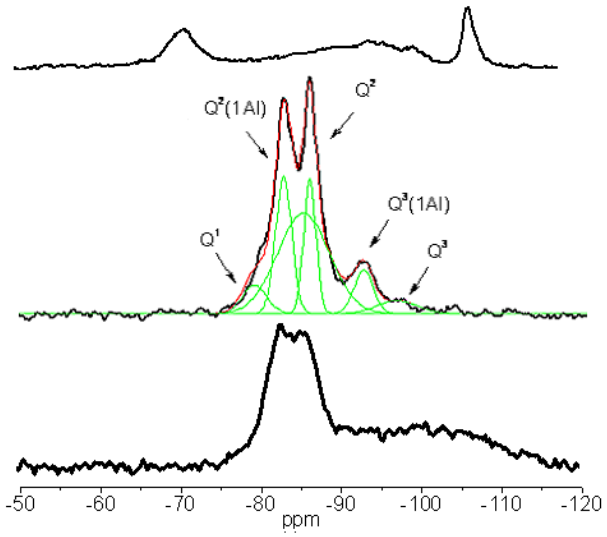

Figure 22. NMR spectra of Set 3. Original ash (sample D) on top, activated ash (sample B) with Gaussian curves in the middle and chemisorbed (sample H) on bottom.

^{29}Si MAS-NMR spectrum of the original old ash is shown at the top of Figures 22 and for new ash on Appendix 5 Figure 1. Both spectra exhibit broad resonance in the chemical shift range from -80 to -110 ppm. This resonance can be assigned to the variety of silicon sites in amorphous fly ash glass. The resonance lines at -71.5 and -107.3 ppm arise from belite (β-Ca_2SiO_4) and quartz, respectively. (Reinik et al. 2007)

The chemical shift values of the ^{29}Si resonance for activated samples, the middle line in Figures 22 and Figure 1 Appendix 5, are typical to the silicon sites in silicate chains of tobermorites or that of silicate hydrate gels. The spectrum of activated samples presents four resonance lines at -80.0, -82.8, -86.2, -92.1 and -97 ppm. According to the ^{29}Si NMR studies of tobermorites, these lines can be assigned to the silicon sites Q^1, Q^2(1Al), Q^2 and Q^3(1Al), respectively. (Reinik et al. 2007)

The resonance spectra for activated ashes demonstrate that the resonance lines at -71.5 and -107.3 ppm for belite and quartz are absent and silica in the original fly ashes is completely converted into tobermorite-like structures. In order to get quantitative characteristics of the activated ash structures, the spectrum by Gaussian lines at given frequencies was fit. The best fit was obtained when added underneath of the well-resolved lines a broad 13ppm width Gaussian background line, which arises from silicon

configurations of amorphous C-S-H phase. Such amorphous phase was obtained to be 11Å tobermorite. (Reinik et al. 2007)

The bottom curves in Figures 22 and Figure 1 Appendix 5 presents the situation after chemisorption. The shapes of the curves are close to that of the activated samples. The highest resonance peaks remain in the original position, which means that the mineral structure has not changed during the chemisorption process. The shapes of the curves for activated and chemisorbed ashes are not identical, so some chemisorption may have occured. Gaussian lines were not available for more specific chemisorption analysis.

8.1.5 X-ray diffraction analysis

X-ray diffraction analysis (XRD) was performed for all the eight samples, to reveal whether the activation process had yielded minerals and to state how the chemisorption process had changed the mineral structure. The XRD graphs for all three samples in set 3 are presented in Figure 23. The similar graphs for the sets 1 and 2 are presented on Appendix 6 in Figures 1 and 2.

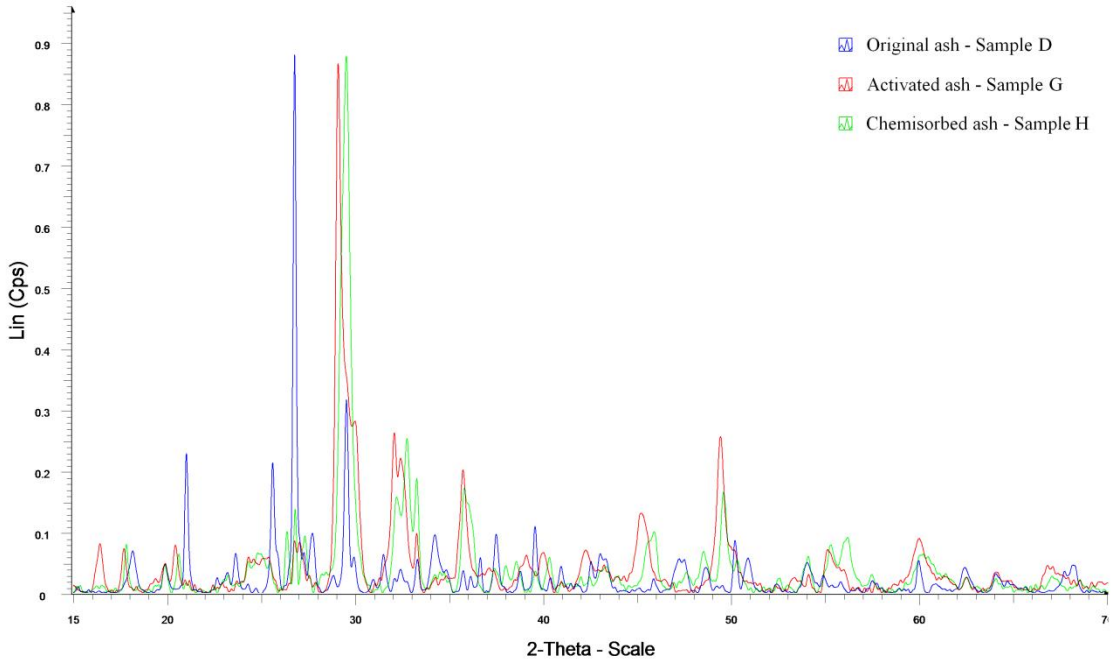

Figure 23. XRD graph of the set 3.

XRD analysis offers diffraction patterns for the samples, but the materials activated (or chemisorbed) did not fully match the XRD database's structural models and therefore the analysis did not yield unanimous mineral compositions and proportions. This is probably, because the crystalline structures of the materials were spread and the mineral structures formed in the activation process weak. XRD analysis revealed that all hydrothermally treated samples may contain mixtures of more or less well defined katoite and tobermorite minerals. The XRD results were too imprecise to quantify the proportions of the minerals. As the analysis shows, all the major peaks in the original ashes were removed after activation phase and new peaks were formed with different locations and heights. For this reason it is expected that the activation process yielded totally new compounds.

Due to lack of reliable proportions of certain minerals, it was not possible to define how much CO_2 had chemisorbed on the material. The XRD analysis did not determine the new compounds formed in chemisorption phase, but the graphs for activated ashes and chemisorbed ashes are mainly at the same locations and the heights of the peaks are approximately the same. These factors suggest that the chemical composition of the samples did not notably change during the chemisorption process and the chemical reaction did not occur to a significant extent. There was a possibility for a small amount of reacted CO_2 to remain, because the curves for activated and chemisorbed ash are not identical.

8.2 Physisorption

8.2.1 Sorptometer

Surface characteristics measured using sorptometer are listed in Table 7.

Table 7. Surface characteristics of samples studied in physisorption.

Sample	BET-surface area [m^2/g]	t-Plot Micro area [m^2/g]	t-Plot External area [m^2/g]	BJH surface area [m^2/g]	BJH average pore diameter [nm]	BET C-value
1. OSA new	6.3	0.8	5.6	7.3	20.0	244
2. OSA old	7.1	0.6	6.5	8.4	18.1	160
3. 4M130 new	64.6	12.0	52.6	61.1	14.9	696
4. 4M130 old	74.3	14.3	60.0	71.7	15.9	930
5. Act. GLS	27.8	1.5	26.3	31.3	13.9	135
6. Act. 50:50 GLS/OSA	38.8	4.1	34.7	40.2	16.1	195
7. Act. 70:30 GLS/OSA	45.4	4.9	40.5	47.2	14.4	208
8. GLS	14.8	0.0	14.9	17.3	16.1	93

The surface structure of original OSA and GLS were scarcely porous, so physisorption of CO_2 does not seem possible in practise without pre-treatment. The measured specific surface areas for untreated oil shale ashes (samples 1 and 2) were only 6 m^2/g and 7 m^2/g and for untreated GLS (sample 8) it was around 15 m^2/g. The hydrothermal activation process for OSA increased the surface areas to 65 and 74 m^2/g. Also GLS increased surface are up to 30 m^2/g (sample 5). t-Plot values show the distribution between micro and mesoporous area. BJH surface area analysis yielded values close to that of BET. For an adsorbent material, that low specific surface areas are still low.

Pore diameter values were determined with BJH method, which predicts the diameters to be between 14 and 20 nm. The diameters are rather wide compared to the width of a CO_2 molecule (0.34 nm), even though the pore diameter distribution is not available. BJH method severely underestimates the pore sizes. (Ravikovitch et al. 2000)

8.2.2 Thermogravimetric analysis

CO_2 adsorption capacity was measured for the eight samples using TGA in atmospheric pressure. CO_2 uptake for sample 4 is presented in Figure 24. The green line represents the weight of the sample, the brown line represents the temperature, in which the TGA is operating. The weight changes for the rest of the samples are presented on Appendix 1 in Figures 1 – 7.

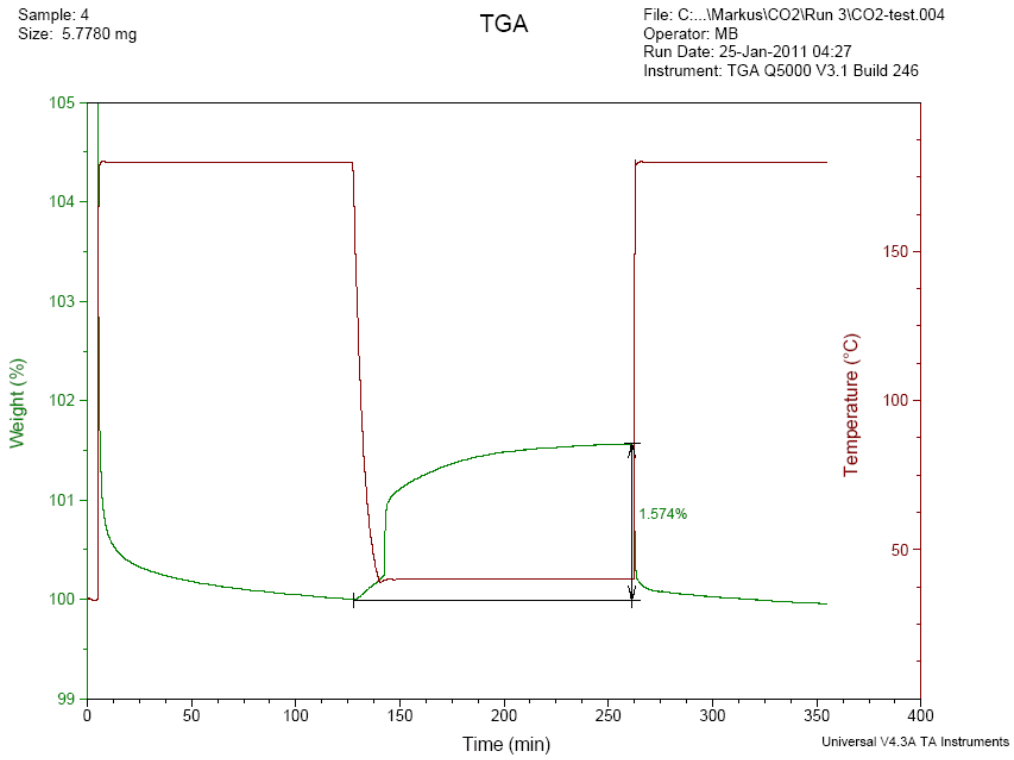

Figure 24. Sample 4: CO_2 adsorption measured with TGA

The TGA CO_2 uptake results for all eight samples are presented in Table 8. The highest CO_2 uptake was measured for sample 4, which is a 4M130 activated sample made of old ash. The CO_2 uptake capacity for the sample was 1.6% of the weight. Sample 3, which was produced in the similar conditions using new ash, had a little weaker CO_2 uptake capacity, 0.9%. Pure ash in both cases, samples 1 and 2, did not indicate any CO_2 uptake capacity.

Pure GLS (sample 8) on the other hand had uptake capacity of 0.1 wt.-%. Activated GLS (sample 5) had 0.23% weight increment. The 50:50 mixture of GLS and old OSA (sample 6) had capacity of 0.48%, which was lower than the average of the precursors individually (which would have been 0.57%).

Table 8. Sample studied and their relative CO_2 uptake.

Sample	CO_2 uptake [%]	Sample	CO_2 uptake [%]
1. OSA new	0.01	5. Act. GLS	0.23
2. OSA old	0.03	6. Act. 50:50 GLS/OSA	0.48
3. 4M130 new	0.91	7. Act. 70:30 GLS/OSA	0.46
4. 4M130 old	1.57	8. GLS	0.09

All mass increments measured were proportional to their specific surface areas, as expected. The samples with greater specific surface areas had better CO_2 uptake capacities.

The results of CO_2 adsorption measured in this work did not indicate high CO_2 uptake abilities. In preliminary tests, almost 4 wt.-% CO_2 adsorption was reached when activated samples were measured. The preliminary tests were performed with reference ash samples. The percentages for non-activated materials in preliminary tests were less than tenth of a percent. These differences may be due to the broken sensor.

The shape of BET N_2 adsorption isotherm indicated rather good adsorption capabilities, shown in Figure 12, but in TGA tests, minimal adsorption was measured. Perhaps the reason for poor CO_2 uptake was that N_2 molecule is so much smaller compared to CO_2 molecule, therefore it can fill micropores and CO_2 molecule cannot. All TGA runs were performed at normal atmospheric pressure. According to literature, the pressure in physisorption should have been elevated. (Walton et al. 2008)

All samples measured in TGA had some physisorption capabilities, but none of them had chemical reactions in these conditions. All CO_2 adsorbed was also able to desorb. Expectant application for these kinds of materials would be in e.g. CO_2 scrubbing at gas purification at a power plant due to fact that physisorption does not provide long term storage.

9 Conclusions

9.1 Activation process

The present study showed that oil shale ash can be used as a precursor for novel materials, such as tobermorites and katoite. The analysis methods used in this work did not define the exact mineral composition or mineral proportion of activated ash. XRD analysis revealed that either the minerals formed in the reaction did not have proper mineral structures or a variety of different minerals was formed. The concentration or reaction temperature was probably not high enough. Oil shale ash can be converted to novel materials, but the reaction conditions should be studied more closely to find the best conditions to yield the desired minerals.

The activation set up did not tolerate temperatures above150°C, so it was not possible to reach the optimal temperature reported in the literature (Reinik et al. 2007, 2008). Higher concentration could yield a better mineral composition and higher concentration (8-10 M) should be tested in the future experiments. In the literature, 8 M solution is common in similar solutions. In this work 4 and 5 M solution were prepared.

Activation of two different batches of ash yielded similar characteristics and mineral compositions under similar reaction conditions (NMR). NMR analysis also revealed that all the silica in the original ashes was converted into a new material, and the Gaussian background lines obtained to a tobermorite-like structure.

No mineralogical analyses (XRD or NMR) were made before chemisorption or physisorption runs. It is possible that the activation reaction did not yield the best achievable crystal structure, or the mineral composition was weak. The work should have been made in two phases, first to analyse the mineralogy of activated ash samples, and then to select the best samples for chemisorption. In this work activation was assessed only on the surface area of the reference samples and to an earlier study about the conditions. The XRD and NMR analyses performed afterwards revealed that the

activation process had formed hydrothermal calcium silicate minerals, tobermorites and katoite as expected.

Activation of green liquor sludge did not yield promising results for CCS. GLS consists of calcium carbonate mainly and it does not have silica as a constituent. Addition of silica may be worthwhile step in the future experiments. On the other hand, calcium carbonate in GLS has already stored a CO_2 molecule.

9.2 Chemisorption process

Feasibility for carbon dioxide chemisorption is measured for activated oil shale ash according to the article by Touze et al. (2004), where the reaction conditions of 150°C and 100 bar are assessed to be adequate for mineral carbonation of CO_2 onto tobermorites. The experiments were carried out in suggested direct reaction between gaseous carbon dioxide and solid activated ash.

As a result of chemisorption, no CO_2 chemisorption was observed on the precursor materials. The highest amount of carbon dioxide reacted on the sample H gained the mass of the sample by 5%, which is equivalent to 90 kg CO_2 uptake per ton of ash. The two other samples had mass increments of 2% and ~0%. The amount of carbon dioxide chemisorbed on the material is minimal. Weighing predicted a small increase in the mass, and surface analysis revealed that the specific surface areas after chemisorption were reduced. These factors reflect that sorption occurred. Unfortunately, it is not possible to say for sure if these changes were due to physisorption. All analyses used in this work are indirect methods and cannot predict whether the chemical reaction occurs.

FESEM, EFTEM or EDS analyses, on the contrary, do not reflect notable elemental or visible changes on the sample surfaces. An approximate particle size for activated ash sample is around 10 µm and the specific surface area around 60 m^2/g. Due to the size of a particle, the vast majority of the hydrothermal minerals formed in the activation reaction are not on the surface. Even if the chemical reaction occurs, chemisorption is a surface reaction and the amount of carbon dioxide sequestered on activated ash is naturally low.

A potential reaction for further studies could be simultaneous activation and chemisorption reaction, in which dissolved active ions are able to react with carbon.

NMR and XRD analyses showed that the peaks for activated and chemisorbed materials remained at the same locations and the heights of the peaks were almost the same, but information of mineral proportion was not available. As the result of these analyses, it was not possible to prove whether chemisorption took place. Total carbon (TC) or Total Organic Carbon (TOC) analyses were not used in this work, but they could have revealed the change in carbonic concentration (Teir et al. 2007). The carbonic concentration would reveal, if carbon dioxide had reacted on the surface.

Teir et al. (2007) have produced magnesium carbonates from serpentinite in pH controlled aqueous solutions where CO_2 was bubbled through the solution. This kind of an aqueous method may be useful for mineral carbonation of CO_2 onto tobermorites as well, if the chemisorption could be conducted simultaneously with the activation process. Better conversion for oil shale ash mineral carbonation could be possible, if the calcium and silicate molecules were pre-dissolved and ready to react.

The processes presented in this work would probably not be realistic, if the CO_2 uptake was not significantly higher. Novel techniques for CO_2 capture and storage are needed and further study of mineral carbonation is necessary. The temperature and pressure requirements are too high for industrial usage, but the process could be possible *in situ* at an oil shale power plant. Carbon dioxide needs to be pressurised, which would increase the cost of a carbonation process, and recovery of sodium hydroxide would be crucial. The CO_2 emitted during the manufacturing of the chemicals, production of energy, and the mineral carbonation process itself may be significant, and should be taken into account in further evaluations. (Teir et al. 2007)

9.3 Physisorption process

The use of OSA and GLS were studied for CO_2 removal from gas streams. The precursors were studied as pure reactants and activated materials. The most important requirement for an efficient physisorption material is the high specific surface area. The surface areas of both precursor materials increased in the activation process. Activated oil shale ashes had BET surface areas up to ten times that of untreated oil shale ash, and micropores had formed as well. However, the size of specific surface areas of activated oil shale ashes were relatively low (65 – 74 m^2/g) for industrial adsorption processes, however, it could be possible to use hydrothermally activated OSA as the CO_2 trap adsorbent. The activation process doubled the specific surface area of GLS up to 30 m^2/g. Advantages of the raw materials are that they are cheap and abundant. In some instances, the materials could be used locally for flue gas purification, for example at an integrated pulp mill and biogas plant or at an oil shale ash power plant.

The highest value measured for CO_2 uptake was 1.6 wt.-%. The reason for the low physisorption uptake was the low operating pressure used in the experiment. Adsorption methods for CO_2 scrubbing are conducted invariably under high pressure. The TGA equipment did not have an opportunity to operate in elevated pressures and the adsorption temperature used was high. Consequently, it might be possible that the crystal water lost in drying caused a collapse of the pore system.

After the TGA measurements, the thermo sensor was noticed to be broken. The sensor did not tolerate CO_2 as a flux gas, as CO_2 causes corrosion at high temperatures. It can be possible that the sensor was not functioning correctly during the experiments and the results may be corrupted.

An article of the result of the physisorption tests is also submitted to Fuel scientific journal to be published. (Reinik et al. 2011)

10 Summary

Carbon dioxide is the most important greenhouse gas produced by human activities, and the CO_2 emissions are a worldwide issue and it is assumed to be the primary cause for the climate change. Carbon dioxide capture and storage is widely researched to moderate the consequences of CO_2 on the environment.

Oil shale ash and green liquor sludge were examined as precursor materials for carbon dioxide capture and storage. Today, both the materials are classified as waste materials and not many applications for their use have been found. However, oil shale ash has a promising calcium and silica composition for alkaline hydrothermal activation to yield calcium silicate minerals, such as tobermorites. Green liquor sludge has a large quantity of calcium and magnesium, but there is insufficient silica. That is why green liquor sludge was examined mostly for CO_2 adsorption.

Carbon dioxide capture and storage capability of these materials are studied in two processes; chemisorption and physisorption. Chemisorption process has a goal to turn tobermorites formed in the activation process into calcium carbonate, which is a geologically stable form for carbon storage. Physisorption is a process to adsorb CO_2 from gas flows in gas purification.

The raw materials need to be pre-treated before they are suitable for carbon dioxide capture and storage. The pre-treatment used in this work was an alkaline hydrothermal activation process with aqueous sodium hydroxide solution. The activation process was conducted for all raw materials and their derivatives. All silica in oil shale ash was converted into calcium silicate minerals. It was detected that the minerals formed in the activation were mostly tobermorites and katoite. Green liquor sludge was activated as an individual material and as a mixture with oil shale ash.

Tobermorites are chemically reactive with carbon dioxide, and reactivity of activated oil shale ash was studied. The reaction between activated OSA and CO_2 was studied directly, where the reaction was performed in CO_2 atmosphere under high temperature and pressure. The end products were analysed using a variety of analysing methods.

Reactivity was evaluated by analysing the materials after chemisorption and comparing them to activated materials. The analyses used in this work did not prove that carbon dioxide reacts with oil shale ash. Nevertheless, the simultaneous activation and mineral carbonation could be reasonable processes to study in the future experiments. The amount of carbon dioxide mineralised on activated oil shale ash was 90 kg CO_2 per ton of ash.

Adsorption of gaseous molecules on a material surface is due to physical forces. Carbon dioxide has higher selectivity for adsorption than methane or air. That is why CO_2 physisorption capabilities were studied using a variety of materials and the actual CO_2 uptake was measured. The activated oil shale ash samples gained 1.6% mass increment due to CO_2 physisorption.

Oil shale ash was found to be a promising raw material for carbon dioxide capture and storage, but in this work, no concrete use was detected. Green liquor sludge did not indicate functional features in carbon dioxide sequestration in this study. However, both waste materials proved to be potential candidates for carbon dioxide capture and storage, therefore, more research is needed.

11 References

Akitt J & Mann B (2000) NMR and Chemistry. An introduction to modern NMR spectroscopy. The UK. Stanley Thornes Ltd. ISBN 0 7487 4344 8

Aleklett K, Höök M, Jakobsson K, Lardelli M, Snowden S & Söderbergh B (2010) The Peak of the Oil Age - analyzing the world oil production Reference Scenario in World Energy Outlook 2008. Energy Policy. Vol 38, 2010, 1398-1414 p.

Al-Wakeel E, El-Korashy A, El-Hemaly S & Rizk M (2001) Divalent ion uptake of heavy metal cations by (aluminum + alkali metals) – substituted synthetic 1.1 nm-tobermorites. Journal of Materials Science 36 2405 – 2415 p.

Baines S & Worden R (2004) Geological storage of carbon dioxide Geological storage of carbon dioxide, London, Special Publications 2004; v. 233; p. 1-6

Beruto D, Botter R & Searcy A (1984) Thermodynamics and Kinetics of Carbon Dioxide Chemisorption on Calcium Oxide. The Journal of Physical Chemistry, Vol. 88, No. 18

Brierley A & Kingsford M (2009) Impacts of Climate Change on Marine Organisms and Ecosystems. Review, Current Biology, Vol 19, No 14, 602-614 p.

Byrappa K & Yoshimura M (2001) Handbook of hydrothermal technology. Japan. ISBN: 978-0-8155-1445-9

Carl Zeiss NTS GmbH, Germany. Manufacturer's website. [Accessed on 4 March 2011] Available on: http://www.zeiss.com

Chowdhury F, Okabe H, Shimizu S, Onoda M & Fujioka Y (2009) Development of novel tertiary amine absorbents for CO_2 capture. Energy Procedia. Vol. 1. 1241–1248 p.

Coleman N (2006) Interactions of Cd(II) with waste-derived 11 Å tobermorites. Separation and purification technology 48 62–70 p.

Drits V & Tchoubar C (1990) X-ray diffraction by disoriented lamellar structures. Theory and application to microdivided silicates and carbons. Springer-Verlag. Germany. ISBN 0-387-51222-5

Dyni J (2006) Geology and Resources of Some World Oil-Shale Deposits: The U.S.A, Geological Survey Scientific Investigations Report 2005–5294, 42 p.

Hitchon B, Gunter , Gentzis T & Bailey R (1999) Sedimentary basins and greenhouse gases: a serendipitous association. Energy Conversion & Management, Vol. 40, 825-843 p.

Hubbert M (1956) Nuclear energy and the fossil fuels. Publication Shell development company. Texas. No 95.

Kauriinoja A (2010) Small-scale biomass-to-energy solutions for northern periphery areas. Oulu, Oulun yliopisto. 95 p.

Karakashev D, Batstone D & Angelidaki I (2005) Influence of Environmental Conditions on Methanogenic Compositions in Anaerobic Biogas Reactors. Applied and Environmental Microbiology, Jan. p. 331–338

Kelleher B, Leahy J, Henihan A, O'Dwyer T, Sutton D & Leahy M (2002) Advances in poultry litter disposal technology. Review. Bioresource Technology, Vol 83, 27–36 p.

Krivovichev S (2008) Minerals as advanced materials I. Tobermorite 11 Å and its synthetic counterparts: Structural relationships and thermal behaviour. Springer. Russia. ISBN 978-3-540-77122-7.

Lepistö M (2005) Hiilidioksidin monet mahdollisuudet. Oulu, Oulun yliopisto. 67 p.

Marini L (2007) Geological sequestration of carbon dioxide: thermodynamics, kinetics, and reaction path modeling. Developments in chemistry. ISBN 978-0-444-52950-3

Maugeri L (2004) Oil: Never Cry Wolf—Why the Petroleum Age Is Far from over. Policy Forum, Science and Industry. Vol 304, 21 May. 1114 – 1115 p.

Meisen A & Shuai X (1997) Research and Development Issues in CO_2 Capture. Energy Convers. Mgrnt, Vol. 38, 37-42 p.

Merlino S, Bonaccorsi E, & Armbruster T (2001) The real structure of tobermorite 11Å: normal and anomalous forms, OD character and polytypic modifications. Eur. J. Mineral. 13, 577–590 p.

Molchanov V & Prikhidko E (1956) Corrosion of silicate glasses by alkaline solutions. Russian chemical bulletin. Vol. 6. 1179-1184 p.

Nuckols M, Purer A & Deason G (1985) Design Guidelines for Carbon Dioxide Scrubbers. NCSC Tech Man. Florida 4110-1-83.

Nurmesniemi H, Pöykiö R, Perämäki P & Kuokkanen T (2005) The use of a sequential leaching procedure for heavy metal fractionation in green liquor dregs from a causticizing process at a pulp mill. Chemosphere, Vol 61, 1475–1484 p.

Oelkers E, Gislason S & Matter J (2008) Elements, An international magazine of mineralogy, Chemistry and petrology. October 2008, volume 4, number 5. 333-337 p. ISSN 1811-5209

Oymael S (2007) Suitability of oil shale ash as a constituent of cement. Oil Shale. Vol. 24. No 1. 45-58 p.

Pinkerton F, Wicke B, Olk C, Tibbetts G, Meisner G, Meyer M & Herbst J (2000) Thermogravimetric Measurement of Hydrogen Absorption in Alkali-Modified Carbon Materials. J. Phys. Chem. B 2000, Vol. 104, No 40, 9460 - 9467 p.

Privalova E, Mäki-Arvela P, Murzin D & Mikkola J.-P. (2010) Capturing CO_2: conventional versus non-conventional technologies for biogas plants. Åbo Akademy University. Preview.

Puertas F, Martinez-Ramirez S, Alonso S & Vazguez T (2000) Alkali-activated fly ash/slag cement Strength behaviour and hydration products. Cement and Concrete Research, Vol 30, 1625 -1632 p.

Qiang J, Wang J & Li S (2003) Oil Shale Development in China. Oil Shale. Vol 20. 356-359 p.

Ravikovitch P, Vishnyakov A, Russo R & Neimark A (2000) Unified Approach to Pore Size Characterization of Microporous Carbonaceous Materials from N_2, Ar, and CO_2 Adsorption Isotherms. Langmuir 2000, Vol. 16, 2311 – 2320 p.

Reinik J, Heinmaa I, Mikkola J.-P. & Kirso U (2007) Hydrothermal alkaline treatment of oil shale ash for synthesis of tobermorites. Fuel. Vol 86, 669–676 p.

Reinik J, Heinmaa I, Mikkola J.-P. & Kirso U (2008) Synthesis and characterization of calcium–alumino-silicate hydrates from oil shale ash – Towards industrial applications Fuel. Vol 87, 1998–2003 p.

Reinik J (2010) Private communication. Umeå, Sweden.

Reinik J, Heinmaa I, Kallaste T, Ritamäki J, Boström D, Pongracz E, Huuhtanen M, Larsson W, Keiski R, Kordas K & Mikkola J.-P. (2011) Study of alkaline hydrothermal action of oil shale fly ash on enhancement of CO_2 adsorption. Fuel. In press.

Schleifer K (2009) Classification of *Bacteria* and *Archaea*: Past, present and future. Systematic and Applied Microbiology. Vol. 32, 533-542 p.

Shawabkeh R, Al-Harahsheh A, Hami M & Khlaifat A (2004) Conversion of oil shale ash into zeolite for cadmium and lead removal from wastewater. Fuel, Vol. 83, 981-985 p.

Sing K, Everett D, Haul R, Moscou L, Pierotti R, Rouquèrol J & Siemieniewska T (1985) Reporting Physisorption Data for Gas/Solid Systems with Special Reference to the Determination of Surface Area and Porosity. IUPAC, Pure & Appl. Chem., Vol. 57, 603—619 p.

Smadi M & Haddad R (2003) The use of oil shale ash in Portland cement concrete. Cement & Concrete Composites. Vol. 25, 43–50 p.

Tegethoff F, Rohleder J & Kroker E (2001) Calcium Carbonate: From the Creataceous Period into the 21st Century. Basel, Birkhäuser Verlag, 342 p. ISBN 3-7643-6425-4

Teir S, Eloneva S, Fogelholm C.-J. & Zevenhoven R (2006) Stability of calcium carbonate and magnesium carbonate in rainwater and nitric acid solutions. Energy Conversion and Management. Vol. 47. 3059-3068 p.

Teir S, Kuusik R, Fogelholm C.-J., Zevenhoven R (2007) Production of magnesium carbonates from serpentinite for long-term storage of CO_2. International Journal of Mineral Processing. Vol 85. 1-15 p.

The Engineering Toolbox. [Accessed on 4 March 2011]. Available on: http://www.engineeringtoolbox.com/boiling-point-water-d_926.html

The EU Emission Trading System (2011) [Accessed on 2 May 2011]. Available on: http://ec.europa.eu/clima/policies/ets/index_en.htm

Topham S (1986) Ullmann's Encyclopedia of Industrial Chemistry. Carbon dioxide. Vol A5, 165-182 p.

Touze S, Bourgeois F, Baranger P & Durst P (2004) Analyse bilantielle de procedes ex situ de sequestration du CO_2. BRGM/RP-53290-FR. 77 p. Translated with Google translator

Tunega D & Zaoui A (2010) Understanding of Bonding and Mechanical Characteristics of Cementitious Mineral Tobermorite From First Principles. Journal of Computational Chemistry Vol. 00, 1-9 p.

Walton K, Millward A, Dubbeldam D, Frost H, Low J, Yaghi O & Snurr R (2008) Understanding Inflections and Steps in Carbon Dioxide Adsorption Isotherms in Metal-Organic Frameworks. J. American Chemical Society, Vol. 130, No. 2, 2008

Ward C (1984) Coal geology and coal technology. Blackwell Scientific Publications. 345p. ISBN 0-86793-096-9

Webb P & Orr G (1997) Analytical Methods in Fine Particle Technology. The USA, Micromeritics Instrument Corporation, 301 p.

Appendix 1 (1/4)

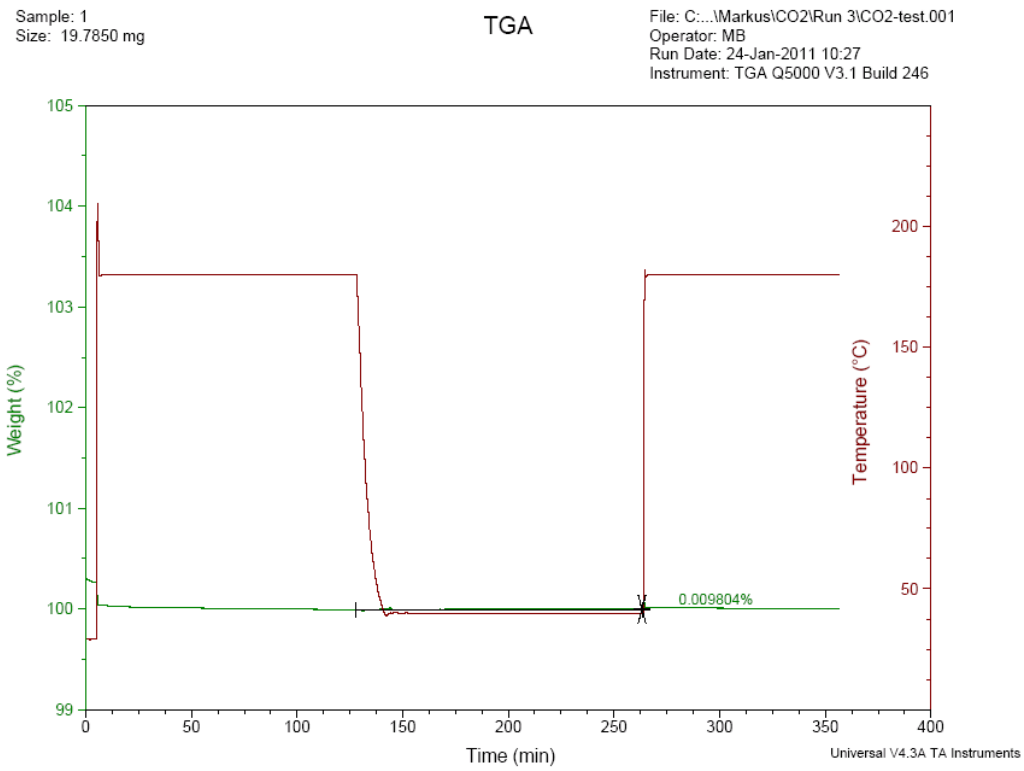

Figure 1. Sample 1, new ash, CO_2 adsorption uptake.

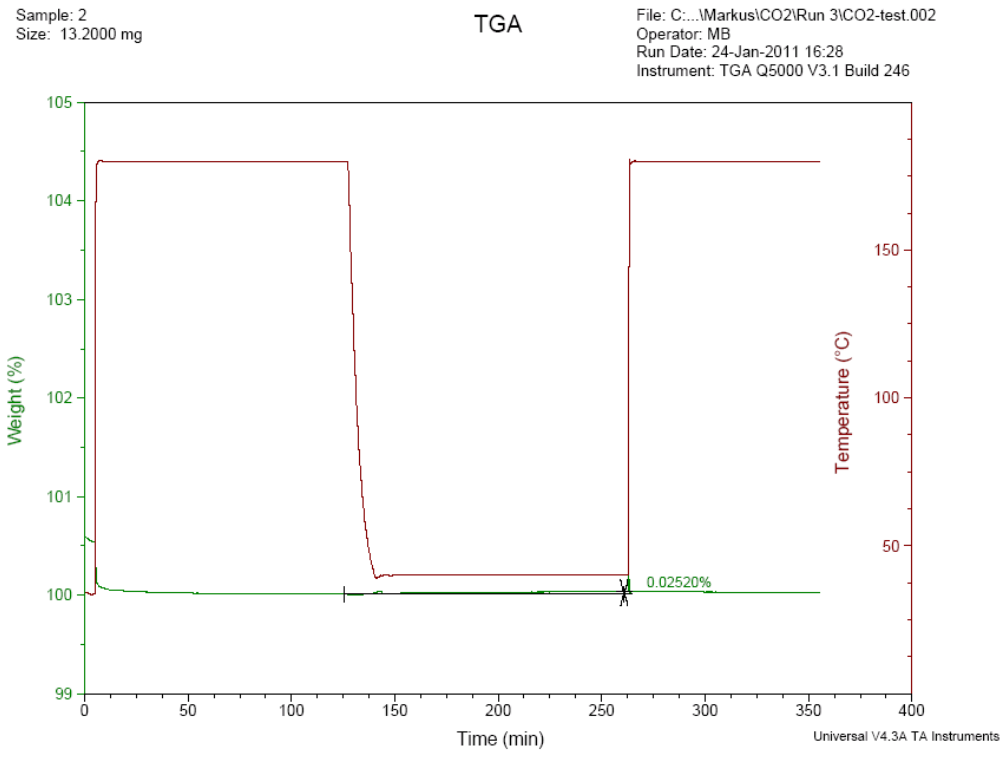

Figure 2. Sample 2, old ash, CO_2 adsorption uptake.

Appendix 1 (2/4)

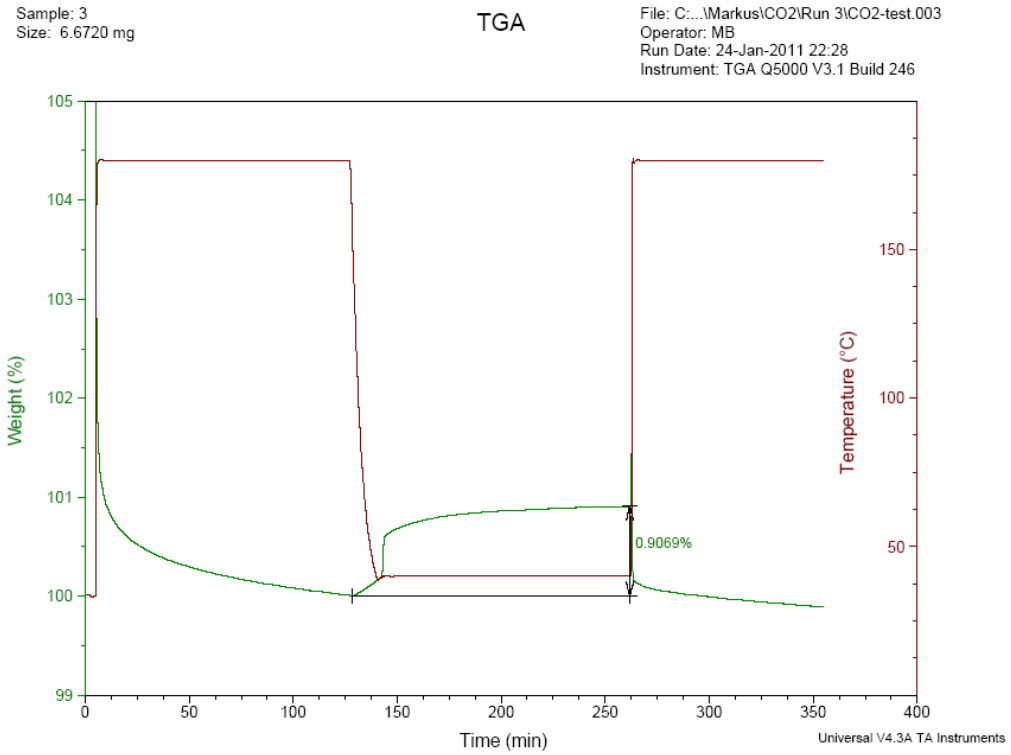

Figure 3. Sample 3, 4M130 old ash, CO_2 adsorption uptake.

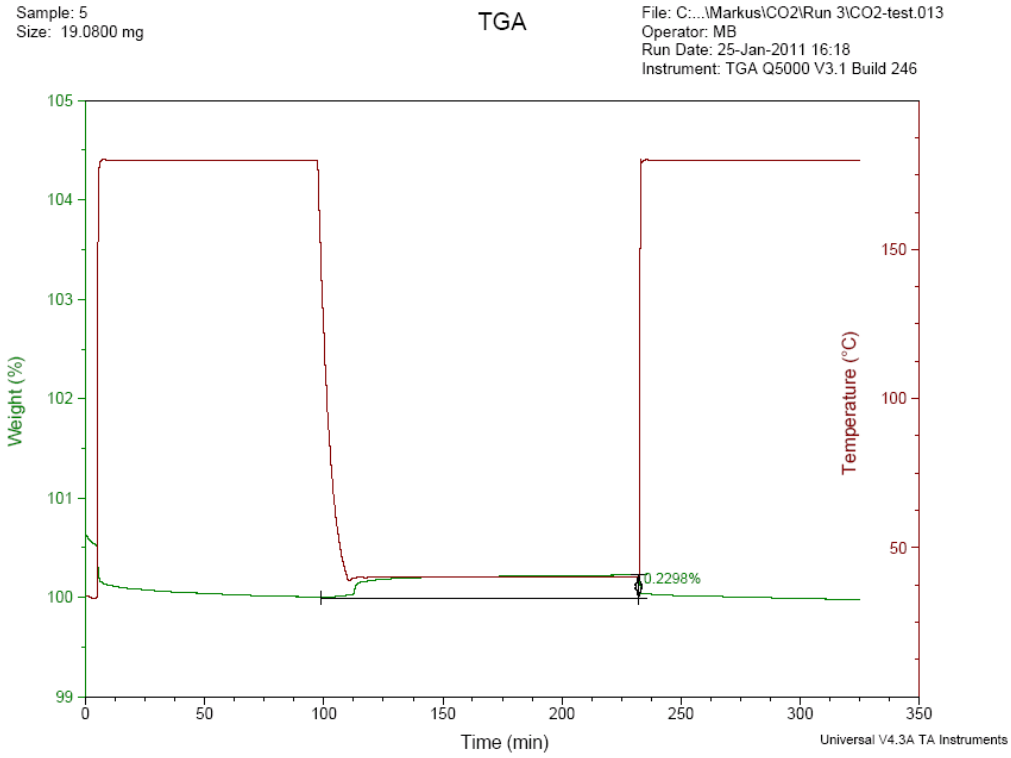

Figure 4. Sample 5, activated GLS, CO_2 adsorption uptake.

Appendix 1 (3/4)

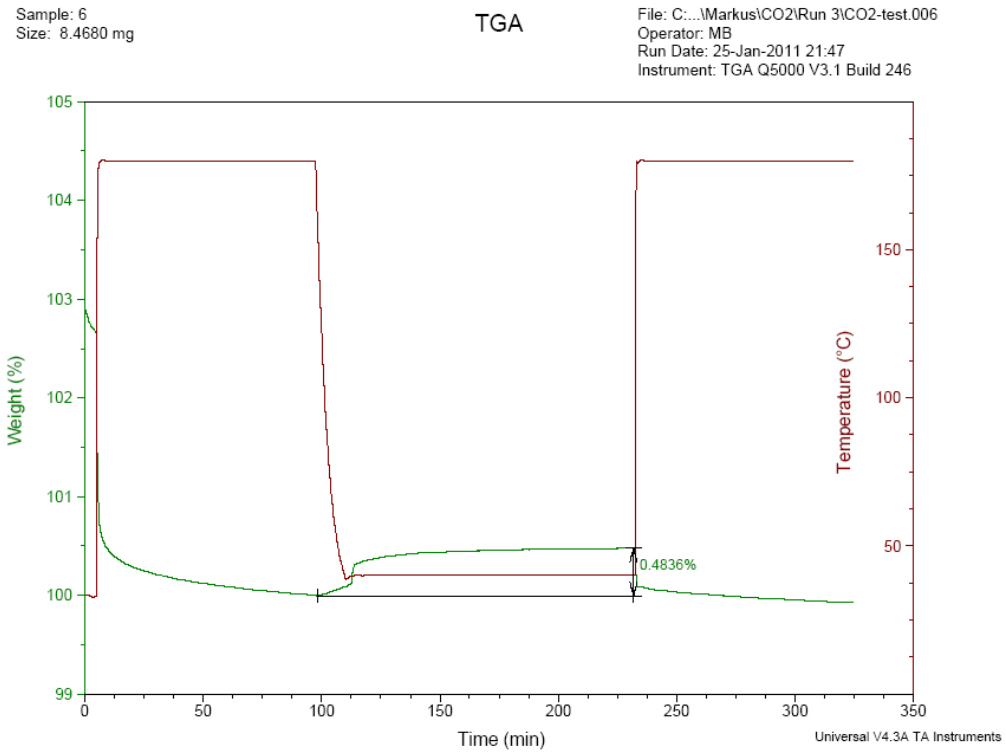

Figure 5. Sample 6, activated 50/50 GLS/OSA mixture, CO_2 adsorption uptake.

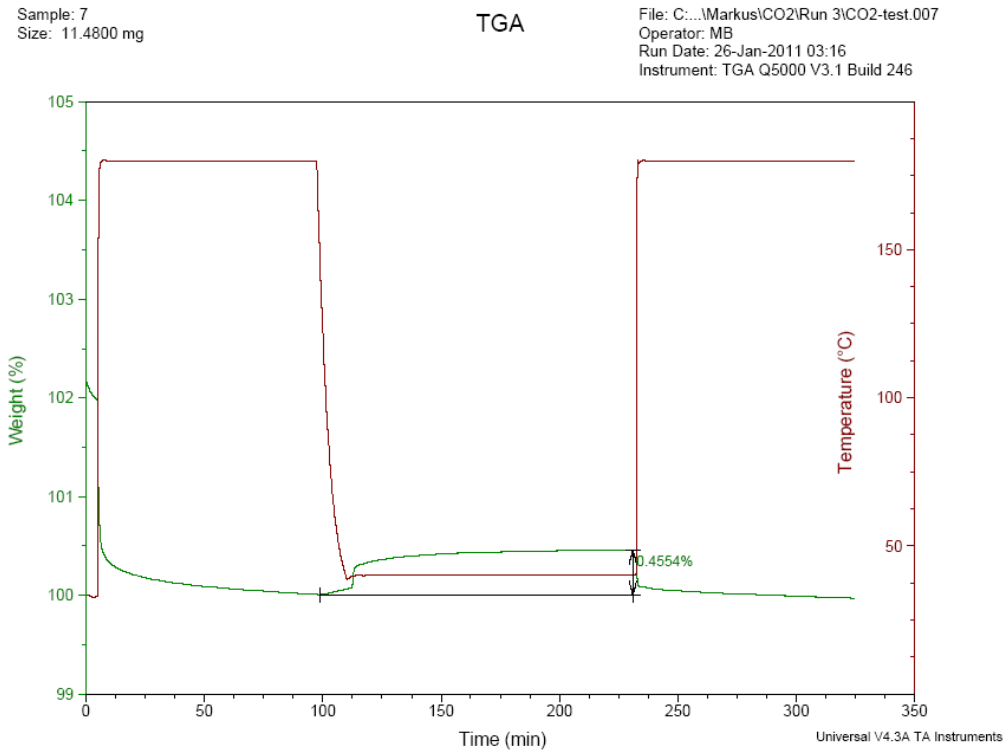

Figure 6. Sample 7, activated 70:30 GLS/OSA mixture, CO_2 adsorption uptake.

Appendix 1 (4/4)

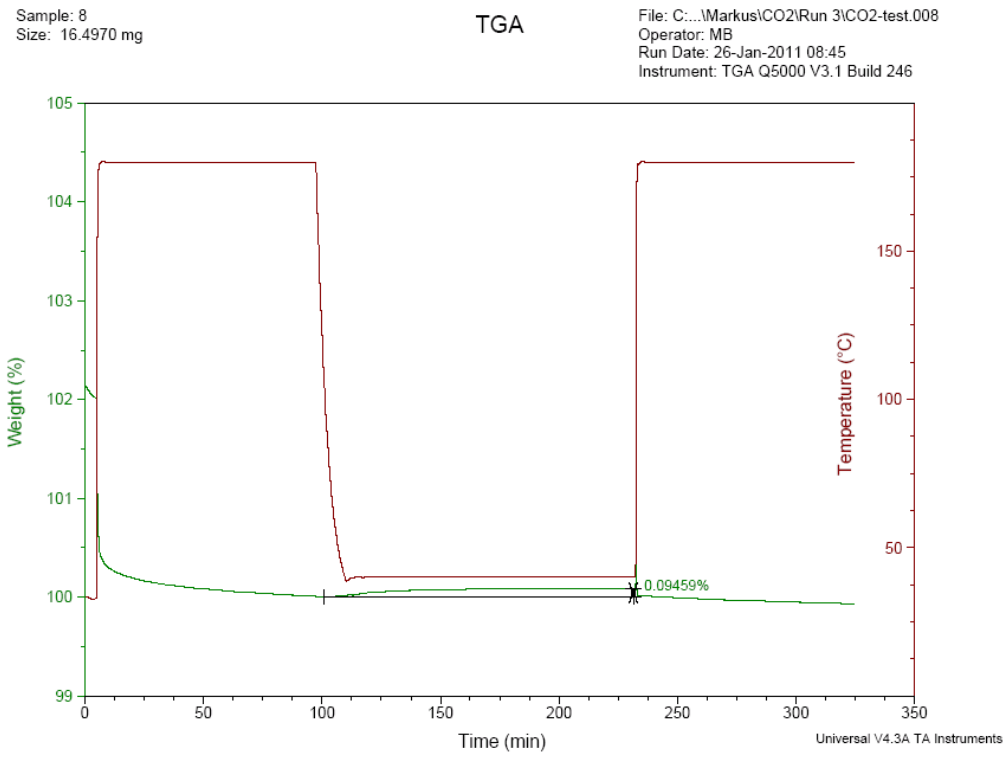

Figure 7. Sample 8, GLS, CO_2 adsorption uptake.

Appendix 2

Table 1. Surface characteristics for all samples.

Sample	BET-surface [m2/g]	t-Plot Micro [m2/g]	t-Plot External [m2/g]	BJH surface area [m2/g]	BJH average pore diameter [nm]	BET C-value
GLS	14.8	0	14.9	17.3	16.1	93
4M130 GLS	27.8	1.5	26.3	31.3	13.9	135
4M130 50/50 GLS/OSA	38.8	4.1	34.7	40.2	16.1	195
4M130 70:30 GLS/OSA	45.4	4.9	40.5	47.2	14.4	208
Old ash	7.1	0.6	6.5	8.4	18.1	160
New ash	6.3	0.8	5.6	7.3	20.0	244
1M130 Reinik	37.5	4.6	32.9	38.3	14.9	236
1M160 Reinik	57.9	11.2	46.6	58.8	16.0	990
3M130 Reinik	58.7	13.6	45.0	57.8	18.2	-1483
3M160 Reinik	49.9	11.2	38.7	49.2	15.9	-6424
5M130 Reinik	60.7	13.6	47.2	60.5	17.8	-2779
5M160 Reinik	46.5	10.4	36.2	45.2	22.1	-6203
8M130 Reinik	70.1	18.1	52.0	67.1	21.4	-636
8M160 Reinik	58.5	14.1	44.4	56.2	16.6	-1243
4M130 new	64.6	12.0	52.6	61.1	14.9	696
5M130 new	66.8	12.4	54.5	63.8	17.4	634
3M145 new	67.8	11.4	45.4	52.4	15.9	1506
5M145 new	64.6	12.2	52.3	58.6	15.6	786
6M145 new	50.1	9.3	40.8	47.3	18.7	795
5M145 - 68h	48.1	9.7	38.4	44.7	18.6	1464
4M130 old	74.3	14.3	60.0	71.7	15.9	930
3M145 old	74.1	14.2	59.8	70.2	13.5	954
4M145 old	67.0	11.9	55.2	65.0	14.0	530
5M145 old	67.9	13.1	54.8	63.5	16.1	992
chem VI	49.0	3.7	45.3	51.9	17.7	145
chem XII	54.3	7.5	46.9	51.1	16.3	276
chem I	62.6	12.1	50.5	57.0	18.5	749
chem VII	45.0	4.1	40.9	48.1	21.1	169
chem IIX	62.0	9.8	52.3	57.9	16.2	352
chem IX	45.7	6.5	39.2	43.4	16.2	278
chem XI	53.0	2.6	50.4	57.3	12.9	127
chem II	60.7	7.4	53.3	62.0	14.6	224
chem III	65.7	10.2	55.5	63.1	16.7	336

Appendix 3

Table 1. Chemisorption conditions and CO_2 uptake.

		Chemisorption conditions		Sample mass		
Chem	Sample	Press. [bar]	Temp. ['C]	Before [g]	After [g]	Diff. [%]
VI	5M160 Reinik	90	150	0.5060	0.5260	+3.9
XIII	5M130 New	100	150	0.9303	0.9544	+2.5
XII	4M130 New	100	150	1.1318	1.1407	+0.8
IV	5M130 New	40	150	0.9163	0.9231	+0.7
V	4M130 New	90	150	1.1268	1.1295	+0.2
I	5M145 New	110	150	1.0278	1.0283	+0.05
VII	5M160 Reinik	100	200	1.4708	1.4935	+1.5
IIX	5M145 New	100	180	0.8154	0.8225	+0.9
IX	5M145 -68 h 50:50	100	150	1.7359	1.7421	+0.4
X	GLS/OSA	90	150	1.2031	1.2083	+0.4
XI	4M130 Old	120	85	-	-	-
III	4M130 Old	100	150	0.8983	0.9485	+5.6
II	5M145 Old	90	150	1.0391	1.0622	+2.2
XIV	5M145 Old	95	150	0.6514	0,6600	+1.3

Appendix 4 (1/3)

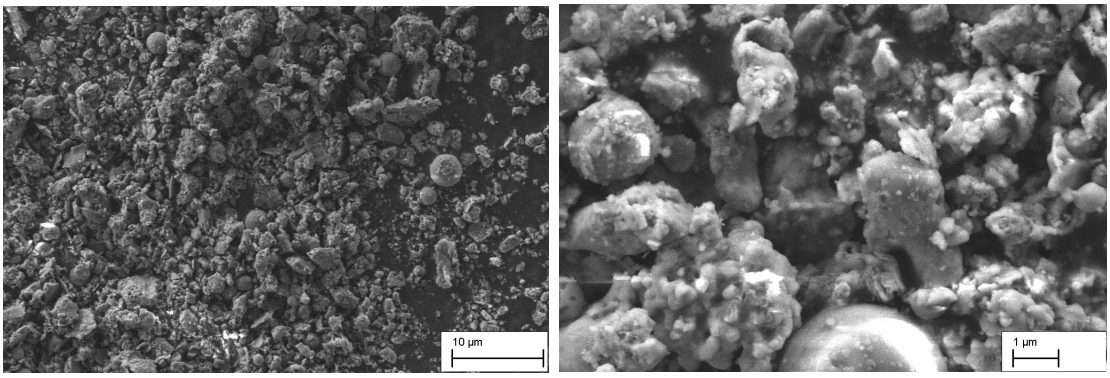

Figure 1. FESEM pictures of sample A. On the left, 5 000x and 25 000x on the right.

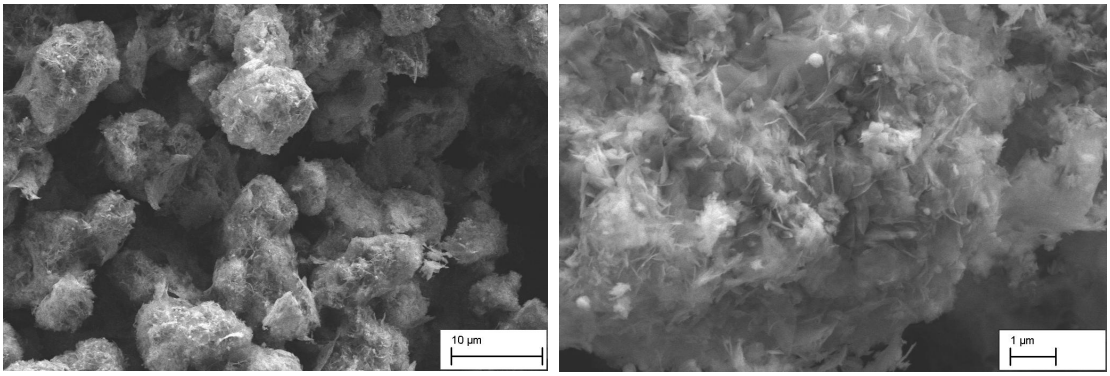

Figure 2. FESEM pictures of sample B. On the left, 5 000x and 25 000x on the right.

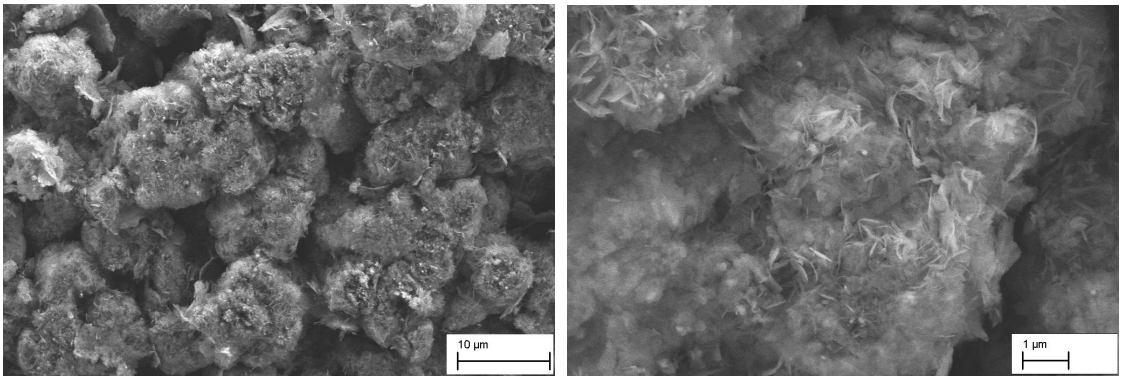

Figure 3. FESEM pictures of sample C. On the left, 5 000x and 25 000x on the right.

Appendix 4 (2/3)

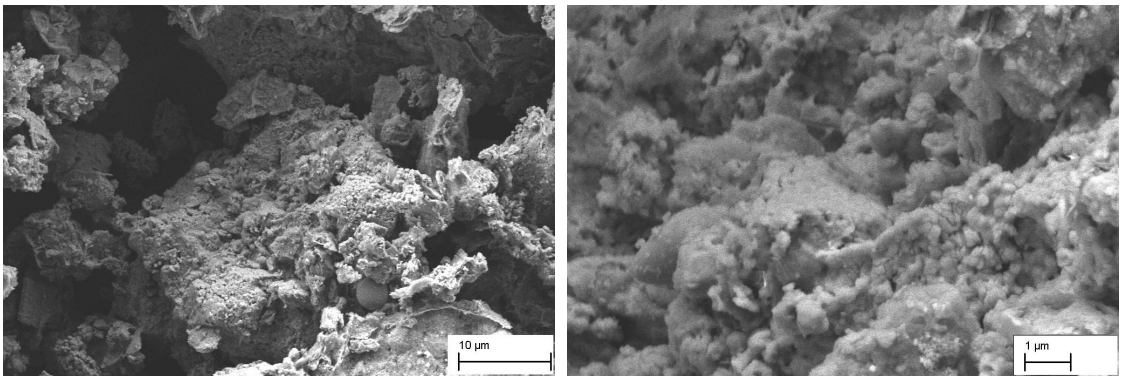

Figure 4. FESEM pictures of sample D. On the left 5 000x and 25 000x on the right.

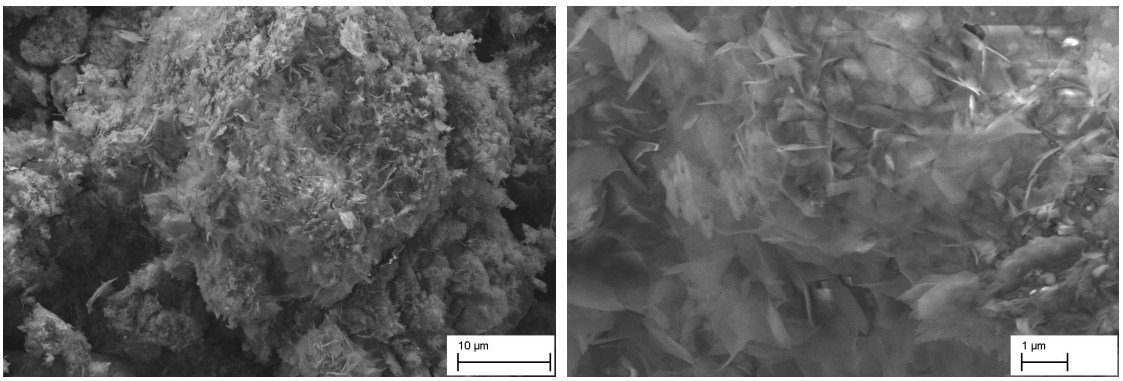

Figure 5. FESEM pictures of sample E. On the left, 5 000x and 25 000x on the right.

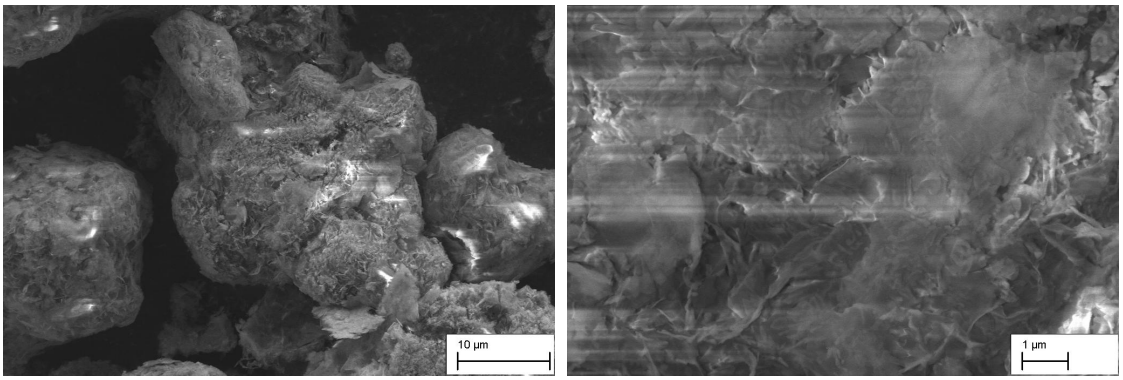

Figure 6. FESEM pictures of sample F. On the left, 5 000x and 25 000x on the right.

Appendix 4 (3/3)

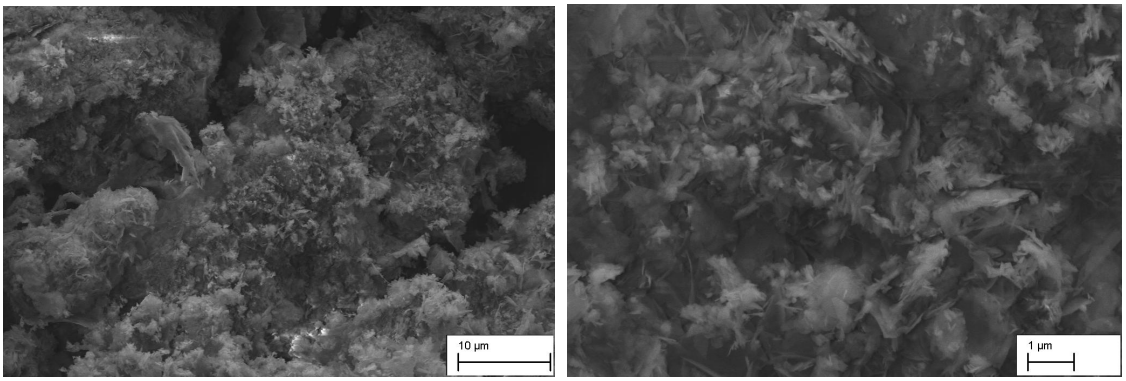

Figure 7. FESEM pictures of sample G. On the left 5 000x and 25 000x on the right.

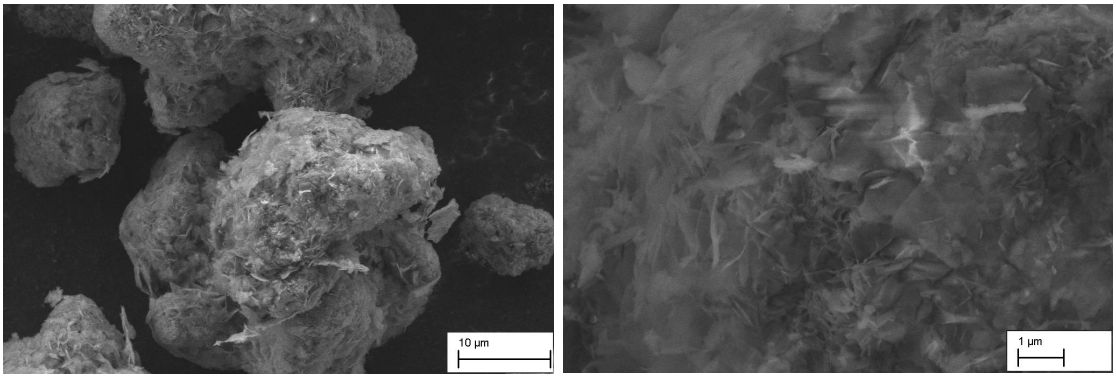

Figure 8. FESEM pictures of sample H. On the left 5 000x and 25 000x on the right.

Appendix 5

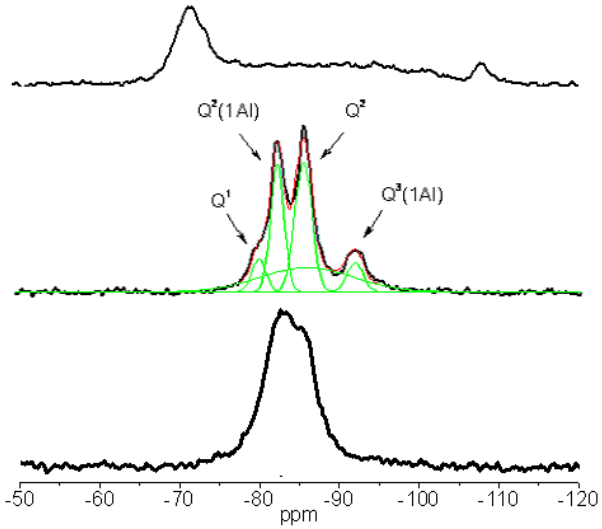

Figure 1. NMR spectra of Set 1. New ash (Sample A) on top, activated 5M145 (Sample B) with Gaussian curves in the middle and chemisorbed sample B on bottom.

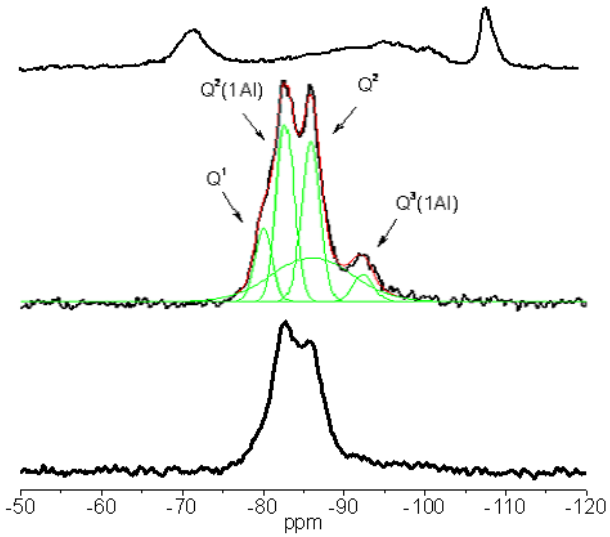

Figure 2. NMR spectra of Set 2. Old ash (Sample D) on top, activated 5M145 (Sample E) with Gaussian curves in the middle and chemisorbed sample F on bottom.

Appendix 6

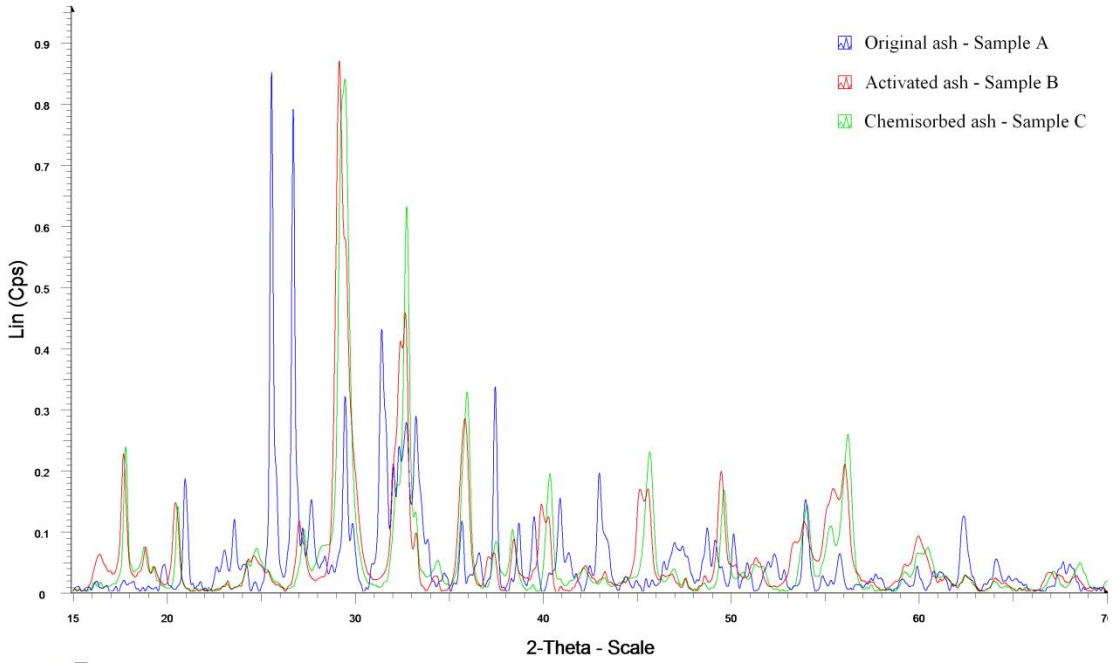

Figure 1. XRD graph of the set 1 for chemisorption.

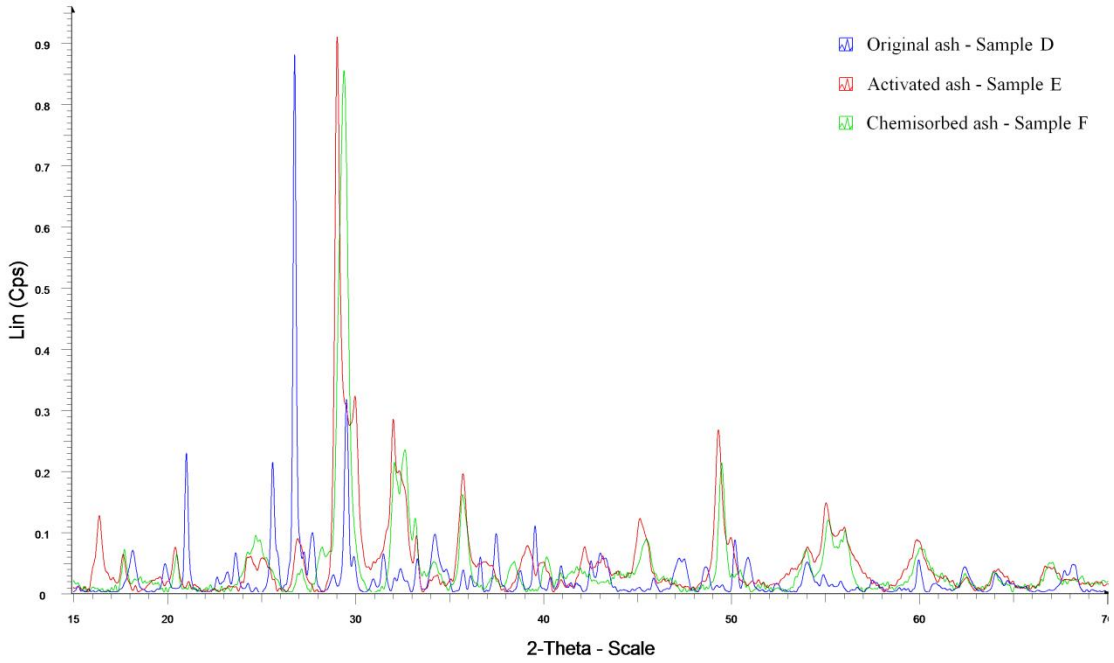

Figure 2. XRD graph of the set 2 for chemisorption.